Caudal Cranium of *Thylacosmilus atrox* (Mammalia, Metatheria, Sparassodonta), a South American Predaceous Sabertooth

Analía M. Forasiepi, Ross D. E. MacPhee, and Santiago Hernandez del Pino

Bulletin of the American Museum of Natural History

CAUDAL CRANIUM OF *THYLACOSMILUS ATROX* (MAMMALIA, METATHERIA, SPARASSODONTA), A SOUTH AMERICAN PREDACEOUS SABERTOOTH

ANALÍA M. FORASIEPI
IANIGLA, CCT-CONICET, Mendoza, Argentina

ROSS D.E. MacPHEE
Department of Mammalogy,
American Museum of Natural History, New York

SANTIAGO HERNÁNDEZ DEL PINO
IANIGLA, CCT-CONICET, Mendoza, Argentina

BULLETIN OF THE AMERICAN MUSEUM OF NATURAL HISTORY
Number 433, 64 pp., 27 figures, 1 table
Issued June 14, 2019

ISSN 0003-0090

CONTENTS

ABSTRACT

The caudal cranium of the South American sabertooth *Thylacosmilus atrox* (Thylacosmilidae, Sparassodonta, Metatheria) is described in detail, with emphasis on the constitution of the walls of the middle ear, cranial vasculature, and major nerve pathways. With the aid of micro-CT scanning of the holotype and paratype, we have established that five cranial elements (squamosal, alisphenoid, exoccipital, petrosal, and ectotympanic) and their various outgrowths participate in the tympanic floor and roof of this species. *Thylacosmilus* possessed a U-shaped ectotympanic that was evidently situated on the medial margin of the external acoustic meatus. The bulla itself is exclusively composed of the tympanic process of the exoccipital and rostral and caudal tympanic processes of the squamosal. Contrary to previous reports, neither the alisphenoid nor the petrosal participate in the actual tympanic floor, although they do contribute to the roof. In these regards *Thylacosmilus* is distinctly different from other borhyaenoids, in which the tympanic floor was largely membranous (e.g., *Borhyaena*) and lacked an enlarged ectotympanic (e.g., *Paraborhyaena*). In some respects *Thylacosmilus* is more similar to hathliacynids than to borhyaenoids, in that the former also possessed large caudal outgrowths of the squamosal and exoccipital that were clearly tympanic processes rather than simply attachment sites for muscles. However, hathliacynids also exhibited a large alisphenoid tympanic process, a floor component that is absent in *Thylacosmilus*. Habitual head posture was inferred on the basis of inner ear features. Large paratympanic spaces invade all of the elements participating in bounding the middle ear, another distinctive difference of *Thylacosmilus* compared to other sparassodonts. Arterial and venous vascular organization is relatively conservative in this species, although some vascular trackways could not have been securely identified without the availability of CT scanning. The anatomical correlates of the internal carotid in relation to other basicranial structures, the absence of a functional arteria diploetica magna, and the network for venous return from the endocranium agree with conditions in other sparassodonts.

INTRODUCTION

Sparassodonta is a wholly extinct radiation of predaceous metatherians thought to be endemic to South America. Fossils of metatherians with hypercarnivorous dentitions have been found on other continents, but in general they are too fragmentary to provide any certainty regarding their likely affinities (Beck, 2015), or are controversial for other reasons (Carneiro, 2018; see discussions in Muizon et al., 2018). Sparassodonta is generally regarded as a monophyletic clade of stem marsupials (e.g., Szalay, 1982; Marshall and Kielan-Jaworowska, 1992; Rougier et al., 1998; Babot, 2005; Forasiepi, 2009; Engelman and Croft, 2014; Forasiepi et al., 2015; Suárez et al., 2016; Muizon et al., 2018). Nearly 60 different species of sparassodonts have been recognized, the majority of Neogene age (fig. 1). *Patene*, a taxon represented in Eocene deposits in Argentina, Brazil and Peru, has been traditionally considered to have the most primitive morphology found in the group (e.g., Simpson, 1948; Marshall, 1981; Goin et al., 1986; Goin and Candela, 2004). Expressing this point in the form of a definition by ancestry, Sparassodonta is the group that includes the common ancestor of *Patene* and all its descendents (e.g., see Forasiepi, 2009; Engelman and Croft, 2014; Forasiepi et al., 2015; Suárez et al., 2016; Muizon et al., 2018).

Although there is broad agreement regarding the overall taxonomic composition of Sparassodonta, there are also persistent areas of controversy. The earliest taxa for which sparassodont affinities have been claimed include the Early Paleocene Tiupampan species *Mayulestes ferox* and *Allqokirus australis* (e.g., Muizon, 1994, 1998; Muizon et al., 1997, 2018). In a recent phylogenetic analysis presented by Muizon et al. (2018), *Mayulestes, Allqokirus,* and *Patene* are shown as forming a monophyletic group at the base of Sparassodonta. However, at least in the

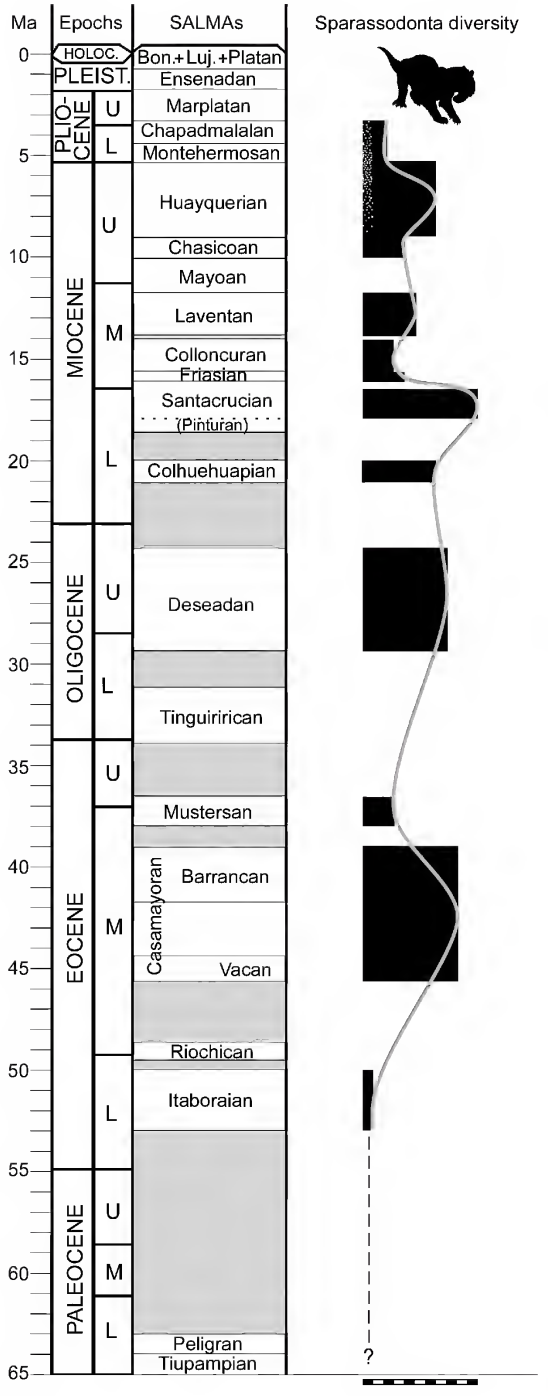

case of *Mayulestes*, alternative phylogenetic positions also have been proposed (Rougier et al., 1998; Goin, 2003; Babot, 2005; Forasiepi, 2009; Engelman and Croft, 2014; Forasiepi et al., 2015; Suárez et al., 2016; Wilson et al., 2016).

Undisputed records of Sparassodonta, including ones for *Patene simpsoni*, begin in the Early Eocene (Itaboraian) and extend through to the Pliocene (Chapadmalalan), when the last of them disappeared (Babot and Forasiepi, 2016; Prevosti and Forasiepi, 2018) (fig. 1). Forasiepi (2009) divided non-Tiupampan taxa into two principal groups, Hathliacynidae and Borhyaenoidea, the latter comprising Borhyaenidae, Thylacosmilidae, and (possibly) Proborhyaenidae (see Babot, 2005; Forasiepi et al., 2015; Babot and Forasiepi, 2016). This arrangement agrees with earlier treatments, such as those of Marshall (1978, 1981; Marshall et al., 1990). However, Proborhyaenidae did not emerge as a natural group in all studies (Babot, 2005; Forasiepi et al., 2015).

Most sparassodonts can be viewed as specialized hypercarnivores (Wroe et al., 2004; Prevosti et al., 2013; Zimicz, 2014, López-Aguirre et al., 2016; Croft et al., 2018), with only 10% of species qualifying as omnivores or mesocarnivores utilizing the criteria of Prevosti and Forasiepi (2018). Perhaps the most famous of all sparassodonts is the so-called "marsupial sabertooth," *Thylacosmilus atrox* (Riggs, 1933, 1934; figs. 2–5).

FIG. 1. Diversity of sparassodonts through time. Lines representing the diversity curve based on number of species (black blocks) as predicted by the fossil record (Lazarus taxa not included). Possible fossil record biases include hiatuses (time spans lacking known fossils), different taxon durations, and averaging of biochronological units. Other biases which may mask the real diversity pattern include inadequate or imprecise chronological ages for associations determined by radiometric dating, as well as differences in sampling effort across temporal units or geographical regions (Prevosti and Forasiepi, 2018). Dot cluster indicates the temporal span of *Thylacosmilus atrox* from the Late Miocene (Huayquerian) to Pliocene (Chapadmalalan). Scale: 1:1 species.

FIG. 2. Artistic reconstruction of *Thylacosmilus atrox* by Jorge Blanco.

Its hypertrophied upper canines and correlated cranial modifications have inevitably invited comparisons to *Smilodon* and other sabertooth placentals —a classic example of convergent evolution (e.g., Riggs, 1933, 1934; Simpson, 1971; Marshall, 1976a, 1977a; Turnbull, 1978; Turnbull and Segall, 1984; Churcher, 1985).

But the dental apparatus is not the only region of striking morphological specialization seen in sabertooth skulls: the auditory regions of *Smilodon* and *Thylacosmilus* are likewise remarkably modified compared with those of their close relatives (Turnbull and Segall, 1984). In his initial description of *Thylacosmilus*, Riggs (1934) provided a brief treatment of its cranial anatomy, based mainly on the holotype (FMNH P14531; figs. 3, 6–8). Turnbull and Segall (1984) reevaluated and extended Riggs' interpretations, adding detailed descriptions of the paratype (FMNH P14344; figs. 4, 9, 10). They identified several otic features of *Thylacosmilus* that, if correctly interpreted, would not only be novel for sparassodonts but unique among metatherians. These identifications are given special attention in this paper.

Thanks to the availability of μCT scanning, we have been able to reevaluate Turnbull and Segall's (1984) descriptions, which by necessity had to be largely based on surface anatomy. However, unexpected difficulties in identifying certain features required examination of other fossil evidence for morphological variation in the sparassodont caudal cranium. This was required in any case because the literature on metatherian cranial morphology is limited compared with that available for eutherians. Although metatherians and eutherians are phylogenetic sisters, these two clades have fol-

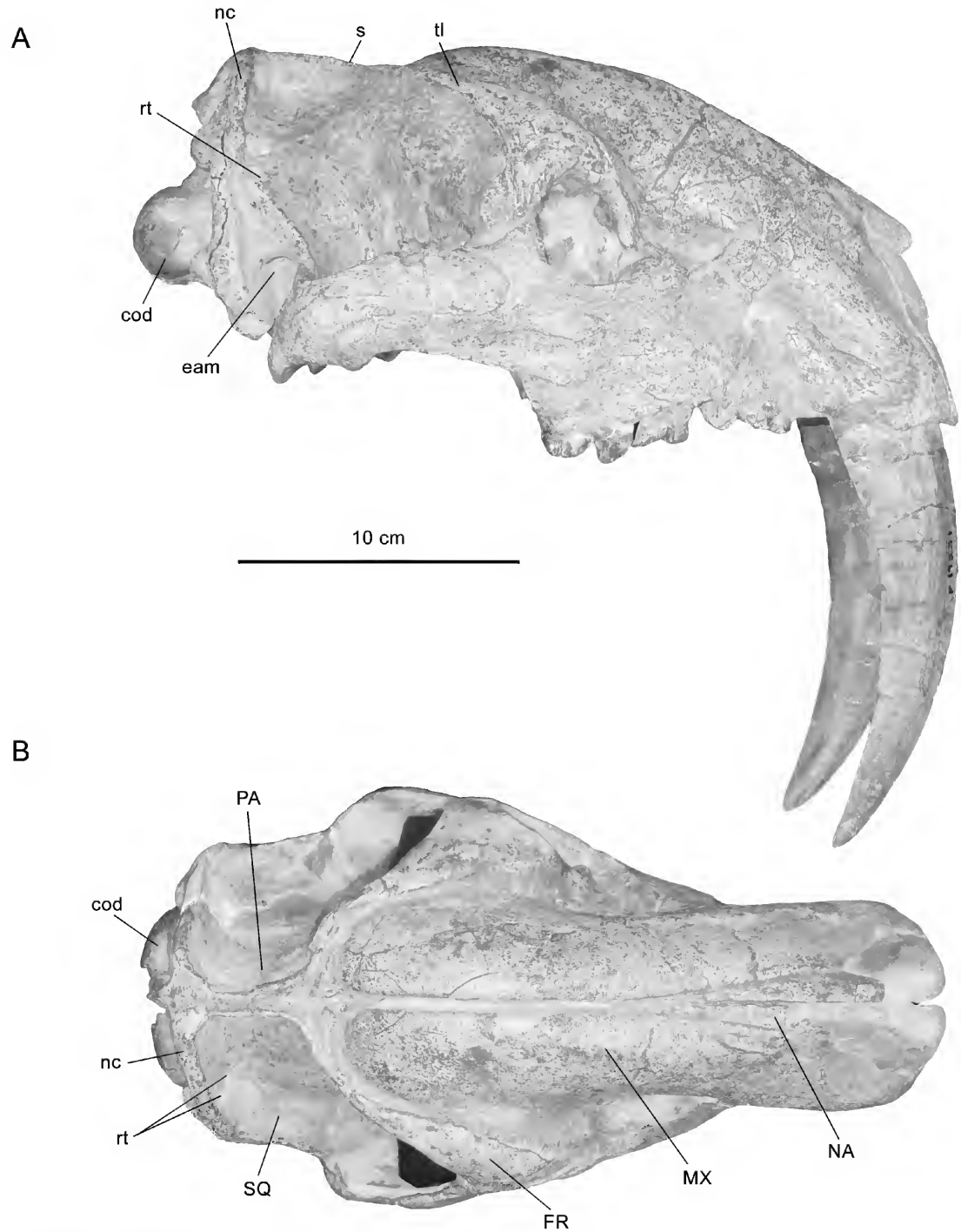

FIG. 3. *Thylacosmilus atrox*, holotype, FMNH P14531 (Hualfin, Catamarca, Argentina; Corral Quemado Formation; Chapadmalalan, mid-Pliocene). Skull in lateral (**A**) and dorsal (**B**) views. Abbreviations: **cod,** occipital condyle; **eam,** external acoustic meatus; **FR,** frontal; **MX,** maxilla; **NA,** nasal; **nc,** nuchal crest; **PA,** parietal; **rt,** rami temporales; **s,** sagittal crest; **SQ,** squamosal; **tl,** temporal line.

lowed different evolutionary (and morphological) trajectories for the past ~130 Ma (O'Leary et al., 2013). As a result, conditions in fossil metatherians need to be interpreted on their own terms, and not merely viewed as special instances of what can be observed in eutherians.

MATERIALS AND METHODS

Specimens

Thylacosmilus: The specimens principally utilized for this study are the holotype (FMNH P14531; figs. 3, 6–8), which is in good condition overall, and the paratype (FMNH P14344; figs. 4, 9, 10), which has suffered considerable erosional damage but retains a reasonably intact caudal cranium. Additional details on basicranial construction were retrieved from *T. atrox* MMP 1443-M (figs. 5, 11). Other specimens reviewed in this paper are listed in table 1.

Goin and Pascual (1987) have shown that the numerous Late Miocene/Pliocene thylacosmilid species named in the 20th century cannot be meaningfully distinguished from one another and should therefore be regarded as synonyms of *Thylacosmilus atrox*, the earliest valid name apart from an unused senior synonym (*Achlysictis lelongi*, now suppressed; see Goin and Pascual, 1987) coined by Ameghino (1891). The amount of individual variation within *T. atrox* as currently defined is certainly substantial (e.g., *Thylacosmilus* FMNH P14531, P14344, and MMP 1443-M; figs. 3–5). Because of their notable difference in size, the holotype and paratype were thought by Riggs (1934: 9) to be of greatly different ontogenetic ages. He described the paratype as "a young adult specimen," basing his assessment on the fact that "the mandible is nearly one fourth smaller in linear dimensions than that of the holotype." However, we found that the dentitions were notably worn in both specimens, indicating that any difference in their ontogenetic ages could not have been very considerable. It is possible that sexual dimorphism, perhaps in combination with or amplified by individual variation (Goin and Pascual, 1987), played an important role in producing such wide ranges in size, even in fossils of similar ontogenetic age. In fact, even though less pronounced than in *Thylacosmilus*, substantial morphological variability has been demostrated for other sparassodonts (e.g., in *Cladosictis patagonica*, expressed as differences in mandibular size and shape; Echarri et al., 2017), just as it has in extant mammals generally (e.g., Lindenfors et al., 2007).

It is important to note that Turnbull and Segall (1984) made modifications to the holotype and paratype in the course of their investigation. First, the apparent outlines of several sutures were drawn with indelible ink on both specimens. Although many of these tracings correspond fairly well to actual boundaries between bone territories as seen in the scans, in some cases they do not, or the situation is ambiguous. For a given suture to be named as such in this paper there must be secure evidence of it, either macroscopically or in the segmental data. This issue principally affects evaluation of bullar composition. Although both specimens can be described as reasonably well preserved, bullar surfaces display hairline breaks that cannot be easily distinguished from sutures. In a second modification of the fossil material, Turnbull and Segall (1984) removed most of the right bulla of the paratype in order to better explore middle ear anatomy. Fortunately, the detached bulla was kept with the rest of the skull, permitting us to provide some additional interpretrations of its morphology.

Other Metatheria: The comparative set of fossil and extant specimens utilized in this paper is listed in table 1. Certain features whose relations or ontogeny are uncertain were traced in serially sectioned pouch young of *Monodelphis domestica* (head length, 8.5 mm; postnatal day 12; DUCEC), *Perameles* sp. (head length, 17.5 mm; ZIUT), and *Macropus eugenii* (head length, 29 mm; ZIUT). For additional information on these specimens, see Sánchez-Villagra and Forasiepi (2017). Other data were obtained from the literature.

Anatomical nomenclature: The nomenclature used in the descriptions largely follows MacPhee (1981) and Wible (2003); a few new

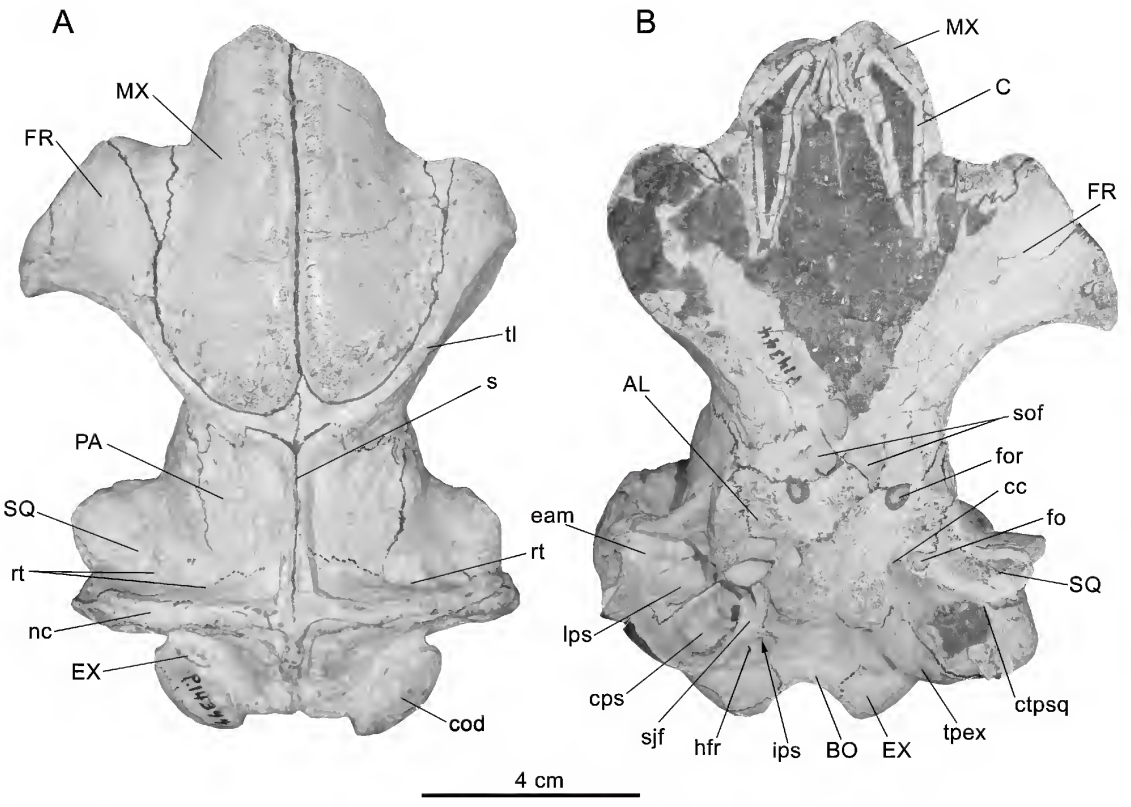

FIG. 4. *Thylacosmilus atrox*, paratype, FMNH P14344 (Río Santa María, Chiquimil, Catamarca, Argentina; Andalgalá Formation; Huayquerian, Late Miocene). Skull in **A,** dorsal and **B,** ventral views. Abbreviations: **AL,** alisphenoid; **BO,** basioccipital; **C,** upper canine; **cc,** carotid canal; **cod,** occipital condyle; **cps,** caudal paratympanic space; **ctpsq,** caudal tympanic process of squamosal; **eam,** external acoustic meatus; **EX,** exoccipital; **fo,** foramen ovale; **for,** foramen rotundum; **FR,** frontal; **hfr,** rostral hypoglossal foramen; **ips,** inferior petrosal sinus; **lps,** lateral paratympanic space (= epitympanic sinus); **MX,** maxilla; **nc,** nuchal crest; **PA,** parietal; **rt,** rami temporales; **s,** sagittal crest; **sjf,** secondary jugular foramen; **sof,** sphenoorbital fissure; **SQ,** squamosal; **tl,** temporal line; **tpex,** tympanic process of exoccipital. Arrow indicates direction to or position of features hidden by other structures.

terms are introduced and defined where they first occur. For all other definitions of anatomical terms, see appendix 1.

CT Scanning and Bone Histology

Thylacosmilus atrox (holotype, FMNH P14531). Originally scanned by Larry Witmer (Ohio University) at O'Bleness Memorial Hospital in Athens, Ohio, using a General Electric Light Speed Ultra MultiSlice CT scanner with a slice thickness of 0.625 mm at 120 kV and 200 mA. This scan resulted in a final stack of 433 slices of 307 × 471 pxl.

Thylacosmilus atrox (paratype, FMNH P14344). Scanned on a GE Phoenix vtomex s240 μCT scanner in the laboratory of Zhe-Xi Luo (University of Chicago) with a slice thickness of 0.07 mm at 210 kV, 190 mA. The scan resulted in a final stack of 2022 slices of 1493 × 1180 pxl.

Sipalocyon gracilis (AMNH VP 9254). Scanned on a GE Phoenix vtomex s240 μCT scanner

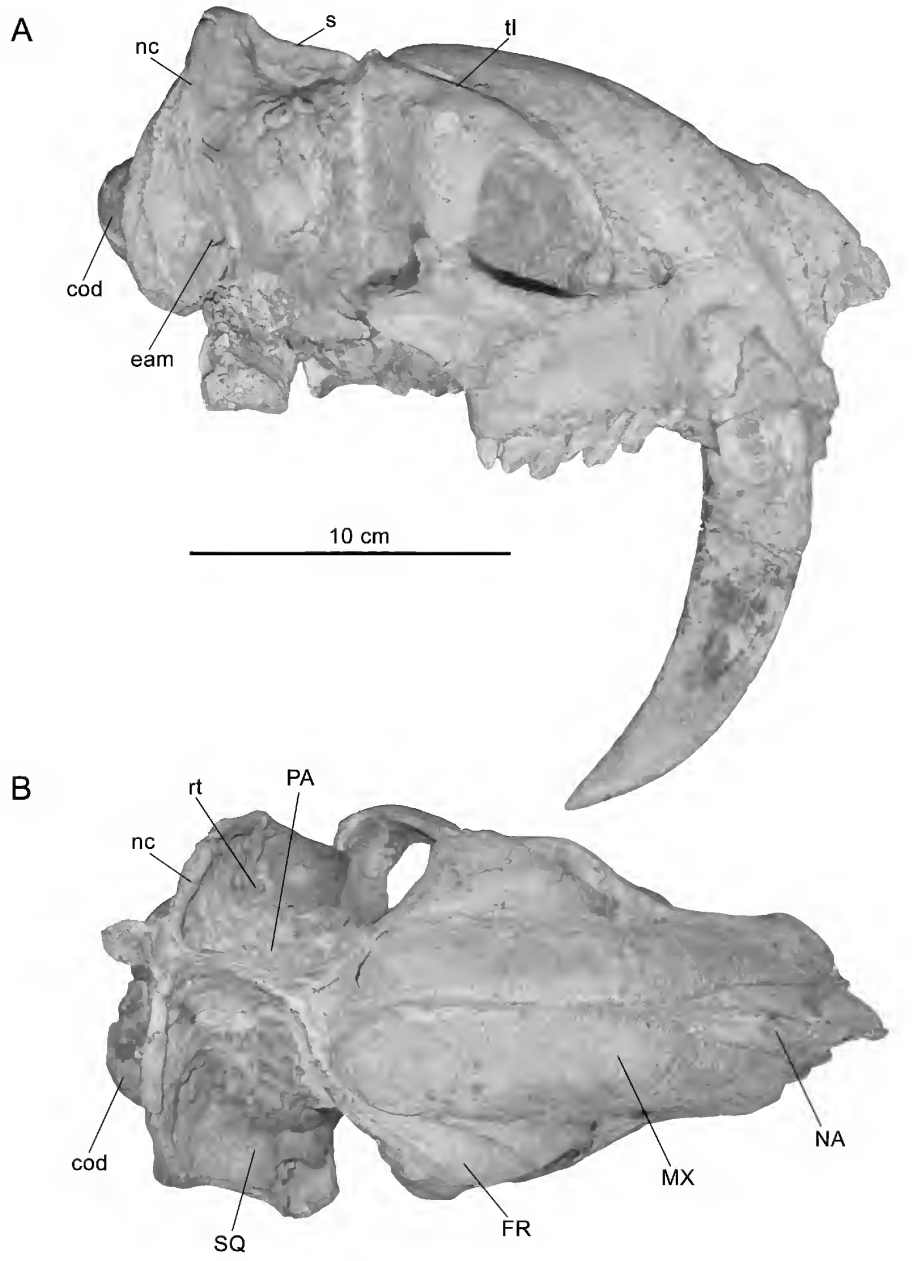

FIG. 5. *Thylacosmilus atrox* MMP 1443-M (Chapadmalal, Buenos Aires, Argentina; Chapadmalal Formation; Chapadmalalan, mid-Pliocene). Skull in **A,** lateral and **B,** dorsal views. Abbreviations: **cod,** occipital condyle; **eam,** external acoustic meatus; **FR,** frontal; **MX,** maxilla; **NA,** nasal; **nc,** nuchal crest; **PA,** parietal; **rt,** ramus temporalis; **s,** sagittal crest; **SQ,** squamosal; **tl,** temporal line.

TABLE 1

List of osteological specimens used for comparisons

Taxon	Specimen	Material	Occurrence	Age
SPARASSODONTA				
Arctodictis sinclairi	MLP 85-VII-3-1	Skull, dentaries, and postcranium	Gran Barranca, Chubut, Argentina	Sarmiento Fm, Early Miocene, Colhuehuapian Age
Borhyaena tuberata	MACN-A 9344	Nearly complete skull	Yegua Quemada, Santa Cruz, Argentina	Santa Cruz Fm, Early Miocene, Santacrucian Age
Borhyaena tuberata	MACN-A 5922	Partial skull	Corriguen Aike (=Puesto Estancia La Costa), Santa Cruz, Argentina	Santa Cruz Fm, Early Miocene, Santacrucian Age
Borhyaena tuberata	YPM PU 15120	Skull and partial postcranium	15 kilometers south of Coy Inlet, Santa Cruz, Argentina	Santa Cruz Fm, Early Miocene, Santacrucian Age
Borhyaena tuberata	YPM PU 15701	Skull, dentaries, and partial postcranium	15 kilometers south of Coy Inlet, Santa Cruz, Argentina	Santa Cruz Fm, Early Miocene, Santacrucian Age
Borhyaena tuberata	MPM-PV 3625	Skull and thoracic vertebra	Puesto Estancia La Costa, Santa Cruz, Argentina	Santa Cruz Fm, Early Miocene, Santacrucian Age
Cladosictis patagonica	MACN-A 5927–5929	Skull, right dentary, and partial postcranium	Corriguen Aike (= Puesto Estancia La Costa), Santa Cruz, Argentina	Santa Cruz Fm, Early Miocene, Santacrucian Age
Cladosictis patagonica	MLP 11-58	Caudal cranium	Santa Cruz, Argentina	Santa Cruz Fm, Early Miocene, Santacrucian Age
Cladosictis patagonica	YPM PU 15170	Skull, both dentaries, and partial postcranium	15 kilometers south of Coy Inlet, Santa Cruz, Argentina	Santa Cruz Fm, Early Miocene, Santacrucian Age
Lycopsis longirostrus	UCMP 38061	Skull and articulated postcranium	La Venta, Colombia	Villavieja Fm, Middle Miocene, Laventan Age
Prothylacynus patagonicus	MACN-A 5931-5937	Skull, fragmentary dentaries and partial postcranium	Corriguen Aike (=Puesto Estancia La Costa), Santa Cruz, Argentina	Santa Cruz Fm, Early Miocene, Santacrucian Age
Prothylacynus patagonicus	YPM PU 15700	Skull, both dentaries, and partial postcranium	Killik Aike N (= Felton´s Ea.), Santa Cruz, Argentina	Santa Cruz Fm, Early Miocene, Santacrucian Age
Sipalocyon gracilis	AMNH VP 9254	Complete skull and fragment of right dentary	Killik Aike N (= Felton´s Ea.), Santa Cruz, Argentina	Santa Cruz Fm, Early Miocene, Santacrucian Age
Sipalocyon gracilis	MACN-A 691–703	Incomplete skull, dentaries, and partial postcranium	Río Sehuen, Santa Cruz, Argentina	Early Miocene, Santacrucian Age

Taxon	Specimen	Material	Occurrence	Age
Sipalocyon gracilis	MACN-A 5952–5953	Incomplete skull and incomplete left dentary	Corriguen Aike (= Puesto Estancia La Costa), Santa Cruz, Argentina	Santa Cruz Fm, Early Miocene, Santacrucian Age
Thylacosmilus atrox	FMNH P14531 (holotype)	Complete skull, dentaries, and partial postcranium	Hualfín (near Puerta del Corral Quemado), Catamarca, Argentina	Corral Quemado Fm, Mid-Pliocene, Chapalmalalan Age
Thylacosmilus atrox	FMNH P14344 (paratype)	Partial skull and part of the postcranium	Rio Santa María, Chiquimil, Catamarca, Argentina	stratum 19 Andalgalá Fm., Late Miocene, Huayquerian Age
Thylacosmilus atrox	MLP 35-X-41-1, ex-FMNH P14474	Partial skull	Hualfín (near Puerta del Corral Quemado), Catamarca, Argentina	Corral Quemado Fm, Mid-Pliocene, Chapalmalalan Age
Thylacosmilus atrox	MMP 1443-M	Skull and dentaries	Chapalmalal, Buenos Aires, Argentina	Chapadmalal Fm, mid-Pliocene, Chapalmalalan Age
cf. *Pharsophurus sp.*	AMNH VP 29591	fragment of a skull (juvenile)	Rinconada de la Sierra de Canquel, Scarritt Pocket, Chubut, Argentina	Deseado Formation, Late Oligocene, Deseadan Age
MARSUPIALIA				
Acrobates pygmaeus	AMNH M 37185	Skull and skin	New South Wales, Australia	
Dasyurus maculatus	AMNH M 65688	Skull	NW Arthur River, Tasmania	
Didelphis marsupialis	AMNH M 95345	Skull and skin	Pura, Rio Tapajos, Brazil	
Didelphis marsupialis	AMNH M 95350	Skull and skin	Pura, Rio Tapajos, Brazil	
Dromiciops gliroides	MACN-Ma 23607	Skull	Llao Llao, Río Negro, Argentina	
Lasiorhinus latifrons	AMNH M 243	Skull	South Australia, Australia	
Monodelphis domestica	AMNH M 133247	Skull	Anapolis, Brazil	
Monodelphis domestica	AMNH M 261242	Skull, postcranium, and skin	Chuquisaca, Porvenir, Bolivia	
Sarcophilus harrisii	AMNH M 65673	Skull, postcranium, and skin	NW Arthur River, Tasmania	
Sarcophilus harrisii	AMNH M 173501	Skull	Columbia Dental College, Australia	
Sarcophilus harrisii	AMNH M 69544	Skull	Tasmania	
Vombatus ursinus	AMNH M 173506	Skull	Columbia Dental College, Australia	

housed at AMNH with a slice thickness of 0.069 mm at 180 kV, 220 mA. The scan resulted in a final stack of 1648 slices of 1037 × 593 pxl.

Borhyaena tuberata (YPM PU 15120, petrosal only). Scanned on a GE Phoenix vtomex s240 μCT scanner housed at AMNH with a slice thickness of 0.012 mm at 180 kV, 220 mA. The scan resulted in a final stack of 1425 slices of 1140 × 886 pxl.

cf. *Pharsophorus* sp. (AMNH VP 29591, petrosal only). Scanned on a GE Phoenix vtomex s240 μCT scanner housed at AMNH with a slice thickness of 0.012 mm at 180 kV, 220 mA. The scan resulted in a final stack of 1925 slices of 1619 × 1166 pxl.

The open source program 3DSlicer (Fedorov et al., 2012) was used for 3-D reconstruction and segmentation of FMNH P14531 and FMNH P14344. VGStudio MAX (Volume Graphics GmbH, Heidelberg, Germany) was used for 3-D reconstruction of the petrosals and inner ear of AMNH VP 9254, YPM PU 15120, and AMNH VP 29591. Linear data were taken using 3DSlicer and open source Fiji (Schindelin et al., 2012).

Histological sections were examined with a stereoscopic microscope (Leica MZ 16®); photos were taken with a Leica DFC 420 C® digital camera at the University of Zürich (Sánchez-Villagra and Forasiepi, 2017).

Institutional and Other Abbreviations

AMNH M, Department of Mammalogy, American Museum of Natural History, New York; AMNH VP, Department of Vertebrate Paleontology, American Museum of Natural History; DUCEC, Duke University Comparative Embryology Collection, Department of Evolutionary Anthropology, Durham, NC; FMNH, Field Museum of Natural History, Chicago; MACN-A, Museo Argentino de Ciencias Naturales "Bernardino Rivadavia," Ameghino Collection, Buenos Aires, Argentina; MLP, Museo de La Plata, La Plata, Argentina; MMP, Museo Municipal de Ciencias Naturales de Mar del Plata "Lorenzo Scaglia," Mar del Plata, Argentina; MPM-PV, Museo Regional Provincial "Padre M.J. Molina," Río Gallegos, Argentina; UCMP, University of California, Museum of Paleontology, Berkeley; YPM PU, Yale Peabody Museum, ex-Collection of Princeton University, New Haven, CT; ZIUT, Zoologisches Institut Universität Tübingen (collection of W. Maier), Germany.

Capital and lower case letters, C/c, canine, P/p, premolar, and M/m, molar, refer to upper and lower teeth, respectively.

COMPARATIVE OSTEOLOGY OF THE CAUDAL CRANIUM OF *THYLACOSMILUS* AND OTHER SPARASSODONTS

Tympanic Floor and Basicranial Composition in *Thylacosmilus*

Because of the effects of extensive remodeling activity during ontogeny, as well as postmortem damage, the components forming the auditory bulla of adult *Thylacosmilus atrox* are difficult to identify by simple inspection. This is well illustrated by the history of differing conclusions regarding tympanic floor composition in this species. The first published observations on the basicranial anatomy of *Thylacosmilus* appeared in Riggs' (1934) monograph, based on notes compiled by Bryan Patterson (and thus cited as such here). Patterson reached no firm conclusions regarding bullar constitution in this taxon, but he did mention, confusingly, that the mastoid, exoccipital, and squamosal appeared to be "overlapping" the bulla, as though the latter were a separate entity. He also stated very tentatively that the alisphenoid might be involved in forming the rostromedial part of the bony tympanic floor, whereas the caudal part was probably formed by the "tympanic wing of the petrosal" (= caudal tympanic process of this element; appendix 1).

In sharp contrast, Turnbull and Segall (1984) concluded that the bulla was not alisphenoid/petrosal in composition, as Patterson seemed to imply, but instead "mastoid"/exoccipital. Without giving definitive reasons, they stated that the bulla is "comprised mainly of the mastoid, which surrounds the [ecto]tympanic, and in part by the exoccipital, which overlaps the mastoid posteriorly" (p.

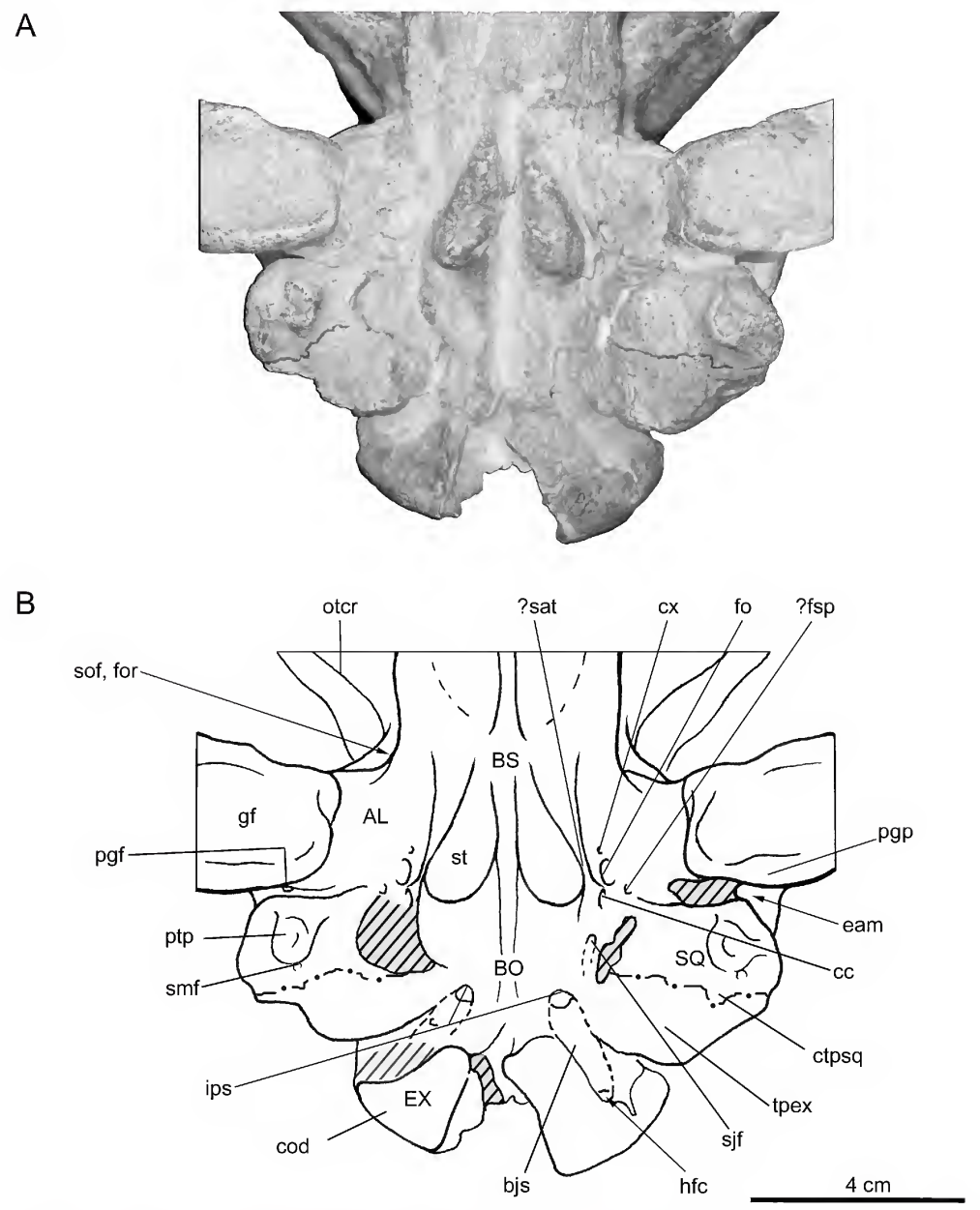

FIG. 6. *Thylacosmilus atrox*, holotype, FMNH P14531. Basicranium in **A,** ventral view, with **B,** key. Shaded areas represent incompletely prepared or restored areas. Foraminal locations mostly indicated on specimen's better-preserved left side. Abbreviations: **AL,** alisphenoid; **bjs,** basijugular sulcus; **BO,** basioccipital; **BS,** basisphenoid; **cc,** carotid canal; **cod,** occipital condyle; **ctpsq,** caudal tympanic process of squamosal; **cx,** canal x (see text); **eam,** external acoustic meatus; **EX,** exoccipital; **fo,** foramen ovale; **for,** foramen rotundum; **?fsp,** foramen spinosum; **gf,** glenoid fossa; **hfc,** caudal hypoglossal foramen; **ips,** inferior petrosal sinus; **otcr,** orbitotemporal crest; **pgf,** postglenoid foramen; **pgp,** postglenoid process of squamosal; **ptp,** posttympanic process of the squamosal; **?sat,** sulcus for the auditory tube; **smf,** stylomastoid foramen; **sof,** sphenoorbital fissure; **SQ,** squamosal; **st,** sphenoidal tubercle; **sjf,** secondary jugular foramen; **tpex,** tympanic process of exocipital. Arrow indicates direction to or position of features hidden by other structures.

252). Their presumptive suture line separating these bone territories can be seen in the basicranial view of the holotype (fig. 6A). In their opinion there were no contributions to the floor from pars cochlearis of the petrosal nor any of the other circumjacent bones (i.e., alisphenoid, basisphenoid, basioccipital, squamosal, or ectotympanic).

By contrast, scanning evidence (figs. 7, 8) conclusively establishes that the tympanic floor in *Thylacosmilus* is formed by the squamosal and exoccipital, without overlapping any other structures except for the ectotympanic. Scans also demonstrate that the ectotympanic does not contribute to any part of the bullar wall but merely contacts it from within (see also fig. 12D). Given previous interpretations, the major surprise is the failure of the petrosal to broadly participate in the formation of the bulla. Scans show that the petrosal bone is relatively small and deeply buried among surrounding elements (fig. 8C, D). There is no projection conforming to the rostral tympanic process on the promontorial surface, and only an insignificant crest at the position of the caudal tympanic process of the petrosal (fig. 19B). The external or "mastoid" surface of pars canalicularis is not exposed caudally, and the rear of the skull is formed solely by occipital and squamosal material (fig. 10).

Unfortunately, scan resolution was not good enough to check whether the bullar suture lines drawn by Turnbull and Segall (1984) were correctly placed. However, assuming their interpretations are correct, in ventral view the squamosal's total contribution would have been somewhat greater than that of the exoccipital (fig. 6). This is certainly possible, but in view of the uncertainties we do not attempt to further refine boundaries of bone territories in the figures. We cannot account for Patterson's observation that the alisphenoid participates in the bullar floor in the form of a tympanic process, although there is a small epitympanic wing of the alisphenoid in the roof of the tympanic cavity (see below and fig. 9).

Turnbull and Segall (1984: 262) inferred that a small collection of bone fragments attached to the tympanic roof on the open right side of the paratype might represent remains of the rostral crus of the ectotympanic and ossicles (fig. 9B, C). The ossicular pieces are too damaged for worthwhile description. The putative ectotympanic fragment (fig. 9C: ?EC) bears no diagnostic features of that element. In any case, the authors inferred from this evidence that the ectotympanic was probably U-shaped: "The main triangular piece [of the rostral crus] is too reduced to be the entire tympanic bone, and we assume that most of the probably very fragile ring portion must be missing."

The scan of the unopened left middle ear of the paratype reveals that their inference regarding the form of the ectotympanic was largely correct: a scatter of small bone fragments, as well as a crescentic, thin-walled structure, identifiable as ectotympanic, can be seen embedded in the matrix filling the tympanic cavity (fig. 12D). The crescentic structure is slightly displaced relative to the porus meatus, perhaps because it was broken away when the middle

FIG. 7. *Thylacosmilus atrox*, holotype, FMNH P14531. **A–E.** Horizontal sections through caudal cranium in ventrodorsal order (see inset). In B, apparent subdivision of foramen ovale is possibly a preparation artifact. E depicts caudalmost portion of petrosal, which is not exposed on external surface of skull. Note throughout large size of tympanic cavity and paratympanic spaces. Abbreviations: **AL,** alisphenoid; **at,** aperture for the auditory tube; **BS,** basisphenoid; **cc,** carotid canal; **CNV_2,** maxillary branch of trigeminal (cranial) nerve; **CNV_3,** mandibular branch of trigeminal (cranial) nerve; **cod,** occipital condyle; **cps,** caudal paratympanic space; **ct,** tympanic cavity; **ctpsq,** caudal tympanic process of squamosal; **cx,** canal x; **eam,** external acoustic meatus; **ecr,** endocranial cavity; **EX,** exoccipital; **fmg,** foramen magnum; **fo,** foramen ovale; **FR,** frontal; **frs,** frontal sinus; **?fsp,** foramen spinosum; **gfis,** glaserian fissure; **iam,** internal acoustic meatus; **ips,** inferior petrosal sinus; **lps,** lateral paratympanic space (= epitympanic sinus); **nc,** nuchal crest; **PE,** petrosal; **pgc/f,** postglenoid canal or foramen; **rtpsq,** rostral tympanic process of squamosal; **sev,** sphenoparietal emissary vein; **sfn,** septum for facial nerve; **sjf,** secondary jugular foramen; **smc,** stylomastoid canal; **SQ,** squamosal; **vps,** ventral paratympanic space.

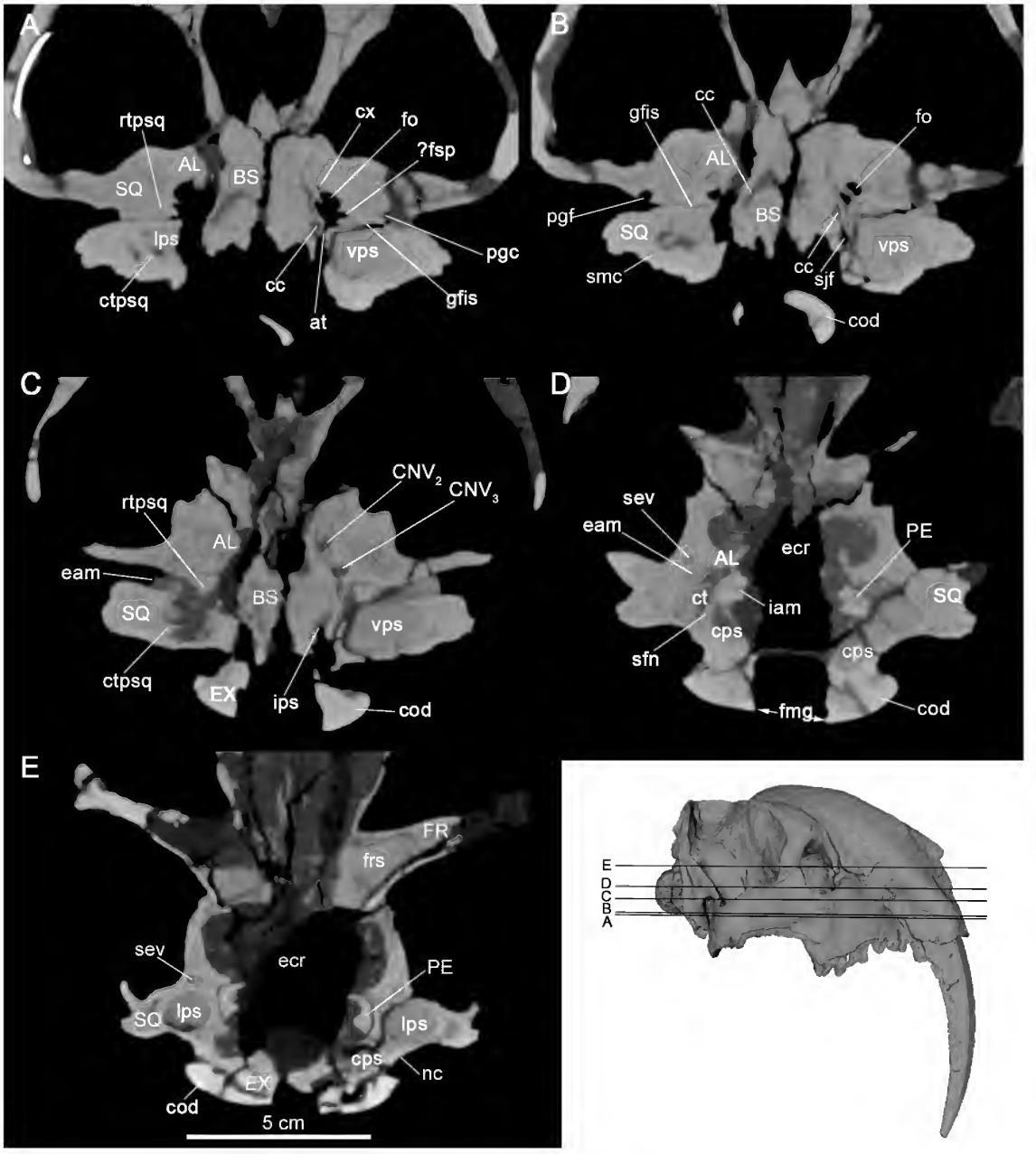
A
rtpsq
cx
fo
?fsp
AL
BS
SQ
lps
vps
pgc
cc
gfis
ctpsq
at
B
gfis
cc
fo
AL
pgf
BS
SQ
vps
smc
cc
sjf
cod
C
CNV2
CNV3
rtpsq
AL
eam
BS
SQ
vps
ctpsq
EX
ips
cod
D
sev
eam
ecr
PE
AL
ct
iam
SQ
cps
sfn
cps
fmg
cod
E
FR
frs
sev
ecr
PE
SQ
lps
lps
cps
nc
EX
cod
5 cm
E
D
C
B
A

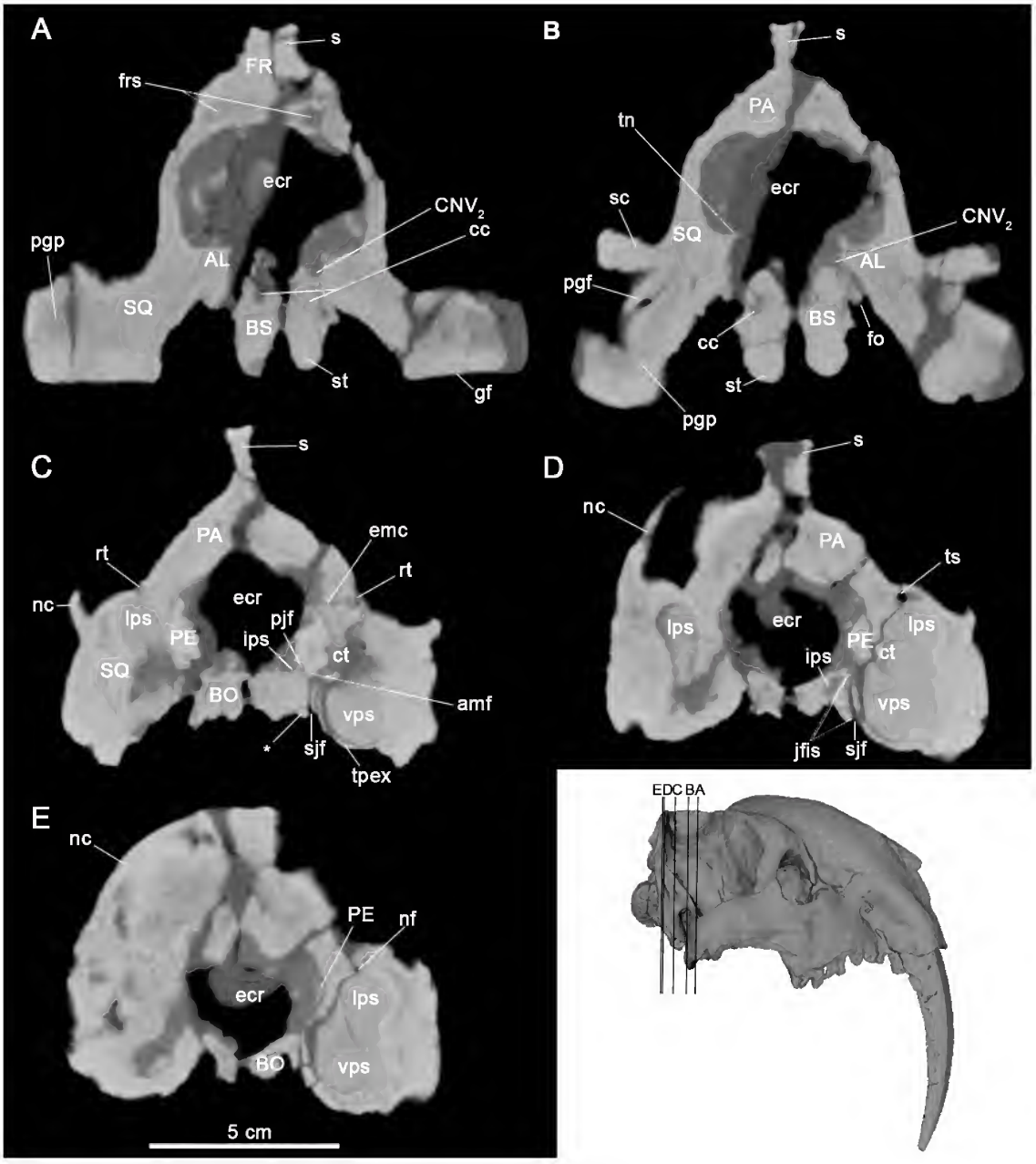
A
s
FR
frs
ecr
CNV2
cc
pgp
AL
SQ
BS
st
gf
B
s
PA
tn
ecr
sc
SQ
CNV2
AL
pgf
BS
fo
cc
st
pgp
C
s
PA
emc
rt
rt
nc
ecr
lps
pjf
PE
ips
ct
SQ
BO
amf
vps
*
sjf
tpex
D
s
nc
PA
ts
lps
ecr
lps
PE
ct
ips
vps
jfis
sjf
E
nc
PE
nf
ecr
lps
BO
vps
5 cm
EDC BA

ear filled with sediment. Nevertheless, in modelling this structure from different perspectives in relation to other otic features we found that it retains its primary orientation, with the preserved part of the crista tympani crossing the ventral part of the element, the incisure facing upward, and the presumed rostral crus facing rostrally. We were able to closely compare this specimen to a detached ectotympanic of *Cladosictis patagonica* (fig. 13). Such features as the crura, crista tympani, and styliform process are closely comparable to their apparent homologs in the latter, justifying the conclusion that the ectotympanic of *Thylacosmilus* was unexpanded and attached to the walls of the tympanic cavity by means of the crural apices (the tips of which were probably broken off during burial). Presumably, the ectotympanic fitted snugly against the medial aspect of the porus, as in the monito del monte (*Dromiciops gliroides*) (Segall, 1969a, see also Sánchez-Villagra and Wible, 2002; Giannini et al., 2004), tree shrews (e.g., *Tupaia* spp.), and lemurs (e.g., *Lemur* spp.) (MacPhee, 1981; Wible, 2009, 2011) whose ectotympanics are somewhat similar in shape and position. In *Thylacosmilus* the element's exact positioning cannot be reconstructed from the evidence at hand. Given its small size and so-called intrabullar or aphaneric position, the ectotympanic could not have made any more than an incidental contribution to meatal walls in *Thylacosmilus*.

The external acoustic meatus of *Thylacosmilus* is a deep funnel (fig. 7C) with a distinctive teardrop shape in lateral view (figs. 3A, 5A, 6). The meatus is rostrally delimited by the entoglenoid region and caudally by the posttympanic process (arising from the caudal tympanic process of the squamosal; appendix 1). The ectotympanic does not participate in this configuration, which is why Patterson (in Riggs, 1934) described it as a "meatus spurius" (in effect, a meatus formed entirely by squamosal material; van der Klaauw, 1931: 138). Turnbull and Segall (1984) noted that the meatal walls converge ventrally to form a deep cleft, corresponding to the glaserian fissure for the passage of chorda tympani (fig. 7A; see Tympanic Floor Composition in the Comparative Set).

In the segmental images we saw nothing unusual in the form of the meatus. However, in the holotype Turnbull and Segall (1984: 252) identified an apparent secondary aperture, in the form of a gap in the meatal wall opening into the "hypotympanic sinus" of the tympanic cavity: "This could have been a direct air channel, bypassing the tympanum, or it could have been membrane-covered and acted as an extension of the tympanum." They did not provide an illustration of this opening in their photographs of the skull, and it cannot be identified on the scanned left side. In any case, on functional and comparative grounds a secondary opening is very unlikely. An opening to the exterior via an accessory "direct air channel" would be the functional equivalent of having a burst eardrum. Even if it were closed off in life by the epithelial lining of the tympanic cavity, the net effect of such an arrangement would probably

FIG. 8. *Thylacosmilus atrox*, holotype, FMNH P14531. **A–E.** Coronal sections through caudal cranium in rostrocaudal order (see inset). Note lengthy course of carotid canal through sphenoidal tubercle (A, B) and great size of total middle ear space (D, E). Abbreviations: **AL,** alisphenoid; **amf,** anteromedial flange; **BO,** basioccipital; **BS,** basisphenoid; **cc,** carotid canal; **CNV_2,** maxillary branch of trigeminal (cranial) nerve; **ct,** tympanic cavity; **ecr,** endocranial cavity; **emc,** emissary canal; **fo,** foramen ovale; **FR,** frontal; **frs,** frontal sinus; **gf,** glenoid fossa; **ips,** inferior petrosal sinus; **jfis,** jugular fissure; **lps,** lateral paratympanic space (= epitympanic sinus); **nc,** nuchal crest; **nf,** nutrient foramen; **PA,** parietal; **PE,** petrosal; **pjf,** primary jugular foramen; **pgf,** postglenoid foramen; **pgp,** postglenoid process of squamosal; **rt,** ramus temporalis; **s,** sagittal crest; **sc,** suprameatal crest; **sjf,** secondary jugular foramen; **SQ,** squamosal; **st,** sphenoidal tubercle; **tn,** tentorium cerebelli (ossified); **tpex,** tympanic process of exoccipital; **ts,** transverse sinus; **vps,** ventral paratympanic space. Asterisk (*) denotes small ridge on lateral margin of basioccipital defining medial wall of jugular fissure. Ramus temporalis connects with both the endocranial cavity (C) and the postglenoid foramen (B).

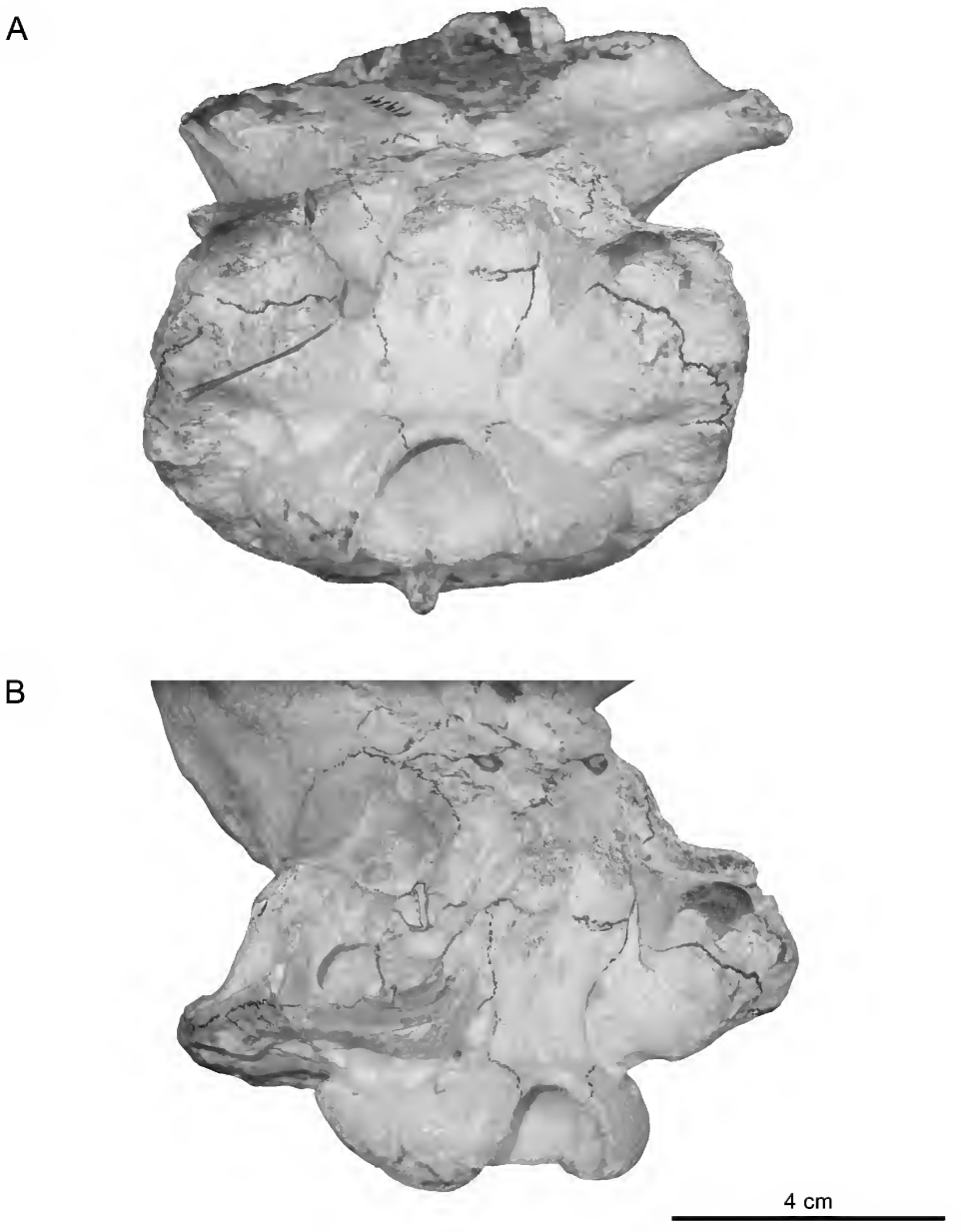

be hearing loss, not gain. The most likely explanation is that the authors misinterpreted the exit aperture of the postglenoid canal, which lies close to and opens within the meatus' rostral wall (transected twice where the bulla was cut away in the paratype; fig. 9A, C: pgc).

We agree from the size of the sphenoid tubercles (figs. 6, 8A, B, 11) that the rostralmost prevertebral neck muscles (longus capitis, rectus capitis ventralis mm.) were greatly enlarged in *Thylacosmilus* (see Turnbull, 1978; Argot, 2004a). The distance from the origins of these muscles to their vertebral insertions would have helped to increase the mechanical advantage of flexion in the cervical vertebrae and therefore the force of the stabbing canines (Wroe et al.,

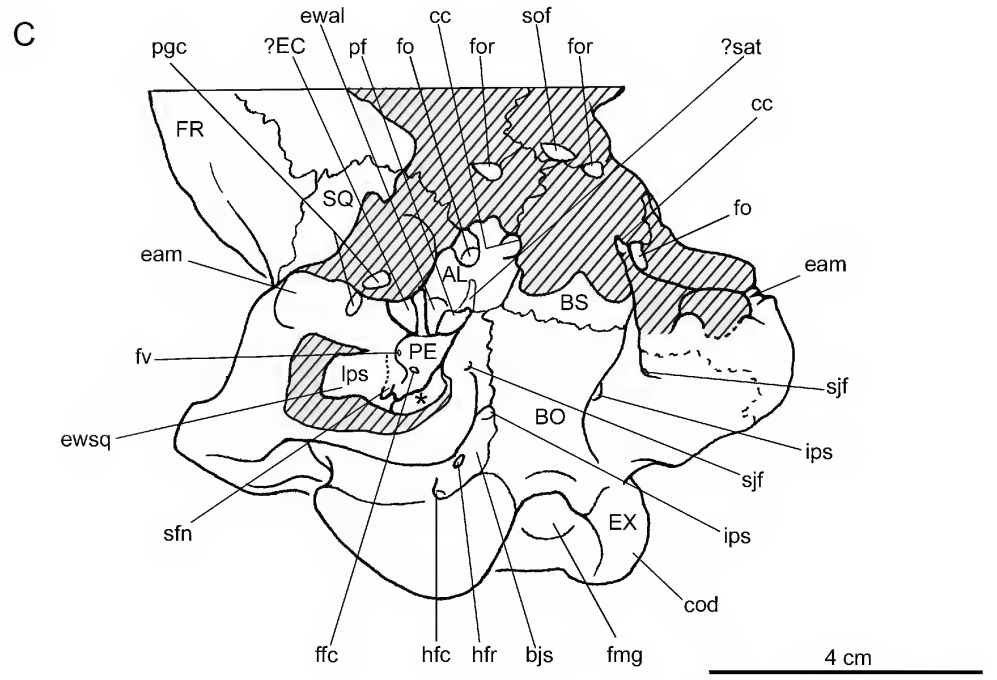

FIG. 9. *Thylacosmilus atrox*, paratype, FMNH P14344, in **A,** oblique ventral and **B,** lateroventral views, with **C,** general key. Note that in A the detached bulla is in its original position. Abbreviations: **AL,** alisphenoid; **bjs,** basijugular sulcus; **BO,** basioccipital; **BS,** basisphenoid; **cc,** carotid canal; **cod,** occipital condyle; **eam,** external acoustic meatus; **?EC,** ?ectotympanic; **ewal,** alisphenoid epitympanic wing; **ewsq,** squamosal epitympanic wing; **EX,** exoccipital; **ffc,** fossula fenestrae cochleae; **fmg,** foramen magnum; **fo,** foramen ovale; **for,** foramen rotundum; **FR,** frontal; **fv,** fenestra vestibuli; **hfc,** caudal hypoglossal foramen; **hfr,** rostral hypoglossal foramen; **ips,** inferior petrosal sinus; **lps,** lateral paratympanic space (= epitympanic sinus); **PE,** petrosal; **pf,** piriform fenestra; **pgc,** postglenoid canal; **?sat,** ?sulcus for the auditory tube; **sfn,** septum for facial nerve; **sjf,** secondary jugular foramen; **sof,** sphenoorbital fissure; **SQ,** squamosal. Dashed line on left bulla marks suture track, the accuracy of which is undetermined. Asterisk (*) indicates unprepared area, within which the primary jugular foramen is located. The canal conducting the internal jugular and cranial nerves through the left bulla to the secondary jugular foramen on the latter's outer wall can be seen in B (broken during removal of right bulla, no longer identifiable on basicranium). Crosshatching indicates damage due to erosion or bullar removal. Arrow indicates the direction to or the position of features hidden by other structures.

2013). Tubercle elongation deepens the central stem significantly as seen in sections (fig. 8A, B). In consequence, the tubercles help to create a lengthy, steep-walled cleft (jugular fissure) between the central stem and the bulla (fig. 8D), positionally equivalent to, but much deeper than, the embryological basicapsular fissure (MacPhee, 1981). The line of the fissure is continued by a small ridge on the lateral margin of the basioccipital, where it nearly abuts the bullar wall (fig. 8C; asterisk). Whether this qualifies as a true tympanic process is moot: the flange may be close to the bullar wall, but it does not actually face onto the middle ear.

Tympanic Floor Composition in the Comparative Set

The usual interpretation of the plesiomorphic metatherian tympanic floor is that it was mem-

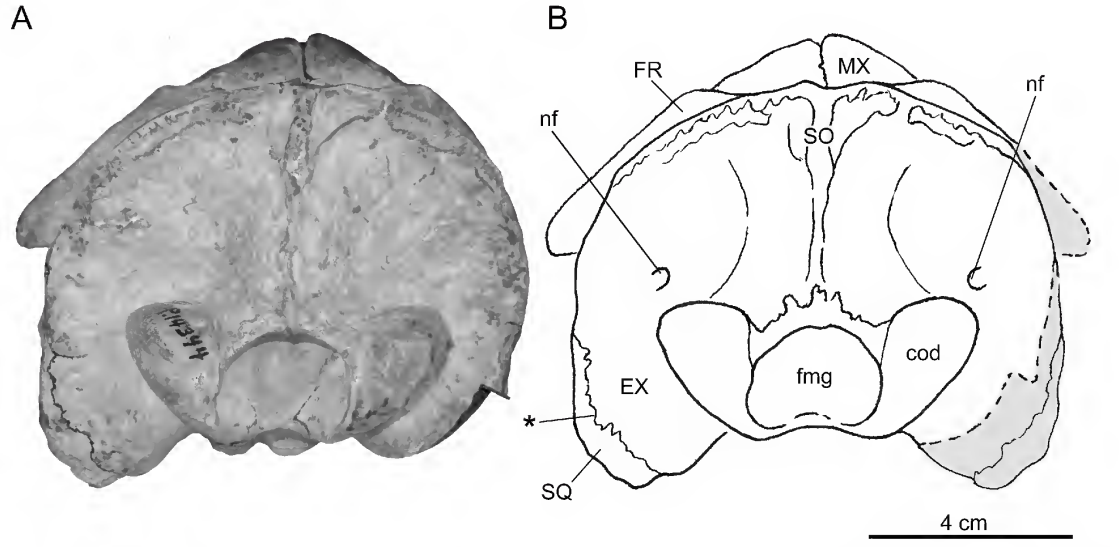

FIG. 10. *Thylacosmilus atrox*, paratype, FMNH P14344, in **A,** caudal view, with **B,** key. Abbreviations: **cod,** occipital condyle; **EX,** exoccipital; **fmg,** foramen magnum; **FR,** frontal; **MX,** maxilla; **nf,** nutrient foramen; **SO,** supraoccipital; **SQ,** squamosal. Asterisk (*) indicates claimed suture between squamosal and exoccipital. Gray areas reconstructed on basis of left side.

branous, lacking any bony contribution other than that provided by the ectotympanic, as in a number of Mesozoic and early Cenozoic nonmarsupial metatherians (e.g., Muizon, 1994, 1998; Marshall and Muizon, 1995; Rougier et al., 1998; Ladevèze and Muizon, 2007; Muizon et al., 2018). Exceptions include *Asiatherium reshetovi*, *Didelphodon vorax*, and herpetotheriids, all of which possessed an alisphenoid tympanic process (Szalay and Trofimov 1996; Horovitz et al., 2008, 2009; Wilson et al., 2016). Presence of the caudal tympanic process of the petrosal can be considered plesiomorphic for both eutherians and metatherians (MacPhee, 1981; Wible, 1984). The presence of entotympanics in marsupials has been claimed several times (e.g., van der Klaauw, 1931; Wood-Jones, 1949; Segall, 1969a,1969b, 1970, 1971; Aplin, 1990; Norris, 1993; Hershkovitz, 1992). However, this structure has never been conclusively demonstrated (e.g., MacPhee, 1979; Reig et al., 1987; Maier, 1989; Sánchez-Villagra and Wible, 2002; Sánchez-Villagra and Forasiepi, 2017). Nevertheless, the possibility deserves further examination (see discussion in Sánchez-Villagra and Forasiepi, 2017).

In extant South American marsupials the composition of the tympanic floor is generally conservative. Apart from the ectotympanic, the only elements involved are tympanic outgrowths of the alisphenoid and petrosal—the latter in the form of the rostral tympanic process of the petrosal only, as seen in didelphids and caenolestids, or both a rostral and a caudal tympanic process of the petrosal as in microbiotheriids (Osgood, 1921; Segall, 1969a, 1969b; 1970; Archer, 1976; Reig et al., 1987; Sánchez-Villagra and Wible, 2002; Voss and Jansa, 2003, 2009; Giannini et al., 2004). In extant Australian marsupials the tympanic floor has a much more variable constitution; e.g., rostral tympanic process of the squamosal in the wombats *Vombatus ursinus* and *Lasiorhinus latifrons* (Wegner, 1964); tympanic process of the exoccipital in the mulgara *Dasycercus cristacauda* (Archer, 1976).

Sparassodonts also differ from the plesiomorphic pattern in the caudal part of the basicranium. In most metatherians (e.g., *Didelphodon*, *Mayulestes*, didelphids, dasyurids; Clemens,

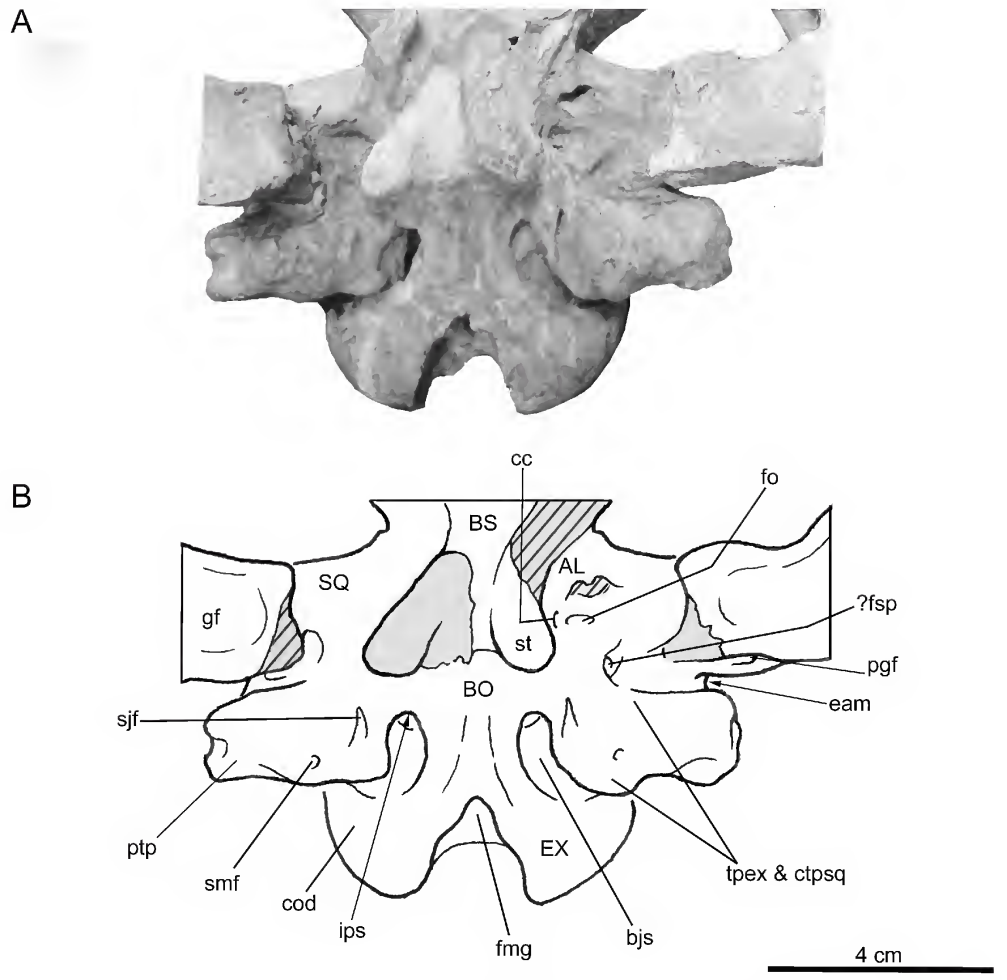

FIG. 11. *Thylacosmilus atrox* MMP 1443-M. **A,** detail of the basicranium, with **B,** key. Abbreviations: **AL,** alisphenoid; **bjs,** basijugular sulcus; **BO,** basioccipital; **BS,** basisphenoid; **cc,** carotid canal; **cod,** occipital condyle; **ctpsq,** caudal tympanic process of squamosal; **eam,** external acoustic meatus; **EX,** exoccipital; **fmg,** foramen magnum; **fo,** foramen ovale; **?fsp,** foramen spinosum; **gf,** glenoid fossa; **ips,** inferior petrosal sinus; **pgf,** postglenoid foramen; **ptp,** posttympanic process of the squamosal; **sjf,** secondary jugular foramen; **smf,** stylomastoid foramen; **SQ,** squamosal; **st,** sphenoidal tubercle; **tpex,** tympanic process of exoccipital. Arrow indicates direction to or position of features hidden by other structures and shading indicates damage or reconstruction.

1966; Reig et al., 1987; Muizon, 1998; Wible, 2003), the occipitals, squamosal, and petrosal consistently bound the walls of the middle ear as seen in caudal view. By contrast, in all sparassodonts that we have examined, this region is exclusively bounded by the squamosal and exoccipital, although the suture separating these bones may be difficult to detect. However, whether they should be considered as tympanic processes is a matter of interpretation. In *Borhyaena* and *Prothylacynus* the projections of the squamosal and exoccipital that caudally border the tympanic cavity per se are functionally related to, and represent continuations of, the nuchal crest for support of musculature of the neck and hyoid. In comparative morphological terms they are more meaningfully identified as posttympanic and paracondylar ("paroccipital")

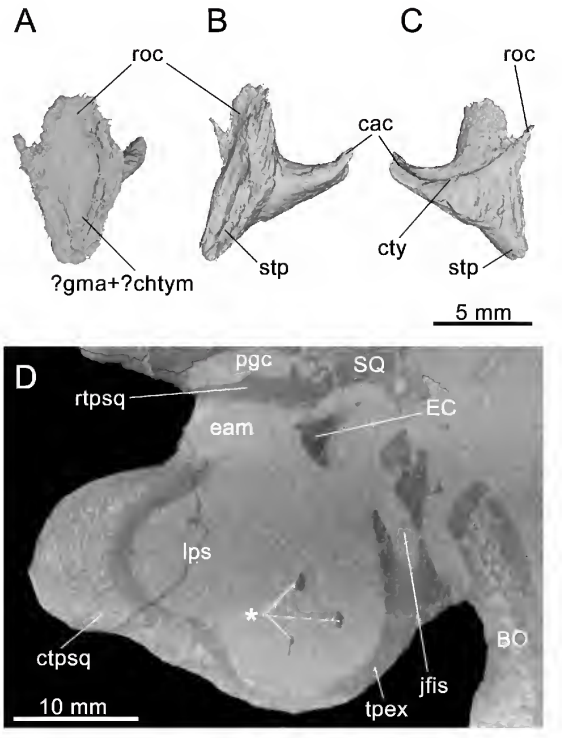

FIG. 12. *Thylacosmilus atrox*, paratype, FMNH P14344. Digital reconstruction of the fragmentary left ectotympanic based on micro-CT data in **A,** rostral, **B,** lateral, and **C,** medial views. **D,** horizontal section of the left middle ear in dorsal view, showing fragments of ectotympanic (asterisk, *). Abbreviations: **BO,** basioccipital; **cac,** caudal crus; **?chtym,** groove for chorda tympani nerve (CNVII); **ctpsq,** caudal tympanic process of squamosal; **cty,** crista tympani; **eam,** external acoustic meatus; **EC,** ectotympanic; **jfis,** jugular fissure; **?gma,** groove for rostral process of malleus; **lps,** lateral paratympanic space (= epitympanic sinus); **pgc,** postglenoid canal; **roc,** rostral crus; **rtpsq,** rostral tympanic process of squamosal; **SQ,** squamosal; **stp,** styliform process (= anterolateral process of ectotympanic); **tpex,** tympanic process of exoccipital.

processes of the squamosal and exoccipital respectively (sensu Evans and Christensen, 1979; see also Wible, 2003, 2009, 2011).

The rostral tympanic process of the petrosal is never conspicuous in Sparassodonta. Although in *Borhyaena* (fig. 20C) and *Prothylacynus* (fig. 15) there are ridges in the expected locations for both rostral and caudal tympanic processes of the petrosal, they are tiny in comparison with skull size. Indeed, the rostral ridge is better interpreted as the margin of the carotid sulcus (on this point, see Muizon et al., 2018).

In all hathliacynids for which there is basicranial evidence, the rostral or rostromedial wall of the bulla is formed by a distinct alisphenoid tympanic process (e.g., *Sipalocyon*, fig. 14 [process broken]), although *Sallacyon* might be an exception (Muizon, 1998; but see also Muizon, 1999). Unlike hathliacynids, which exhibit nearly complete bullae, the borhyaenoid tympanic floor was membranous (apart from the ectotympanic), lacking both an alisphenoid contribution as well as the rostral tympanic process of the squamosal. The only known exception to the unossified tympanic floor among borhyaenoids is *Thylacosmilus*, with its compound squamosal/exoccipital bulla (fig. 6).

In a number of metatherians, Muizon (1994, 1998, 1999; Muizon et al., 1997) has described a fingerlike deviation of the squamoso-alisphenoid

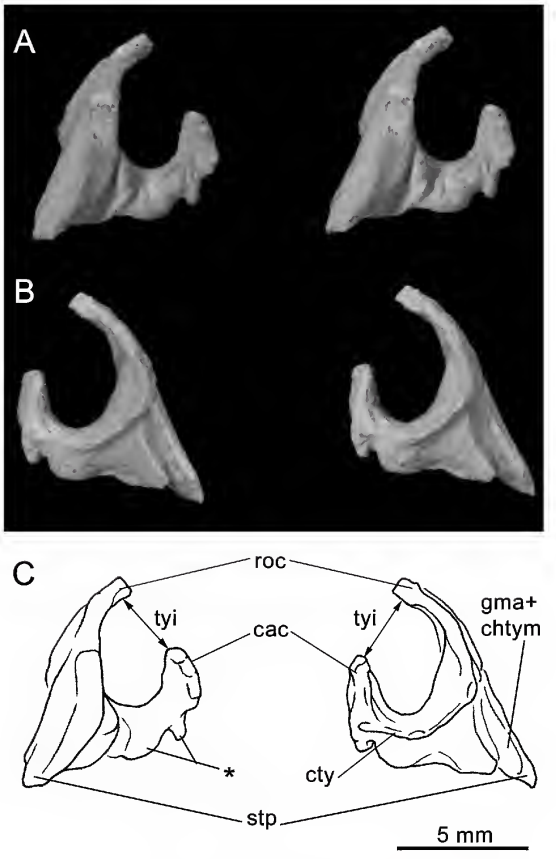

FIG. 13. *Cladosictis patagonica* YPM PU 15170, from locality 15 km south of Coy Inlet, Santa Cruz, Argentina; Santa Cruz Formation, Santacrucian, Early Miocene. Stereo pairs of left ectotympanic in **A,** lateral and **B,** medial views, with **C, D,** keys. Abbreviations: **cac,** caudal crus; **chtym,** groove for chorda tympani nerve (CNVII); **cty,** crista tympani; **gma,** groove for rostral process of malleus; **roc,** rostral crus; **stp,** styliform process (= anterolateral process of the ectotympanic); **tyi,** tympanic incisure. Asterisk (*) indicates tubercles.

suture in the entoglenoid region (his medial process of the squamosal), such that the suture extended toward or even intersected the lateral border of foramen ovale. Utilizing this definition of the medial process of the squamosal, he found this feature in *Pucadelphys*, *Andinodelphys*, *Mayulestes*, and some sparassodonts, including *Sallacyon* (Muizon, 1994: fig. 2B) *Notogale* (Muizon, 1999: fig. 4), and *Cladosictis*, *Sipalocyon*, *Prothylacynus*, *Borhyaena*, and *Paraborhyaena* (Muizon, 1999). The process is also seen in some extant marsupials (vombatiforms; Muizon, 1999). However, we were unable to identify such a projection in either *Prothylacynus* (fig. 15) or *Borhyaena* (fig. 16), and this feature appears also to be absent in *Hondadelphys* and *Arctodictis* (Forasiepi, 2009). In each of these cases, the suture between the squamosal and the alisphenoid lacks any medial deviation toward foramen ovale in the manner described by Muizon. Sutures in this area of the skull are obliterated in the *Thylacosmilus* holotype and MMP 1443-M. If one accepts Turnbull and Segall's (1984) suture line in the paratype, alisphenoid territory bounds the foramen ovale (fig. 4B), and there is no fingerlike deviation of the squamoso-alisphenoid suture. Conditions in other sparassodont specimens examined for this study (e.g., *Cladosictis*,

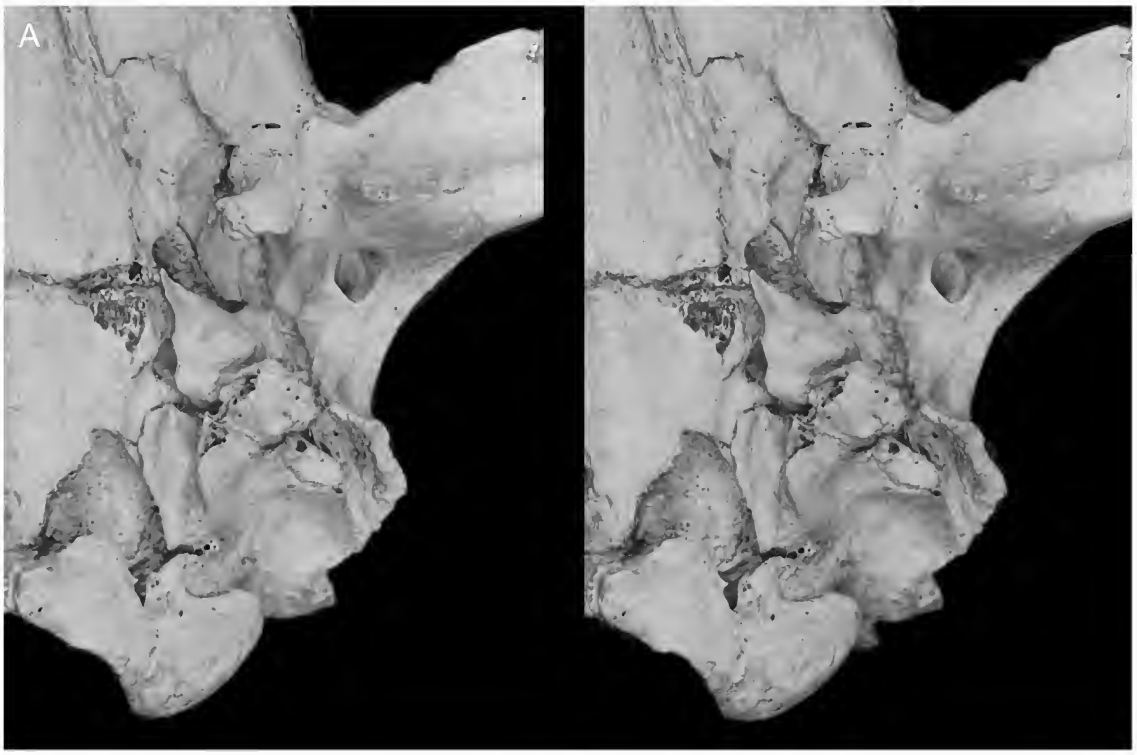
A

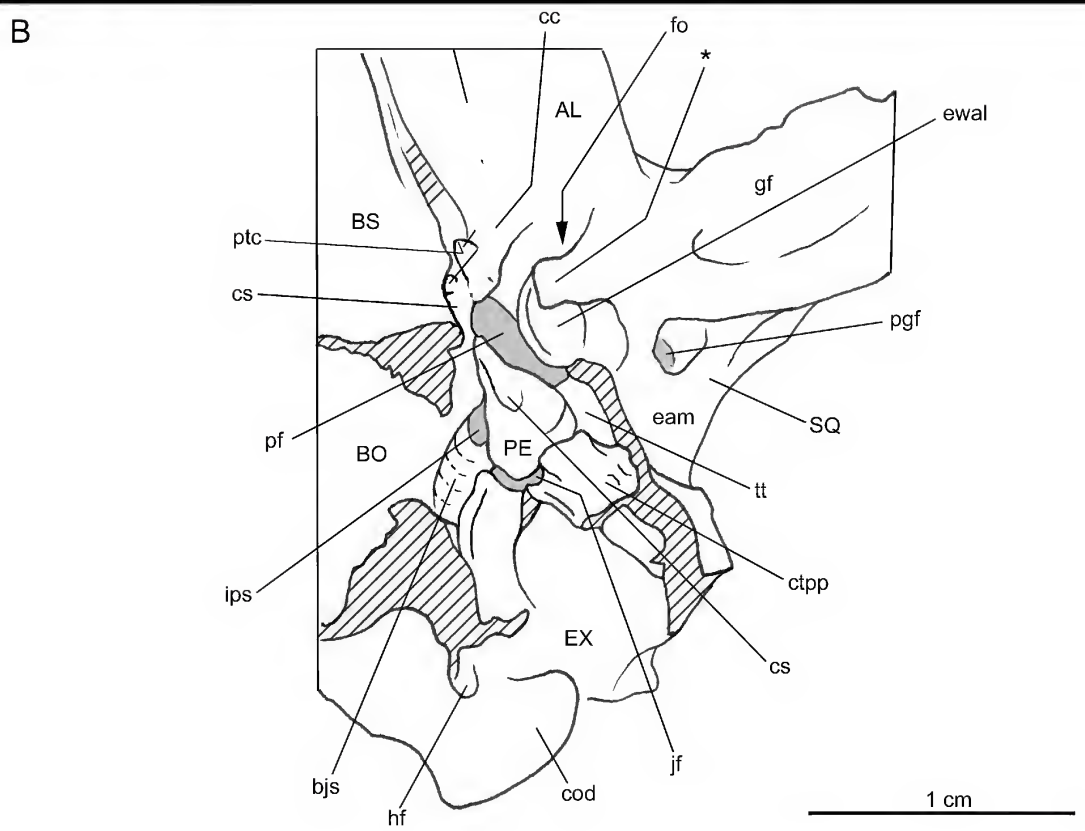
B
cc
fo
*
AL
ewal
gf
BS
ptc
cs
pgf
pf
eam
SQ
BO
PE
tt
ctpp
ips
EX
cs
jf
bjs
hf
cod
1 cm

Sipalocyon) are ambiguous, as sutures in this region are either poorly defined, obliterated, or still covered in matrix. However, if medial deviation of the squamoso-alisphenoid suture is specifically a hathliacynid synapomorphy, its inconstant appearance in other sparassodont clades must reflect separate acquisition, in which case it cannot be regarded as a synapomorphy of the whole order.

More recently, Muizon et al. (2018: 403, char. 185 [1]) redefined the medial process as that part of the squamosal that "extends into the middle ear and forms part of the roof of the hypotympanic sinus" (i.e., tympanic roof, as understood in this paper). In their treatment, character 185(1) is one of three synapomorphies uniquely defining Pucadelphyda. However, it will be interesting to test whether participation of the squamosal in the tympanic roof is actually primitive for metatherians, as it also appears to be for eutherians (MacPhee, 1981).

The ectotympanic is unknown in most borhyaenoids. In *Paraborhyaena boliviana*, Petter and Hoffstetter (1983) described an ectotympanic that is not U-shaped, but is instead mediolaterally expanded into an elongated tube that must have been only lightly attached to the skull, given the absence of a larger bony framework that would have been provided by other floor components. This configuration is remarkably convergent on the ectotympanic of extant *Vombatus* (e.g., Wegner, 1964), which in this taxon assumes the form of a lengthy funnel produced by complete crural fusion along the ectotympanic's axis of elongation. The two taxa differ in that the tympanic floor of *Paraborhyaena* was otherwise not significantly ossified, as it lacked the alisphenoid tympanic process (Muizon, 1999).

Evidence for the ectotympanic in hathliacynids is more abundant. This element is preserved to some extent in a number of specimens (e.g., *Cladosictis patagonica* MLP 11-58, YPM PU 15705, YPM PU 15170, MPM 4326; *Notogale* cf. *mitis* MNHN SAL 271; *Acyon myctoderos* MNHN-Bol-V-003668; see Patterson, 1965; Muizon, 1999; Forasiepi et al., 2006). The following notes are mainly based on *Cladosictis patagonica* YPM PU 15170, the detached right ectotympanic of which is very well preserved (fig. 13). In this species the bulla is incomplete and the ectotympanic is thus only partly enclosed by tympanic processes of the alisphenoid and squamosal. Apparent facets for these processes occur on the ectotympanic crura, suggesting there may have been sutural contact among these bone territories. The rostral crus is longer, wider, and straighter than the caudal crus, a similarity to *Acyon* and apparently *Notogale* (Muizon, 1999; Forasiepi et al., 2006) (fig. 13). The caudal crus exhibits three small tubercles, the rostralmost being largest. The ectotympanics of *Notogale* and *Acyon* are similar in this regard (Muizon, 1999; Forasiepi et al., 2006). The narrow gap (tympanic incisure) between the free ends of the rostral and caudal crura is about 3 mm, representing about half the maximum rostrocaudal length of the bone.

The rostral crus features several shallow grooves, including a longitudinal channel on its medial side that presumably housed the rostral process of the malleus (cf. condition in *Thylacosmilus*; fig. 12A). From the base of the rostral crus a styliform process (van der Klaauw, 1931) juts toward the entoglenoid region of the squamosal, where it entered a small impression that continues forward as a groove. This arrangement marks the position of the glaserian fissure in mammals with

FIG. 14. *Sipalocyon gracilis* AMNH VP 9254, from Felton's Estancia, Santa Cruz, Argentina; Santa Cruz Formation; Santacrucian, Early Miocene. Stereopair in **A,** ventral view, with **B,** key. Abbreviations: **AL,** alisphenoid; **bjs,** basijugular sulcus; **BO,** basioccipital; **BS,** basisphenoid; **cc,** carotid canal; **cod,** occipital condyle; **cs,** carotid sulcus; **ctpp,** caudal tympanic process of petrosal; **eam,** external acoustic meatus; **ewal,** alisphenoid epitympanic wing; **EX,** exoccipital; **fo,** foramen ovale; **gf,** glenoid fossa; **hf,** hypoglossal foramen; **ips,** inferior petrosal sinus; **jf,** jugular foramen; **PE,** petrosal; **ptc,** pterygoid canal (partially broken); **pf,** piriform fenestra; **pgf,** postglenoid foramen; **SQ,** squamosal; **tt,** tegmen tympani. Asterisk (*) indicates bridge of the alisphenoid tympanic process — the anteromedial bullar lamina, following Pavan and Voss (2016) separating primary and secondary oval foramina. Crosshatching indicates damage. Arrow indicates the direction to or the position of features hidden by other structures.

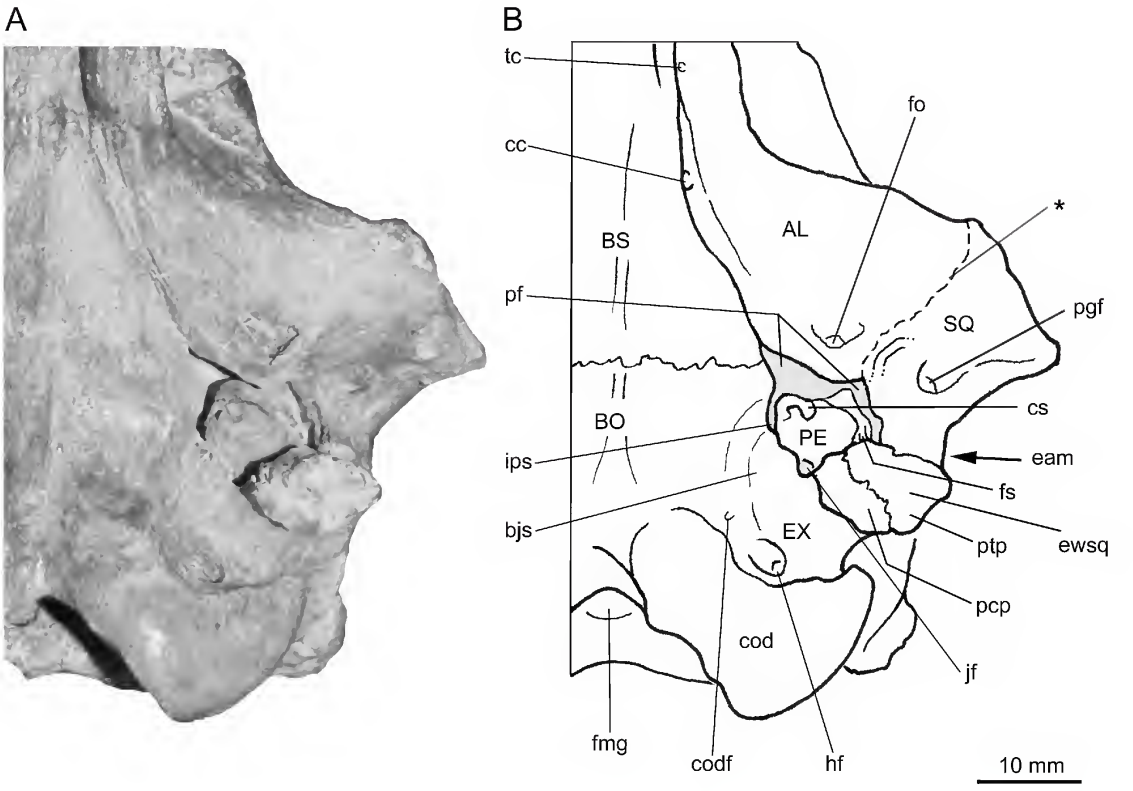

FIG. 15. *Prothylacynus patagonicus* MACN-A 5931 from Corriguen-Kaik, Santa Cruz, Argentina; Santa Cruz Formation; Santacrucian, Early Miocene. Ventral view of **A,** the caudal cranium, with **B,** key. Abbreviations: **AL,** alisphenoid; **bjs,** basijugular sulcus; **BO,** basioccipital; **BS,** basisphenoid; **cc,** carotid canal; **cod,** occipital condyle; **codf,** condyloid foramen; **cs,** carotid sulcus; **eam,** external acoustic meatus; **ewsq,** squamosal epitympanic wing; **EX,** exoccipital; **fmg,** foramen magnum; **fo,** foramen ovale; **fs,** facial sulcus; **hf,** hypoglossal foramen; **ips,** inferior petrosal sinus; **jf,** jugular foramen; **pcp,** paracondylar process; **PE,** petrosal; **pf,** piriform fenestra; **pgf,** postglenoid foramen; **ptp,** posttympanic process; **SQ,** squamosal; **tc,** transverse canal. In this taxon, the more rostral foramen, opening into the basijugular sulcus, is tiny, and it presumably did not carry the hypoglossal nerve. For this reason, we identify it as a strictly venous foramen. Asterisk (*) indicates putative suture between alisphenoid and squamosal. Arrow indicates the direction to or the position of features hidden by other structures.

more complete bullae. It is reasonable to assume that the neurovascular grooves on the ectotympanic and entoglenoid were aligned, and doubtless also accommodated the chorda tympani (CN VII) as it departed the auditory region for the infratemporal fossa to be relayed by the lingual nerve of CN V_3. Similar grooves on the entoglenoid region of the squamosal have been observed in other hathliacynids (Muizon, 1999) and borhyaenoids, including the *Thylacosmilus atrox* holotype and MMP 1443-M, *Prothylacynus patagonicus* MACN-A 5931, and *Borhyaena tuberata* YPM PU 15701. The combination of styliform process and distinct entoglenoid groove has not been observed in the comparative set of living marsupials (e.g., *Didelphis*, *Monodelphis*, *Dasyurus*, *Sarcophilus*, *Vombatus*, *Lasiorhinus*; figs. 17, 18).

Petrosal Morphology

External morphology: Based on the 3-D model of the left petrosal of the paratype illus-

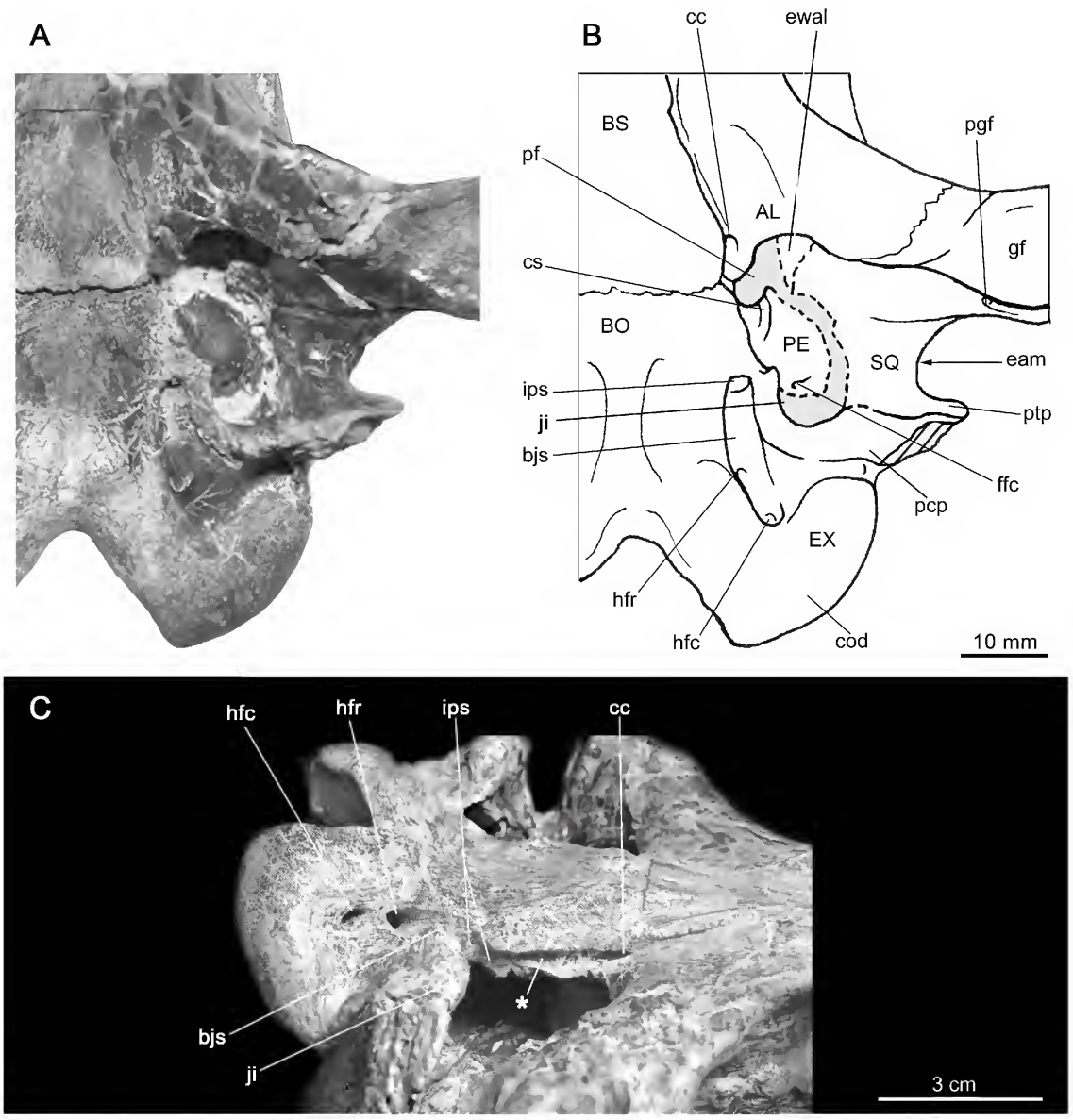

FIG. 16. *Borhyaena tuberata* MPM-PV 3625 from Puesto Estancia La Costa, Santa Cruz, Argentina; Santa Cruz Formation; Santacrucian, Early Miocene. Ventral view of **A,** the caudal cranium, with **B,** key; and MACN-A 5922 (**C**). Abbreviations: **AL,** alisphenoid; **bjs,** basijugular sulcus; **BO,** basioccipital; **BS,** basisphenoid; **cc,** carotid canal; **cod,** occipital condyle; **cs,** carotid sulcus; **eam,** external acoustic meatus; **ewal,** alisphenoid epitympanic wing; **EX,** exoccipital; **ffc,** fossula fenestrae cochleae; **gf,** glenoid fossa; **hfc,** caudal hypoglossal foramen; **hfr,** rostral hypoglossal foramen; **ips,** inferior petrosal sinus; **ji,** jugular incisure; **pcp,** paracondylar process; **PE,** petrosal; **pf,** piriform fenestra; **pgf,** postglenoid foramen; **ptp,** posttympanic process; **SQ,** squamosal. Unusually, in this specimen the caudal aperture of the inferior petrosal sinus is completely ringed by basioccipital bone. More often, the aperture opens in the basicapsular fissure, between the petrosal and basioccipital, in advance of the jugular foramen. Because the roof of the tympanic cavity is incompletely prepared, actual boundaries of the piriform fenestra are unknown. Asterisk (*) indicates groove for medial contact of petrosal. Arrow indicates the direction to or the position of features hidden by other structures.

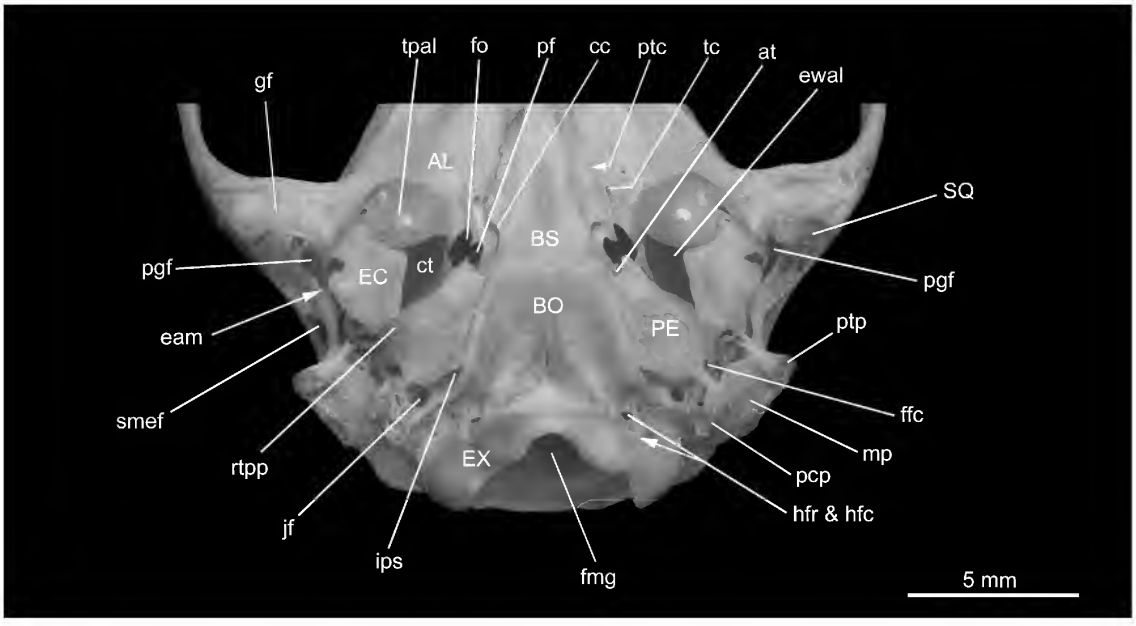

FIG. 17. *Monodelphis domestica* AMNH M 133247. Ventral view of the caudal cranium. Abbreviations: **AL,** alisphenoid; **at,** aperture for auditory tube; **BO,** basioccipital; **BS,** basisphenoid; **cc,** carotid canal; **ct,** tympanic cavity; **eam,** external acoustic meatus; **EC,** ectotympanic; **ewal,** epitympanic wing of alisphenoid; **EX,** exoccipital; **ffc,** fossula fenestrae cochleae; **fmg,** foramen magnum; **fo,** foramen ovale; **gf,** glenoid fossa; **hfc,** caudal hypoglossal foramen; **hfr,** rostral hypoglossal foramen; **ips,** inferior petrosal sinus; **jf,** jugular foramen; **mp,** mastoid process of petrosal; **pcp,** paracondylar process; **PE,** petrosal; **pf,** piriform fenestra; **pgf,** postglenoid foramen; **ptc,** pterygoid canal; **ptp,** posttympanic process; **rtpp,** rostral tympanic process of petrosal; **smef,** suprameatal foramen; **SQ,** squamosal; **tc,** transverse canal; **tpal,** tympanic process of alisphenoid. Arrow indicates the direction to or the position of features hidden by other structures.

trated in figure 19, no part of the petrosal is externally visible, as noted previously; the bone is deeply recessed within the basicranium and making no contribution to the bulla. Microstructural detail in segmental data is consistent with appositional bone having been extensively deposited on both the cochlear and canalicular portions of the petrosal during ontogeny. This has produced some morphological complexity, such as the long, spitlike anteromedial flange on the rostral pole (fig. 19A).

In contrast to most extant marsupials, hathliacynids, and indeed most mammals, the major axis of the petrosal in *Thylacosmilus* is not parallel to the rostrocaudal horizontal plane of the skull but is instead positioned nearly vertically (fig. 8C). This unusual orientation is, however, seen in other borhyaenoids (e.g., *Paraborhyaena*, Petter and Hoffstetter, 1983; *Callistoe*, Babot et al., 2002; *Australohyaena*, Forasiepi et al., 2015; see also Muizon et al., 2018), indicating that it is not correlated with bullar hypertrophy. To avoid confusion our descriptions will utilize conventional directions, as though the petrosal were oriented in a more typical manner.

The 3-D model indicates that, despite damage (fig. 19: asterisks), major features of the petrosal can still be reliably identified. In tympanic view (fig. 19A), the gently rounded promontorium displays neither a rostral process nor any sulci on its ventral surface that might be attributed to the passage of vessels or nerves. The fossula fenestrae cochleae, slightly enlarged by breakage, opens caudomedially while the fenestra vestibuli faces directly caudally. These features are partly bordered by the diminutive caudal tympanic process

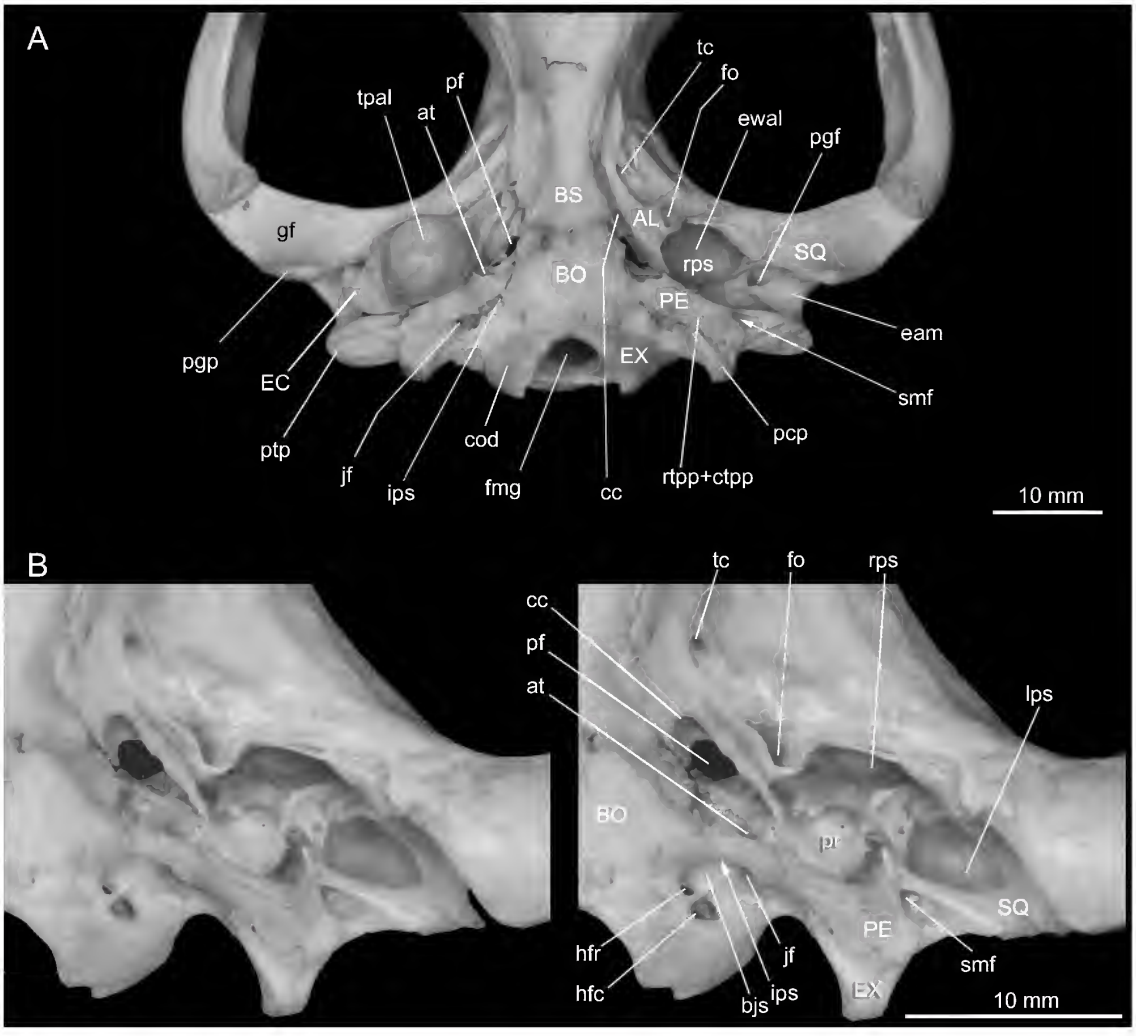

FIG. 18. *Sarcophilus lanarius* AMNH M 65673. Caudal cranium in **A,** ventral and **B,** detailed oblique views. The tympanic floor is formed by the ectotympanic in the meatal area, plus the alisphenoid tympanic process and the rostral and caudal tympanic processes of the petrosal (last two fused into one structure). The exoccipital makes no contribution. Note extratympanic piriform fenestra. Abbreviations: **AL,** alisphenoid; **at,** aperture for auditory tube; **bjs,** basijulugar sulcus; **BO,** basioccipital; **BS,** basisphenoid; **cc,** carotid canal; **cod,** occipital condyle; **ctpp,** caudal tympanic process of petrosal; **eam,** external acoustic meatus; **EC,** ectotympanic; **ewal,** alisphenoid epitympanic wing; **EX,** exoccipital; **fmg,** foramen magnum; **fo,** foramen ovale (represented by its secondary aperture, which is bridged by a projection of the alisphenoid tympanic process—the anteromedial bullar lamina, following Pavan and Voss, 2016); **gf,** glenoid fossa; **hfc,** caudal hypoglossal foramen; **hfr,** rostral hypoglossal foramen; **ips,** inferior petrosal sinus; **jf,** jugular foramen; **lps,** lateral paratympanic space (= epitympanic sinus); **pcp,** paracondylar process; **PE,** petrosal; **pf,** piriform fenestra; **pgf,** postglenoid foramen; **pgp,** postglenoid process; **pr,** promontorium; **ptp,** posttympanic process; **rps,** rostral paratympanic space; **rtpp,** rostral tympanic process of petrosal; **smf,** stylomastoid foramen; **SQ,** squamosal; **tc,** transverse canal; **tpal,** tympanic process of alisphenoid. Arrow indicates the direction to or the position of features hidden by other structures.

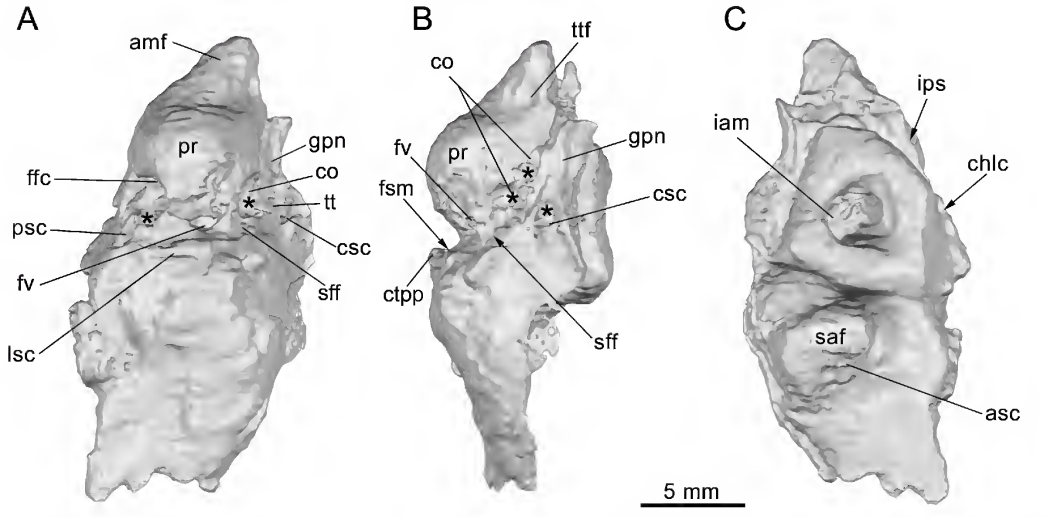

FIG. 19. *Thylacosmilus atrox*, paratype, FMNH P14344. Model of the left petrosal based on 3-D reconstruction from micro-CT data, in **A,** tympanic, **B,** lateral, **C,** and cerebellar views. The petrosal is damaged and the osseous labyrinth is partly exposed. Abbreviations: **amf,** anteromedial flange; **asc,** anterior semicircular canal (exposed by breakage); **chlc,** cochlear canaliculus (= aqueductus cochlearis); **co,** cochlea (exposed by breakage); **csc,** cavum supracochleare (exposed by breakage); **ctpp,** caudal tympanic process of petrosal; **ffc,** fossula fenestrae cochleae (= round window); **fsm,** fossa for stapedius muscle; **fv,** fenestra vestibuli (= oval window); **gpn,** groove for greater petrosal nerve; **iam,** internal acoustic meatus; **ips,** sulcus for inferior petrosal sinus; **lsc,** lateral semicircular canal (exposed by breakage); **pr,** promontorium; **psc,** posterior semicircular canal (exposed by breakage); **saf,** subarcuate fossa; **sff,** secondary facial foramen; **tt,** tegmen tympani; **ttf,** tensor tympani fossa. Asterisk (*) indicates breakage.

(fig. 19B), which also partly borders the fossa for the stapedius muscle. The lateral surface displays a narrow shelf, here regarded as a small tegmen tympani, that is deeply grooved by a sulcus for the greater petrosal nerve. Identification is based on the fact that the groove emanates from the cavum supracochleare, the chamber housing the geniculate ganglion (exposed by breakage; fig. 19A, B). The facial sulcus can be seen emanating from the caudal end of the cavum. Arising from the rostral pole, the anteromedial flange presents a large depression on its lateral surface that we tentatively identify as the fossa for tensor tympani muscle (fig. 19B).

The major features on the cerebellar surface (fig. 19C) are the internal acoustic meatus and subarcuate fossa. Large borhyaenoids are characterized by a very shallow to essentially nonexistent subarcuate fossa (e.g., *Lycopsis*, Marshall, 1977b; *Arctodictis*, Forasiepi, 2009). In comparison to these large borhyaenoids, the subarcuate fossa of *Thylacosmilus* is actually deep, with its greatest diameter at the level of its aperture. The internal acoustic meatus is also deeper than in most other sparassodonts (e.g., *Sipalocyon*, fig. 20A; *Borhyaena*, fig. 20B; but see *Arctodictis*, Forasiepi, 2009). The cochlear canaliculus was identifiable on the petrosal's ventromedial margin, but in the 3-D model the aperture for the endolymphatic duct was not evident (see Internal morphology).

There is no "mastoid" exposure of pars canalicularis in the rear of the skull in *Thylacosmilus*, which is a similarity to several other sparassodonts (e.g., *Sallacyon*, *Notogale*, *Cladosictis*, *Lycopsis*, *Prothylacynus*, *Borhyaena*, *Arctodictis*, *Australohyaena*, *Paraborhyaena*; see Muizon, 1999; Forasiepi, 2009; Forasiepi et al., 2015; Muizon et al., 2018). We tentatively confirm that there is no mastoid exposure in *Sipalocyon*.

Although there is an enlargement of the lateral part of pars canalicularis (fig. 20A: asterisk), the occipital area of the skull is broken and the mastoid exposure cannot be definitely confirmed.

In the scanned specimens of *Thylacosmilus* definite evidence of a prootic canal for the lateral head vein is lacking. However, as noted by Muizon et al. (2018), in *Borhyaena* YPM PU 15120 there is a channel, partly broken, for this vessel (fig. 20C). It is oriented toward the superior border of the petrosal, where it presumably met the prootic sinus in life. There is also an identifiable prootic canal in *Sipalocyon* AMNH VP 9254 (see also Muizon et al., 2018), which is complete. It can be traced from the external lip of the secondary facial foramen to the dorsal surface of the petrosal, where it intersects the large channel for the prootic sinus (fig. 20A).

Lastly, misattributed specimens are a separate category of concern in studies of cranial morphology, as they may affect character analysis of the group to which they have been assigned. A case in point is the isolated petrosal (fig. 20E, F) attributed to the borhyaenoid cf. *Pharsophorus* sp. by Marshall (1978). The specimen has long been associated with a juvenile skull attributed to the genus *Pharsophorus* (AMNH VP 29591), found near but not within the famous Scarritt Pocket (Deseadan) excavated by George Gaylord Simpson. Chaffee (1952: 515), who described the skull, explicitly stated that it was "badly crushed" and "lacking the basicranial region," making it uncertain what the source of the isolated petrosal actually was. It is important to emphasize that this specimen differs from known sparassodont petrosals in several ways, including: (1) tegmen tympani very large, (2) expanded, shelflike medial margin of the petrosal, and (3) ?mastoid exposure on cranial sidewall. The tegmen tympani is characteristically small in marsupials, and often lacks the rostral portion commonly found in placentals (van Kampen, 1905). In marsupials the medial margin of pars cochlearis normally ends flush with the bones comprising the central stem. In the attributed petrosal, this margin is significantly expanded into a shelf (fig. 20E: double asterisks), resembling to some degree petrosal conformation in certain South American native ungulates (see Billet, 2011). Finally, the region caudal to the fossula fenestrae cochleae is smooth surfaced rather than roughened (as would be expected for a sutural surface) and it is punctuated by foramina (fig. 20E: triple asterisks). This combination of features suggests that the isolated petrosal is not that of a sparassodont, but belonged to some other, as yet unidentified, eutherian (possibly but not certainly a South American native ungulate).

Internal morphology: Figure 21A–C presents a 3-D model of the left osseous labyrinth of the paratype, compared to models of *Sipalocyon* AMNH VP 9254 (fig. 21D–F) and *Borhyaena* YPM PU 15120 (fig. 21G–I) in similar orientations. Although there is clearly variation among these taxa, comparative data on the inner ear of sparassodonts is currently too limited for assessment of any systematic or functional significance this variation implies.

In *Thylacosmilus* the maximum length of the canalicular portion is short, at least in relation to the length of the cochlear portion. The cochlea in *Thylacosmilus* displays approximately 2.5 complete turns, comparable to some modern marsupials (e.g., Sánchez-Villagra and Schmelzle, 2007). In nonmarsupial metatherians the cochlea is less coiled (e.g., *Herpetotherium*, 1.6 turns; Horovitz et al., 2008; see also Meng and Fox, 1995). A low number of turns is also seen in Australian marsupials (Sánchez-Villagra and Schmelzle, 2007). In *Sipalocyon* (~2.2; fig. 21E) and in particular *Borhyaena* (~1.9; fig. 21H), the number of cochlear turns is lower. In this latter taxon cochlear coiling is also less compact. The height/length of the anterior semicircular canal is greater than that of the posterior semicircular canal, a feature that has been correlated with a tendency toward upright body posture in a variety of vertebrates (Witmer et al., 2003; Sánchez-Villagra and Schmelzle, 2007). However, there is no basis for making this assumption about body posture in *Thylacosmilus*, whose locomotor adaptations suggest quadrupedalism with some degree of cursoriality (Argot, 2004a, 2004b). The

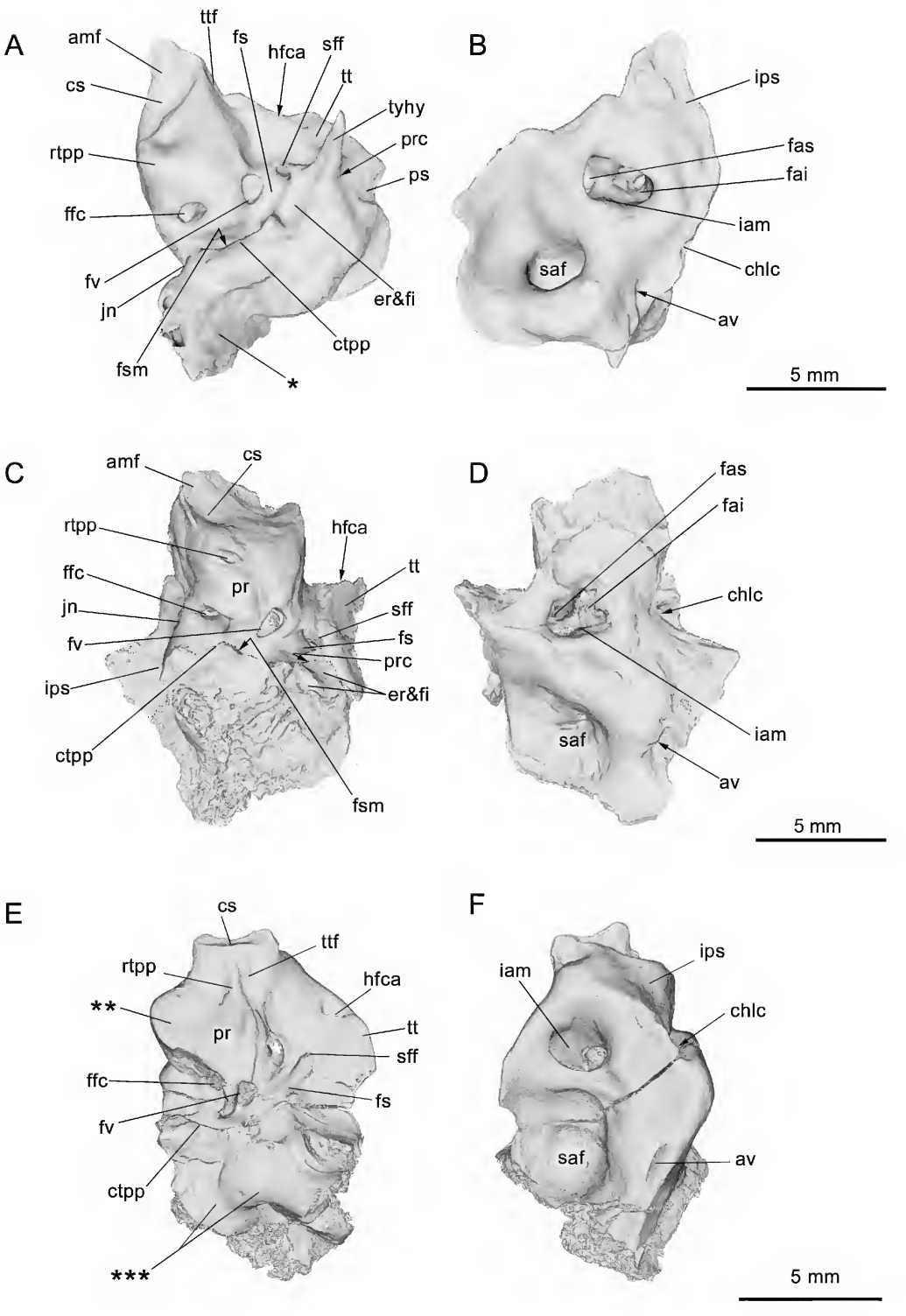
A
amf
ttf
fs
hfca
sff
tt
cs
tyhy
prc
rtpp
ps
ffc
fv
jn
er&fi
ctpp
fsm
*
B
ips
fas
fai
iam
saf
chlc
av
5 mm
C
amf
cs
rtpp
hfca
tt
ffc
pr
jn
sff
fv
fs
prc
ips
er&fi
ctpp
fsm
D
fas
fai
chlc
iam
saf
av
5 mm
E
cs
ttf
rtpp
hfca
**
pr
tt
sff
ffc
fs
fv
ctpp
***
F
ips
iam
chlc
saf
av
5 mm

disproportion seen between the anterior and posterior semicircular canals is much less marked in *Sipalocyon* and *Borhyaena* (fig. 21D, G). The lateral semicircular canal of *Borhyaena* (fig. 21G) displays a curious undulation not seen in the other examined sparassodonts, although it is present in *Vombatus* and *Phascolarctos* (Sánchez-Villagra and Schmelzle, 2007).

The secondary crus commune, formed by the junction of the lateral and posterior semicircular canals at their entry into the vestibule, has been found in a wide variety of extant marsupials (e.g., some didelphids, paucituberculatans, dasyurids, peramelids), as well as some fossil taxa (e.g., *Herpetotherium*, *Mimoperadectes*, *Diprotodon*, *Thylacoleo*, *Palaeothentes*; Sánchez-Villagra and Schmelzle, 2007; Schmelzle et al., 2007; Horovitz et al., 2008, 2009; Alloing-Séguier et al., 2013; Forasiepi et al., 2014). Wide distribution combined with much within-clade variation suggests its presence may be plesiomorphic, perhaps at the level of Mammaliaformes (Ruf et al., 2013). None of the three sparassodonts examined here has a secondary crus commune.

In dorsal view, the length of the lateral semicircular canal in *Thylacosmilus* (fig. 21C) is similar to that of the posterior semicircular canal, as in *Borhyaena* (fig. 21I), while in *Sipalocyon* the posterior semicircular canal is slightly longer (fig. 21F). On the basis of conditions in diprotodontians, Sánchez-Villagra and Schmelzle (2007) hypothesized that in this case equal canal length is correlated with arborealism, the argument being that relative lengthening of the lateral canal increases the sensitivity of equilibration. However, among the sparassodonts examined here, only *Sipalocyon* is considered to have been arboreal or scansorial. The other two taxa are reconstructed as having been exclusively terrestrial (see Argot, 2003a, 2003b; 2004a, 2004b; Ercoli et al., 2012).

Head position in *Thylacosmilus*: For any vertebrate, habitual head posture is an important functional constraint on the kinds of activities that can be efficiently undertaken (Spoor et al., 2007; Coutier et al., 2017). Because of data limitations, head posture in *Thylacosmilus* can be estimated only on the basis of the paratype, which is highly incomplete (fig. 22A–C). As the basisphenoid is badly eroded in this specimen, as a proxy we chose the flattest portion of the basioccipital as seen in a micro-CT segment passing close to the midsagittal plane. Next, we superimposed on this image two points marking the ends of the lateral

FIG. 20. Digital 3-D reconstructions of right petrosal (inverted in figure) of *Sipalocyon gracilis* AMNH VP 9254, collected at La Costa, Santa Cruz, Argentina (Santa Cruz Formation, Santacrucian, Early Miocene), in **A,** tympanic and **B,** cerebellar views. Right petrosal (inverted in figure) of *Borhyaena tuberata* YPM PU 15120, collected 15 kilometers south of Coy Inlet, Santa Cruz, Argentina (Santa Cruz Formation, Santacrucian, Early Miocene), in **C,** tympanic and **D,** cerebellar views. Left petrosal of cf. *Pharsophurus* sp. AMNH VP 29591, collected at Rinconada de la Sierra de Canquel, near Scarritt Pocket, Chubut, Argentina (Sarmiento Formation, Deseadan, Late Oligocene), in **E,** tympanic and **F,** cerebellar views. Abbreviations: **amf,** anteromedial flange; **av,** aqueductus vestibuli; **chlc,** cochlear canaliculus (= aqueductus cochlearis); **cs,** carotid sulcus; **ctpp,** caudal tympanic process of petrosal; **er,** epitympanic recess; **fai,** foramen acusticum inferius; **fas,** foramen acusticum superius; **ffc,** fossula fenestrae cochleae; **fi,** fossa incudis; **fs,** facial sulcus; **fsm,** fossa for stapedius muscle; **fv,** fenestra vestibuli (= oval window); **hfca,** hiatus of facial canal (= hiatus Fallopii); **iam,** internal acoustic meatus; **ips,** sulcus for inferior petrosal sinus; **jn,** jugular notch; **pr,** promontorium; **prc,** prootic canal; **ps,** sulcus for prootic sinus; **rtpp,** rostral tympanic process of petrosal; **saf,** subarcuate fossa; **sff,** secondary facial foramen; **tt,** tegmen tympani; **ttf,** tensor tympani fossa; **tyhy,** tympanohyal. In *Sipalocyon* (A), there is a projection of the lateral part of pars canalicularis (black asterisk, *); however, since the specimen is damaged along the nuchal crest, it is uncertain if the petrosal bone was exposed in occipital view. In cf. *Pharsophurus* (E), white asterisk (*) indicates breakage; black double asterisks (**) identify a shelflike expansion of the petrosal toward the central stem, while triple asterisks (***) indicate a smooth surface, evidently external, that we interpret as the lateral sidewall of the skull. Arrow indicates direction to or position of features hidden by other structures.

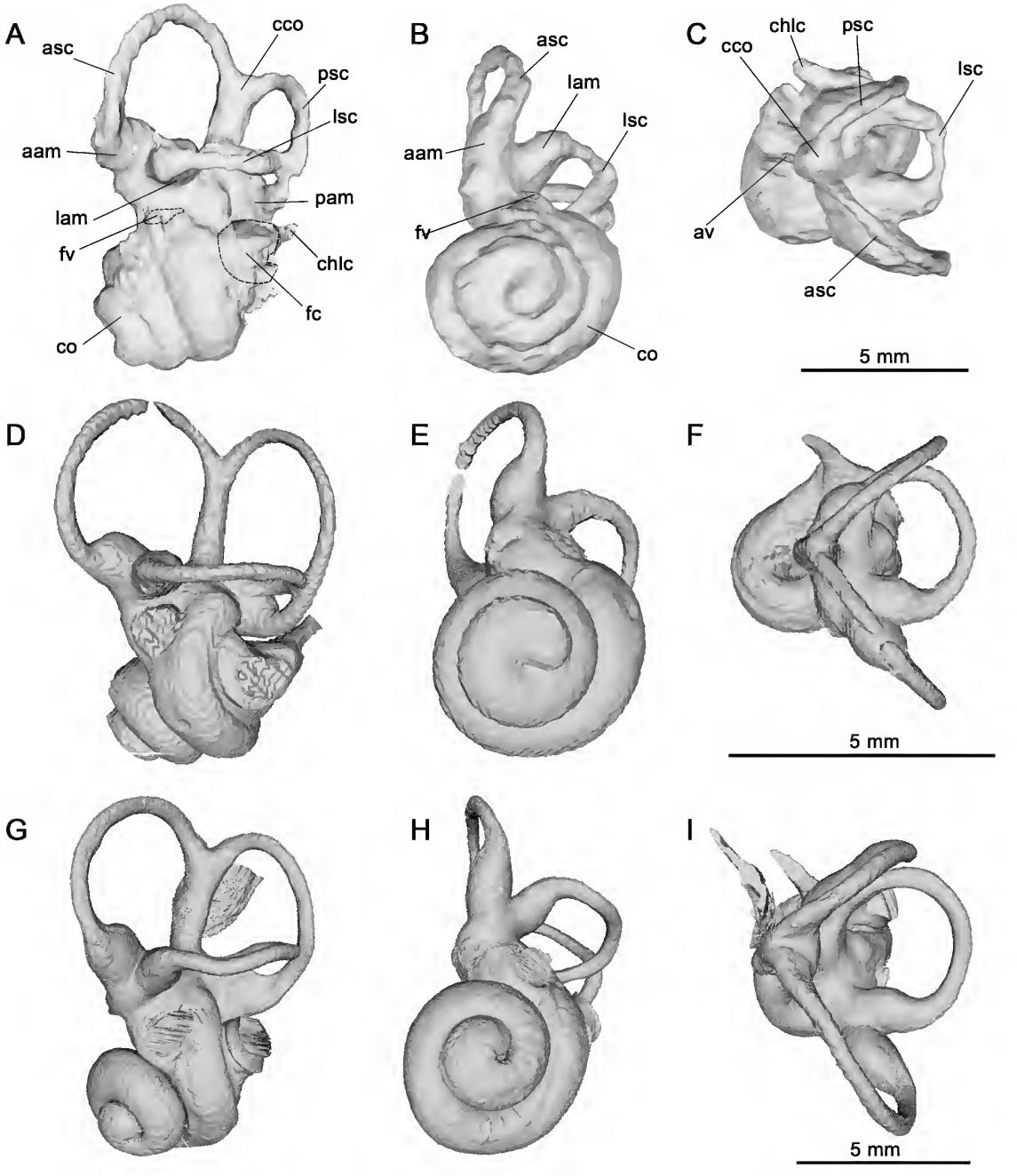

FIG. 21. Digital 3-D reconstructions of the left osseous labyrinth of selected sparassodonts, based on micro-CT data in **A, D, G,** lateral, **B, E, H,** ventral, and **C, F, I,** dorsal views. *Thylacosmilus atrox*, paratype, FMNH P14344 (**A–C**); *Sipalocyon gracilis*, AMNH VP 9254 (**D–F**), and *Borhyaena tuberata*, YPM PU 15120 (**G–I**; right petrosal inverted). Abbeviations: **aam,** anterior ampulla; **asc,** anterior semicircular canal; **av,** aqueductus vestibuli; **cco,** crus commune; **chlc,** cochlear canaliculus (= aqueductus cochlearis); **co,** cochlea; **fc,** fenestra cochleae; **fv,** fenestra vestibuli; **lam,** lateral ampulla; **lsc,** lateral semicircular canal; **pam,** posterior ampulla; **psc,** posterior semicircular canal.

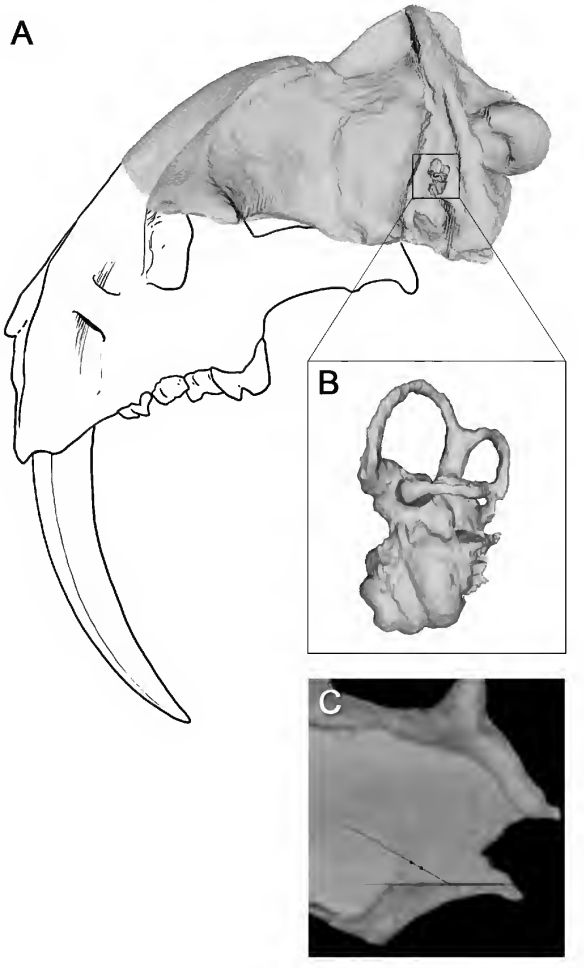

FIG. 22. *Thylacosmilus atrox*, paratype, FMNH P14344, showing the angular relationship between plane of horizontal lateral semicircular canal (LSC) and the floor of the skull following De Beer (1947). **A,** Reconstruction of skull in lateral view oriented with horizontal LSC; **B,** inner ear in lateral view as positioned in the head; and **C,** parasagittal section, illustrating method of measurement (see text).

semicircular canal (fig. 22C). The dihedral angle (30°) formed by lines passed through these points and intersecting the basioccipital planum provides the basis for estimating head posture (De Beer, 1947). To present the result pictorially (fig. 22A), the paratype in lateral aspect was superimposed on a depiction of the holotype in the same aspect, slightly distorted to accommodate the paratype's smaller dimensions. Functionally, the importance of the ability to significantly incline the head, and therewith the snout, is that it maximizes the visual field. This was presumably critical for *Thylacosmilus* as a pursuit carnivore (Argot, 2004a) presumably capable of some degree of binocular vision.

The most serious limitation with our procedure is that the angle between the basioccipital planum and the basisphenoid (which is normally used for head posture estimation) is unknown in the paratype. However, given the form of the planum in *Thylacosmilus* our overall posture estimate is probably close to a minimum.

Tympanic Roof Composition and Middle Ear Pneumatization in *Thylacosmilus* and Comparative Set

The tympanic roof of *Thylacosmilus* is composed of the epitympanic wings of four bones (alisphenoid, squamosal, exoccipital, and petrosal; appendix 1), plus the ventral bulge of the cochlea. Apart from highly autapomorphous *Thylacosmilus*, there is little variation in tympanic roof features in Sparassodonta. This also applies to middle ear pneumatization: most sparassodonts exhibit an uninflated, uncompartmentalized middle ear cavity, whereas *Thylacosmilus* presents the opposite extreme. We have not undertaken a thorough survey of pneumatization in metatherians and therefore restrict ourselves to observations having a direct bearing on the morphological interpretation of *Thylacosmilus* (fig. 23A–C).

There is notable variation in the degree of bullar inflation in the three *Thylacosmilus* specimens described in this contribution (figs. 6, 9, 11). Most of this is probably related to either sex or individual variation. However, one area affected by variable pneumatization has proven difficult to interpret.

Piriform fenestra: The gap in the base of the skull between the auditory capsule and its outgrowths and the epitympanic wings of the alisphenoid and squamosal (= piriform fenestra; appendix 1) seems to have been affected by the degree of pneumatization. In the paratype, the fenestra was excluded from the middle ear cavity (fig. 9B, C). This is harder to establish in the other two specimens because of breakage or incomplete preparation. As far as we can determine, the bullae of the holotype and MMP 1443-M (figs. 6, 11) are more inflated rostromedially than is the case in the paratype, and thus encroach on the fenestra's borders to a greater extent. In most other sparassodonts the piriform fenestra lies external to the tympanic cavity, with some portion of the fenestra remaining patent into adulthood. In some taxa the unossified portion of the tympanic roof is so extensive that the fenestra can be properly said to lie within the definitive middle ear (e.g., *Prothylacynus*, *Borhyaena*; figs. 15, 16). In the specimens of *Thylacosmilus*, the fenestra is best seen on the prepared right side of the paratype (fig. 9B, C), where it is exposed adjacent to the bulla's rostromedial extremity. Probably the only structures that actually passed through, as opposed to across, the fenestra were emissary veins and the greater petrosal nerve (CN VII) traveling from the hiatus of the facial canal to meet the deep petrosal nerve in the pterygoid canal.

Epitympanic wings: The alisphenoid contribution to the roof of the tympanic cavity (= alisphenoid epitympanic wing; appendix 1) is small in *Thylacosmilus*, framing only the lateral margin of the piriform fenestra (fig. 9B, C). The exoccipital epitympanic wing is somewhat larger and is deeply indented by the primary jugular foramen. Largest is the squamosal epitympanic wing, which makes up almost all of the lateral part of the roof except for a zone of uncertain extent adjacent to the lateral aspect of the promontorium. Turnbull and Segall (1984) drew a line across this part of the paratype's right tympanic roof (fig. 9B), which implies that they detected a suture in this position (although they did not specifically mention this in their text). Given its location, the bone areas involved would have to be the squamosal wing just mentioned and the tegmen tympani. However, the area attributable to the tegmen on the basis of suture position is comparatively large, at least for a marsupial, and thus requires confirmation. Conditions in the paratype as revealed by scanning are somewhat unclear because of breakage, but in our 3-D model of the entire petrosal (fig. 19A), the shelf extending from pars canalicularis is much narrower than would be expected on the basis of Turnbull and Segall (1984)'s suture line. Likewise, cross sections (e.g., fig. 7D) indicate that the petrosal is not expanded laterally to any significant extent in this specimen. We conclude that they may have misinterpreted, as a suture line, a break in the sediment that still fills this part of the tympanic roof. In sum, the tegminal portion of the roof could not have been as large as Turnbull and Segall (1984) indicated, although

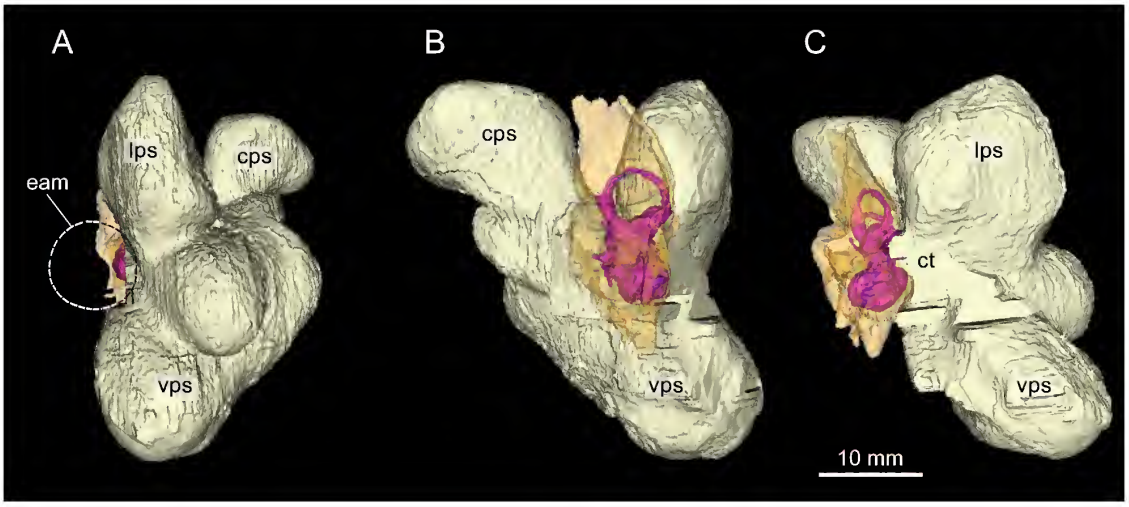

FIG. 23. *Thylacosmilus atrox*, paratype, FMNH P14344. Pneumatization of the left middle ear based on 3-D reconstructions from micro-CT data in **A,** lateral, **B,** medial, and **C,** rostral views. Osseous labyrinth in pink and petrosal shown as semitransparent. Minor evaginations of the ventral paratympanic space not separately identified. Abbreviations: **cps,** caudal paratympanic space; **ct,** tympanic cavity; **eam,** external acoustic meatus; **lps,** lateral paratympanic space (= epitympanic sinus); **vps,** ventral paratympanic space.

it was possibly somewhat larger than the tiny tuberculum tympani usually distinguished in marsupials as the apparent homolog of the placental tegmen tympani (Wible, 2003).

As noted, many sparassodonts have relatively unexpanded middle ear cavities. Although there is little variation in tympanic roof content in terms of contributing elements, their relative sizes and dispositions vary to some extent. Thus, in *Borhyaena* (fig. 16) the roof remained largely membranous due to the failure of the squamosal and alisphenoid to produce epitympanic wings large enough to substantially reduce the size of the piriform fenestra during ontogeny, something also seen in some placentals (e.g., soricids, tenrecoids; MacPhee, 1981). Nor does the petrosal make any significant epitympanic contribution in this borhyaenid (fig. 20C). By contrast, in *Sipalocyon* (fig. 14) the tuberculum tympani/tegmen tympani fills much of the posterolateral part of the roof, whereas in *Notogale*, according to Muizon (1999), the petrosal contribution is even more extensive. In *Arctodictis* (Forasiepi, 2009) the alisphenoid epitympanic wing is effectively absent as such, the body of the alisphenoid merely providing a rostral border for the piriform fenestra. In hathliacynids, however, the alisphenoid epitympanic wing can be quite extensive, as in *Notogale* (Muizon, 1999), where it helps to enclose a large paratympanic space (= "hypotympanic" sinus; van der Klaauw, 1931; see also appendix 1). Clearly, however, the size of the alisphenoid contribution is not solely dependent on the degree to which the middle ear expands rostrally, because the wing in *Thylacosmilus* is tiny despite the overall degree of pneumatization in this taxon.

Paratympanic spaces: Turnbull and Segall (1984: fig. 7A, B) used silicone rubber to produce a cast of the right middle ear of the paratype, but the result as illustrated in their paper is difficult to orient because of the lack of landmarks. They also developed a complicated terminology to describe these spaces, which we will avoid here. Renderings produced from segmental data (fig. 23A–C) give a better idea of how various chambers are situated relative to other structures, such as the faces of the petrosal bone. Any shape differences between these renderings and the Turn-

bull-Segall model are presumably due to the failure of the silicone rubber to completely penetrate certain pockets.

Turnbull and Segall (1984) correctly noted that the greatly enlarged middle ear cavity of *Thylacosmilus* deeply penetrates most of the bones of the caudal cranium, thereby creating a series of continuous but quasidiscrete paratympanic spaces (their "hypotympanic sinus" and its several divisions). In figure 23, the middle ear cavity is oriented in relation to the horizontal plane as indicated by the lateral semicircular canal. This facilitated naming the dilatations of the middle ear cavity according to their relative position in life. The ventral, lateral, and caudal paratympanic spaces are the easiest to define morphologically because they can be delimited by small constrictions and inflations that follow the shape of the bones they invaded. In *Thylacosmilus* the comparatively large volume contained within the middle ear was mostly disposed ventrally and caudally, so that (unlike the case with many mammals with large middle ear cavities) there were no spaces produced by pneumatization of the more dorsal portions of the squamosal or petromastoid. However, the functional result was presumably the same.

The medial end of the external acoustic meatus, which in life would have been closed by the tympanic membrane, is represented by the area above the promontorium in figure 23A (circle), which depicts the model in lateral view. The major diverticula lying ventral to the promontorium are organized along a sharp incline, with the lateral paratympanic space (= epitympanic sinus; see van der Klaauw, 1931) extending above the position of the tympanic cavity per se (fig. 23C). The caudal paratympanic space arches dorsally and caudally, which reflects the fact that this diverticulum hollows out much of the exoccipital almost to the level of the condyles (which are themselves dorsal to the plane of the external acoustic meatus). The relative positioning of major spaces is similar in medial perspective (fig. 23B). The ventral paratympanic space displays some accessory bulges that can be correlated with the unnamed swellings seen on the external bullar surface (fig. 9).

Also noteworthy is the difference in bullar proportions in specimens of *Thylacosmilus*. In MMP 1443-M, the lateral wall of the bulla extends outward much more than it does in the holotype, suggesting a relatively more inflated lateral paratympanic cavity (figs. 6, 11). Like spots on balloons blown up to different degrees, differences in bullar inflation presumably explain the slightly different relative locations of the posttympanic process and the stylomastoid foramen in these specimens.

In living mammals, large tympanic membrane areas and voluminous, compliant middle ear spaces correlate to a significant degree with low frequency audition (Rosowski, 1994), although cochlear architecture of course plays the dominant role (Manoussaki et al., 2008). However, an accurate measure of the size of the tympanic membrane of *Thylacosmilus* is not possible given the fossil material at hand, it is reasonable to infer that the large size of the paratympanic spaces helped to reduce impedance and the transfer of sound energy to the ossicular chain.

Features Related to Nerves and Blood Vessels in *Thylacosmilus* and Comparative Set

Although the anatomical correlates of cranial arteries have been studied by vertebrate paleontologists and morphologists for more than a century (e.g., van Kampen, 1905; Gregory, 1910, 1920; van der Klaauw, 1931), the venous network has been mostly ignored. CT scanning allows an unprecedented opportunity to improve our understanding of vascular morphology in underexamined taxa such as metatherians.

Most of the apertures perforating or crossing the basicranium of *Thylacosmilus* can be plausibly identified by reference to known conditions in extant marsupials. Here we concentrate on

vascular features that have proven difficult to interpret or have been incorrectly identified in other investigations. Channels that are easily and securely identified are depicted in the figures but not otherwise discussed.

Carotid foramen and canal: Turnbull and Segall (1984: 252, fig. 2B) did not indicate or discuss the position of the carotid foramen in *Thylacosmilus*. They noted that in the holotype a "sizeable [foramen lacerum] medium borders the anteromedial end of the [petrosal] at the medial end of the chamber" (Turnbull and Segall, 1984: 262), which is equivalent to the piriform fenestra of this paper. However, they did not attribute any function to the fenestra, which in any case never transmits the internal carotid in metatherians (in contrast to the case in some eutherians; see Discussion).

In fact, there is a true carotid foramen on the basicranium of the holotype of *Thylacosmilus,* but it is located in an incompletely prepared area on the basisphenoid between the hypertrophied sphenoidal tubercle and the medial bullar wall (fig. 6). Segmental data reveal that each carotid foramen opens into a canal that passes through the substance of the ipsilateral sphenoidal tubercle, to meet the canal for the opposite carotid artery at the hypophyseal fossa (fig. 8A). There the vessels presumably joined to form the rostral terminus of the circulus arteriosus. In the holotype the foramen is located slightly more caudally on the basicranium (relative to foramen ovale) than in the paratype or MMP 1443-M, perhaps because of the hypertrophy of canal walls (figs. 9, 11).

We have since identified carotid foramina in all sparassodont taxa that we were able to examine, and indeed its position in this group has never been controversial, with a few exceptions. For example, Patterson (1965; followed by Marshall, 1976b, 1977b, 1978) claimed that the typical carotid foramen was missing in *Cladosictis* YPM 15705. Instead, he identified a "posterior carotid foramen," which, he conjectured, accommodated a branch destined for the circulus arteriosus (see also Basijugular sulcus and inferior petrosal sinus). The basis for his inference stemmed from a dissection of a fresh specimen of *Didelphis marsupialis*, in which he found a "small branch leaving the internal carotid artery at the level of the foramen lacerum posterius [= jugular foramen], passing into the cranial cavity through the posterior carotid foramen and there joining the circle of Willis" (Patterson, 1965: 6). The misidentification of the basicranial aperture of the inferior petrosal sinus as a "posterior carotid foramen" in marsupials goes back at least as far as a note in Gregory's (1910) monograph, because at that time it was widely accepted that two internal carotids, a medial and a lateral, had primitively existed in mammals. At that time there were few comparative data on cephalic veins apart from the internal jugular, and it was assumed that the large port near the jugular foramen must have been for a major artery. This hypothesis has been conclusively refuted on comparative anatomical grounds: there is only one internal carotid in mammals (Presley, 1979; Cartmill and MacPhee, 1980; Wible, 1983). Wible (1984) allowed that Patterson might have seen an unusual anastomosis between the circulus arteriosus and a small branch given off at the carotid furcation, possibly homologous with the ascending pharyngeal artery, but he did not consider it likely.

We have two additional observations to add to Wible's. First, although foraminal positions in *Cladosictis* skulls are often difficult to recognize because of damage or obscuring matrix, in at least a few examples (e.g., MPM 4323, MACN-A 5927, MLP 11-58) the carotid foramen is located precisely where one would expect, that is, along the track of the carotid sulcus rostral to the basioccipital-basisphenoidal synchondrosis (see Discussion). Second, we were unable to identify any arterial vessels within the confines of the channel for the inferior petrosal sinus in serially sectioned pouch young of *Monodelphis* and *Perameles* (figs. 24, 25). This suggests that the distribution of Patterson's vessel among extant marsupials, if it exists, is restricted taxonomically.

A similar case occurs in the evaluation of the cranial vasculature of *Lycopsis* (Marshall, 1977b). Marshall assumed that the internal carotid released a branch within the neck that separately joined the circulus arteriosus via the "bilobate" foramen lacerum posterius (= jugular foramen). Like Patterson, Marshall (1976b, 1978) failed to recognize the inferior petrosal sinus, apparently universally present in marsupials.

A final relevant example is Petter and Hoffstetter's (1983: fig. 4) failure to illustrate or discuss the carotid foramen of *Paraborhyaena* MNHN SAL 5, leaving it uncertain whether or not this taxon possessed this feature at all. However, they did note that a foramen, "qui apparaît ... à faible distance en avant du bord postérieur de l'alisphénoïde, est interprété comme le foramen d'un canal transverse" ["which appears a sight distance in front of the posterior margin of the alisphenoid, is interpreted as the foramen of a transverse canal"]. As depicted by them, this foramen is relatively large compared to the transverse foramina of other sparassodonts, and its position is much more consistent with its being the carotid foramen. The transverse foramen, by contrast, is a variable feature in this group and its absence in *Paraborhyaena* would not be especially remarkable.

Sphenoorbital fissure and foramen rotundum: Turnbull and Segall (1984) thought that the apertures near the front end of the badly eroded skull of the *Thylacosmilus* paratype (figs. 4B, 9) were the optic canals. Scans show that they are instead the remnants of the sphenoorbital fissures (= optic-sphenorbital fissure of Muizon et al., 2018, and optic-orbital foramen of Marshall and Muizon, 1995; Muizon, 1998), which in metatherians transmit not only CN II but also CN III, IV, V_1 and VI, plus the ophthalmic artery and vein. Immediately caudolateral to the sphenoorbital fissure is the foramen rotundum, which transmits CN V_2 (figs. 4B, 9). The foramen rotundum is bilaterally exposed in this specimen because erosion had removed much of the rostral portion of the cranium. A separate foramen rotundum for CN V_2 is the usual case in marsupials (see Voss and Jansa, 2009), and it was present in all sparassodonts examined in which the relevant area was preserved. The sphenoorbital fissure and foramen rotundum are not visible in ventral aspect in the holotype of *Thylacosmilus* because these apertures are hidden by a projecting shelf related to the pterygoids.

?Foramen spinosum: How the stem of the middle meningeal artery was supplied in sparassodonts is uncertain. Since the proximal stapedial is evidently absent in all adult metatherians (Wible, 1990; Wible and Hopson, 1995; Marshall et al., 1995), including sparassodonts, it is reasonable to infer that the meningeal distribution area of the embryonic stapedial ramus superior would have been pirated by other trunks—a frequent occurrence in mammals (Wible, 1987). In the holotype and MMP 1443-M the lateral margin of the foramen ovale bears a small aperture that cannot be attributed to any of the structures that typically pass through or near the glaserian fissure in mammals (chorda tympani, stapedial ramus inferior, lesser petrosal nerve, goniale) (figs. 6, 7A, 11). A comparable aperture could not be discriminated in the segmental data for the paratype, indicating that it may be inconstant. One plausible interpretation of the aperture's function is that it was the equivalent of the foramen spinosum of *Homo*—that is, it transmitted an anastomotic link (ramus anastomoticus) between the middle meningeal and maxillary artery.

Such a link has not been previously identified in metatherians, but its presence would not necessarily be surprising. In therians in which the proximal stapedial artery involutes, the ramus superior and its meningeal area of supply is typically taken over by the maxillary division of the external carotid (Bugge, 1974) or by the arteria diploetica magna (Wible, 1984). Other connections may also occur, although with less frequency (Bugge, 1974). Wible (1984) has shown that in some extant marsupials, the connection between the external carotid and meningeal supply occurs via the postglenoid artery (e.g., *Wallabia rufogrisea*). Further, in a pouch specimen of *Peramales nasuta* he detected a branch of the

maxillary artery that passed through foramen ovale and terminated in the vicinity of the trigeminal ganglion. Although there are no other published observations of this latter vessel in a marsupial, the fact that it terminated morphologically shortly after entering the floor of the cranial cavity is consistent with its supplying tissues in the immediate area, including local meninges. Absence of a separate foramen spinosum occasionally occurs as an anomaly in humans; in such cases the stem of the artery presumably passes through foramen ovale (Standring, 2016). Assuming that this train of inference is correct, then individual variation would have to be invoked to explain the apparent absence of an independent foramen in the paratype. An equivalent to the foramen spinosum was not found in skulls of other sparassodonts available for study.

Transverse canal: No canal for the transverse venous sinus is evident in the holotype, paratype, or MMP 1443-M, which agrees with Riggs' (1934) similar observation. Among sparassodonts, the transverse canal has been reported as present in some taxa (e.g., *Prothylacynus*, Forasiepi, 2009; *Lycopsis*, Marshall, 1977b), but absent in others (e.g., *Borhyaena*, Sinclair, 1906).

Marshall (1977b) identified what he took to be a "remnant of the carotid canal" on the margin of foramen ovale in *Lycopsis* UCMP 38061, as well as a separate "foramen lacerum medium" 13 mm rostromedial to the former. If correctly described, his "carotid canal" on the lip of foramen ovale occurs in other taxa (e.g., *Arctodictis*, Forasiepi, 2009; *Didelphis* AMNH M 95350), but in these metatherians there is also a definite carotid canal in the usual place on the lateral aspect of the basisphenoid. A "rudimentary transverse canal" is mentioned as lying between these apertures in his text, but it is not identified as such in his figure 3. As in the case of *Paraborhyaena*, according to its position and relations Marshall's (1977b) transverse canal is much better interpreted as the true carotid foramen. Finally, Marshall's (1977b: fig. 3C) "foramen lacerum anterium," positioned adjacent to the rostroventral surface of the petrosal, is the piriform fenestra of this paper.

Pterygoid canal: In mammals, blood vessels, nerves, and other elements traveling through the pharyngeal area are forced by space constraints to run in close association. Depending on position and taxon, these associations may include the internal carotid artery and vein(s), artery of the pterygoid canal, deep and greater petrosal nerves, tubal cartilage, and tensor tympani. In marsupials, the passageway for these bundles is often signaled by a prominent set of parallel grooves on the central stem, usually referred to as the carotid sulcus after the largest member of the group. The deep and greater petrosal nerves quickly diverge from other structures to travel thereafter within or along the pterygoid/basisphenoid suture as the nerve of the pterygoid canal, sometimes in company with the similarly named artery (MacPhee, 1981; Wible, 2003). However, these structures are small and related features can be difficult to identify (cf. *Monodelphis*; fig. 17). For example, a caudal aperture for the pterygoid canal could not be identified in the holotype or paratype of *Thylacosmilus*, either externally or in scans. Possibly the carotid canal conducted the nerve of the pterygoid canal partway toward its morphological termination in the sphenopalatine ganglion, but breakage obscures its precise routing.

In *Sipalocyon* AMNH VP 9254 (fig. 14) the carotid canal occupies its usual place, with a large sulcus leading into it. There is, however, a second sulcus, also large, adjacent and parallel to the first, which continues rostrally. Its track resembles that expected for the nerve of the pterygoid canal, although its size suggests it conducted a vessel as well (artery of pterygoid canal, or a large vein?). In other sparassodonts this second sulcus is not in evidence, although this area tends to be poorly preserved in fossils.

Glaserian fissure: As Turnbull and Segall (1984) noted, the glaserian (= tympanosquamosal) fissure in *Thylacosmilus* appears as a lengthy slit between the postglenoid process of the squamosal and the rostral wall of the bulla, which is

also squamosal in origin (fig. 7A). This happens because the ectotympanic is aphaneric in *Thylacosmilus* and therefore does not appear in the bullar wall. Normally, the chorda tympani and related structures escape the middle ear between the rostral crus of the ectotympanic and the squamosal (see Tympanic Floor Composition in Comparative Set).

Foramen ovale: Riggs (1934: fig. 1) inverted the leaders identifying foramen ovale and carotid foramen in the illustration of the paratype of *Thylacosmilus*; his foramen caroticum is actually foramen ovale, and conversely. The foramen ovale appears to lie wholly within the alisphenoid and is essentially coplanar with the rest of the basicranium. It does not form the kind of short, anterolaterally directed canal formed by outgrowths of the alisphenoid tympanic process (= anteromedial bullar lamina; Pavan and Voss, 2016) seen in some marsupials (e.g., *Didelphis*), and whose exit from the skull base is sometimes distinguished as the secondary foramen ovale. (See Gaudin et al., 1996; Voss and Jansa, 2003, 2009, for additional remarks on this latter feature.)

In undamaged hathliacynid material, the foramen ovale lies entirely within the alisphenoid (e.g., *Cladosictis*, *Sipalocyon*, *Notogale*, *Acyon*; see Muizon, 1999; Forasiepi et al., 2006; Forasiepi, 2009), enclosed by outgrowths from the alisphenoid tympanic process, and thus interpreted as the secondary foramen ovale. Borhyaenids (*Borhyaena*, *Arctodictis*) and proborhyaenids (*Callistoe*) differ in that the foramen is simply a notch (incisura ovalis) that opens into the piriform fenestra between the alisphenoid and the petrosal (and not the ectotympanic; contra Sinclair, 1906: 349). The stem borhyaenid *Prothylacynus* differs slightly in that the foramen ovale opens within the alisphenoid (fig. 15). For completeness we note that there is a rod of bone defining, or at least circumscribing, a bony foramen ovale. The rod does not, however, qualify as a component of the alisphenoid tympanic process (such as the anteromedial bullar lamina) because it does not participate in bounding the middle ear cavity (fig. 15) and thus we do not distinguish the aperture as a secondary foramen ovale.

In *Monodelphis*, the foramen ovale and the piriform fenestra are confluent (fig. 17; cf. Wible, 2003). Also, large veins, presumably homologous with the emissary plexus of the foramen ovale found in *Homo* (Mortazavi et al., 2012), pass through this joint aperture and drain to the maxillary vein (fig. 24A, B). Although there are no morphological indicators of the presence of this plexus in *Thylacosmilus*, the foramen ovale is probably a frequent port for cephalic drainage in metatherians (cf. Archer, 1976), just as it is known to be in the few extant eutherians (e.g., horse; Ellenberger and Baum, 1894; Sisson and Grossman, 1953).

In sum, in the therian embryo, the potential space between the ala temporalis and the auditory capsule is eventually subdivided by the growth of sheets of bone, principally the alisphenoid but also the petrosal and sometimes the squamosal (see fig. 27). Typically, gaps of various sizes remain; smaller ones by convention are named foramina, but there is often a relatively large dehiscence that may persist into the adult stage between the petrosal and alisphenoid. If there is little ossification of this part of the tympanic roof, as in extant perissodactyls, some afrosoricoids, and many lipotyphlans (MacPhee, 1981), the mandibular branch of the trigeminal nerve (CN V_3), greater petrosal nerve (part of CN VII), internal carotid and veins (if present; see Discussion) may pass through membrane rather than separate, bony foramina. Whether the mandibular nerve passes through a "complete" or "incomplete" bony foramen ovale will depend on the competitive growth rates of the leading edges of the alisphenoid and petrosal.

Canal x: A small aperture opens on the rostral lip of the left foramen ovale in the holotype, but it is absent on the right side. A similarly located and variable feature was detected by Muizon (1999) in *Notogale* MNHN SAL 271 and by Forasiepi (2009) in *Borhyaena* MACN-A 5922 and *Arctodictis* MLP 85-VII-3-1. Marshall (1977b) mentioned (but did not illustrate) the existence of

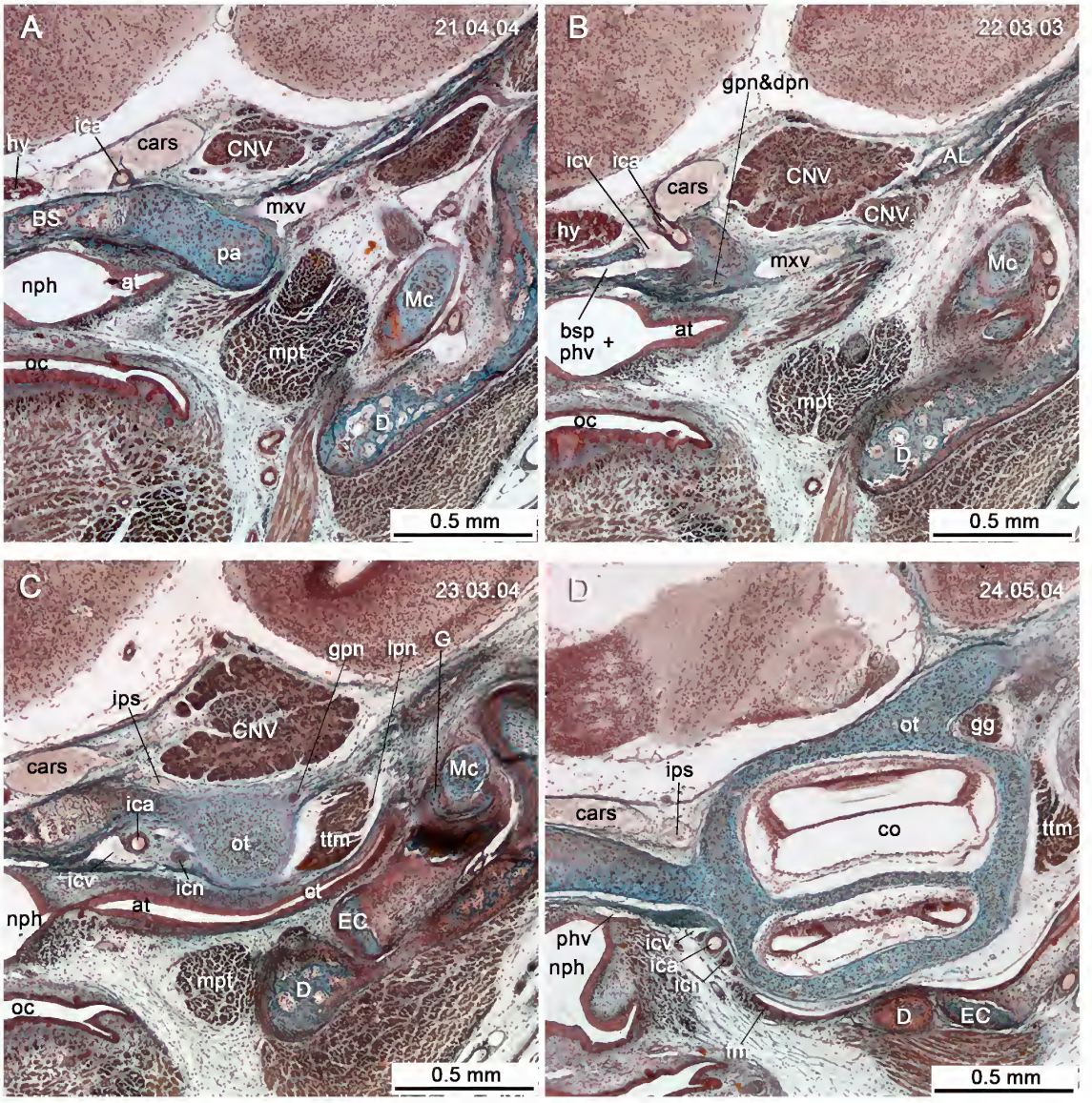

FIG. 24. *Monodelphis domestica* (DUCEC), pouch young, coronal sections through the auditory region. In **A–C**, the internal carotid artery is seen passing into the endocranium in company with the internal carotid vein. Also indicated is the formation of the nerve of the pterygoid canal by the conjunction of the greater petrosal and deep petrosal nerves. In **D,** note position of the inferior petrosal sinus, situated intracranially adjacent to the central stem and otic capsule. Abbreviations: **AL,** alisphenoid; **at,** auditory tube; **BS,** basisphenoid; **bsp,** basilar plexus; **cars,** cavernous sinus; **CNV,** trigeminal (cranial) nerve; **CNV$_3$,** mandibular branch of trigeminal (cranial) nerve; **co,** cochlear duct; **ct,** tympanic cavity; **D,** dentary; **dpn,** deep petrosal nerve (icn fibers passing out of tympanic plexus); **EC,** ectotympanic; **fm,** fibrous membrane of tympanic cavity; **G,** gonial; **gg,** geniculate ganglion (CNVII); **gpn,** greater petrosal nerve (CNVII); **hy,** hypophysis; **ica,** internal carotid artery; **icn,** internal carotid nerve (to tympanic plexus); **icv,** internal carotid vein; **ips,** inferior petrosal sinus; **lpn,** lesser petrosal nerve (CNIX); **Mc,** Meckel's cartilage; **mpt,** medial pterygoid muscle; **mxv,** maxillary vein; **nph,** nasopharynx; **oc,** oral cavity; **ot,** otic capsule; **pa,** processus alaris; **phv,** pharyngeal venous plexus; **ttm,** tensor tympani muscle. Histological serial section number indicated at top left. Numbers ascend in caudal direction.

a tiny hole in approximately the same position in *Lycopsis* UCMP 38061 (see Transverse canal) and we have seen it in *Didelphis* AMNH M 95350 as well. We identify it here as canal x.

In the case of *Notogale*, Muizon (1999: 490) called this feature the "lateral opening of the canal entovale," and described it as a conduit between the carotid canal and foramen ovale. He thought that a small branch of the internal carotid might have passed along it. Although this possibility cannot be discounted, we regard it as unlikely. It cannot be the artery of the pterygoid canal, since canal x is directed away from, rather than toward, the position of the pterygopalatine ganglion. It is more probable that this channel transmitted a vein, the likeliest candidate for which is the sphenoidal (or Vesalian) emissary vein. In *Homo*, this vessel passes through an inconstant foramen (canaliculus sphenoidalis) on the medial side of the foramen ovale, to connect the cavernous sinus with the pterygoid plexus at the base of the skull (Mortazavi et al., 2012). It is likely present in many other mammals.

Sulcus and aperture for auditory tube: Turnbull and Segall (1984: 262) identified on the paratype a "depressed area on the caudomedial side of the squamosal and the medial side of the [ecto]tympanic" as the probable site of the auditory tube's passage toward the middle ear. This description appears to apply to a small groove on the ventral surface of the basicranium that lies in advance of the carotid foramen and is directed toward the rostromedial quadrant of the bulla (figs. 6, 9). Although features like this one are frequently attributed to the passage of the auditory tube, as an endothelial pharyngeal structure the tube is unlikely to leave a bony impression. The cartilage associated with the tube is a better candidate, but that structure is formed in most living marsupials by dense connective tissue (e.g., Maier et al., 1996). In a few known examples (e.g., *Tarsipes* and *Dromiciops*) cartilaginous or precartilagenous tissue is in fact present (see Aplin, 1990; Sánchez-Villagra, 1998; Sánchez-Villagra and Forasiepi, 2017, and references herein; see also fig. 24). For the most part, any sulci grooving bones immediately rostromedial to the auditory region are much more likely to relate to vascular structures and nerves, but since we cannot offer a definitive explanation for the function of this particular feature in *Thylacosmilus*, we simply designate it as "?sulcus for auditory tube" (?sat).

Postglenoid foramen and suprameatal foramen: In a table comparing *Thylacosmilus* to several Santacrucian borhyaenids, Riggs (1934: 29) stated that there was a foramen in the former that "perforates the squamosal within the external acoustic meatus, external foramen not in evidence." He contrasted this with the condition in Santacrucian taxa in which a "large vascular foramen perforates the squamosal above the opening of auditory meatus," a feature lacking in *Thylacosmilus*. These statements refer to two different vascular structures, although the two are related as venous sinuses. The postglenoid foramen is clearly present as an elongated canal in all specimens of *Thylacosmilus* (e.g., fig. 9). Contra Riggs (1934), its outlet is situated within the confines of the meatus. The suprameatal foramen (= subsquamosal foramen sensu Archer, 1976; Pavan and Voss, 2016) is situated in the roof of the meatus as defined by the suprameatal crest in *Didelphis, Monodelphis,* and many other marsupials. It carries a temporal branch of the postglenoid artery and vein to the temporal fossa (for discussion of homologies, see Wible, 2003). Although, as Riggs (1934) noted, *Thylacosmilus* lacks a suprameatal foramen, this aperture's functional role would presumably have been taken up by one of the canals for rami temporales (figs. 3–5). Thus, the ramus canal identified in figure 8C, D communicates with both the endocranium and the postglenoid foramen, implying that meningeal venous return would have joined with that from the sphenoparietal emissary vein (= postglenoid vein) (Wible, 2003; see also fig 25A, B). This arrangement is also seen in well-studied placentals (e.g., horse; Ellenberger and Baum, 1894), and it may well be a therian plesiomorphy.

Primary and secondary jugular foramen: A remarkable feature of the basicranium of

Thylacosmilus is that the primary jugular foramen—the aperture through which the internal jugular vein and several cranial nerves (CN IX, X, and XI) depart the endocranium for the upper neck—is not externally visible. The jugular foramen, as seen on the medial aspect of the bulla, is actually secondary; after leaving the primary foramen the neurovascular bundle had to then pass through the medial bullar wall in order to depart the skull (fig. 8D). This extended routing was presumably a consequence of the greatly expanded exoccipital tympanic process growing over structures, such as the petrooccipital suture, that would normally lie outside the middle ear. Other sparassodonts, which lack a complex bulla, do not express a secondary jugular foramen like that of *Thylacosmilus* (e.g., *Sipalocyon*, *Cladosictis*, *Prothylacynus*; figs. 14, 15). The relatively small width of the jugular passageway has implications for venous drainage in *Thylacosmilus* and possibly other sparassodonts (see Basijugular sulcus and Inferior petrosal sinus).

Stylomastoid foramen and septum for facial nerve: The stylomastoid foramen is situated relatively caudoventrally, at the level of the ventral border of the external acoustic meatus and caudal to the level of the posttympanic process (fig. 6). How the hyoid apparatus articulated with the basicranium is unclear because there is no pit marking the location of the tympanohyal articulation.

On the dissected right side of the paratype, a low septum protrudes from the internal bullar wall opposite the position of the stylomastoid foramen. Originally this would have been continuous with the partial septum on the petrosal (fig. 9C: sfn), which conducted the facial nerve from the secondary facial foramen. The septum is presumably a pneumatization-related feature, and thus is absent in other sparassodonts with less inflated or nonexistent bullae. In *Thylacosmilus*, the septum for the facial nerve serves to morphologically separate the caudal and lateral paratympanic spaces.

Hypoglossal foramina (rostral and caudal): Based on comparisons with living marsupials (e.g., Archer, 1976; Wible, 1990, 2003), we infer that the two large apertures located immediately rostral to the occipital condyles in *Thylacosmilus* carried separate portions of the hypoglossal nerve (fig. 9B, C). These ports were identified as "precondylar foramina" by Riggs (1934) and Turnbull and Segall (1984). In light of our reconstruction of venous networks in this part of the caudal cranium (see Basijugular sulcus and inferior petrosal sinus), we infer that they also carried emissary veins, evidently of large size.

In *Homo*, the fibers forming CN XII pass through the single hypoglossal foramen as two semidiscrete, dura-lined bundles, which then rejoin in the upper neck to form a single trunk. These bundles are occasionally separated by a narrow spicule of bone within the foramen, but completely separate foramina are rare in humans (Standring, 2016) and probably most other placentals. By contrast, metatherians commonly display two foramina, which are sometimes differentiated as condyloid rather than hypoglossal foramina (or as "hypoglossal and accessory foramina"; Sinclair, 1906). Wible (2003) mentioned that in sectioned specimens of *Monodelphis*, *Dasyurus*, and *Didelphis,* these foramina regularly transmit separate bundles of hypoglossal fibers, thus confirming their suspected function. These ports are here distinguished as rostral and caudal hypoglossal foramina. We confirm by means of sectioned fetuses that the same dual bundle-foramina arrangement occurs also in *Dromiciops* (Sánchez-Villagra and Forasiepi, 2017) and *Perameles* (fig. 25C, D). Since this configuration frequently occurs in extant marsupials, it is reasonable to assume that nonmarsupial metatherians varied in the same way. *Hondadelphys*, hathliacynids, and some borhyaenoids (e.g., *Prothylacynus* and *Lycopsis*: figs. 15, 26B), have a single hypoglossal foramen, whereas two foramina are found in *Pucadelphys*, *Mayulestes*, Borhyaenidae, *Paraborhyaena*, and *Thylacosmilus* (Marshall and Muizon, 1995; Muizon, 1998; Horovitz and Sánchez-Villagra, 2003; Babot, 2005; this paper). In the case of *Paraborhyaena*, Petter and Hofstetter (1983) interpreted the more caudal and larger aperture as the condylar fora-

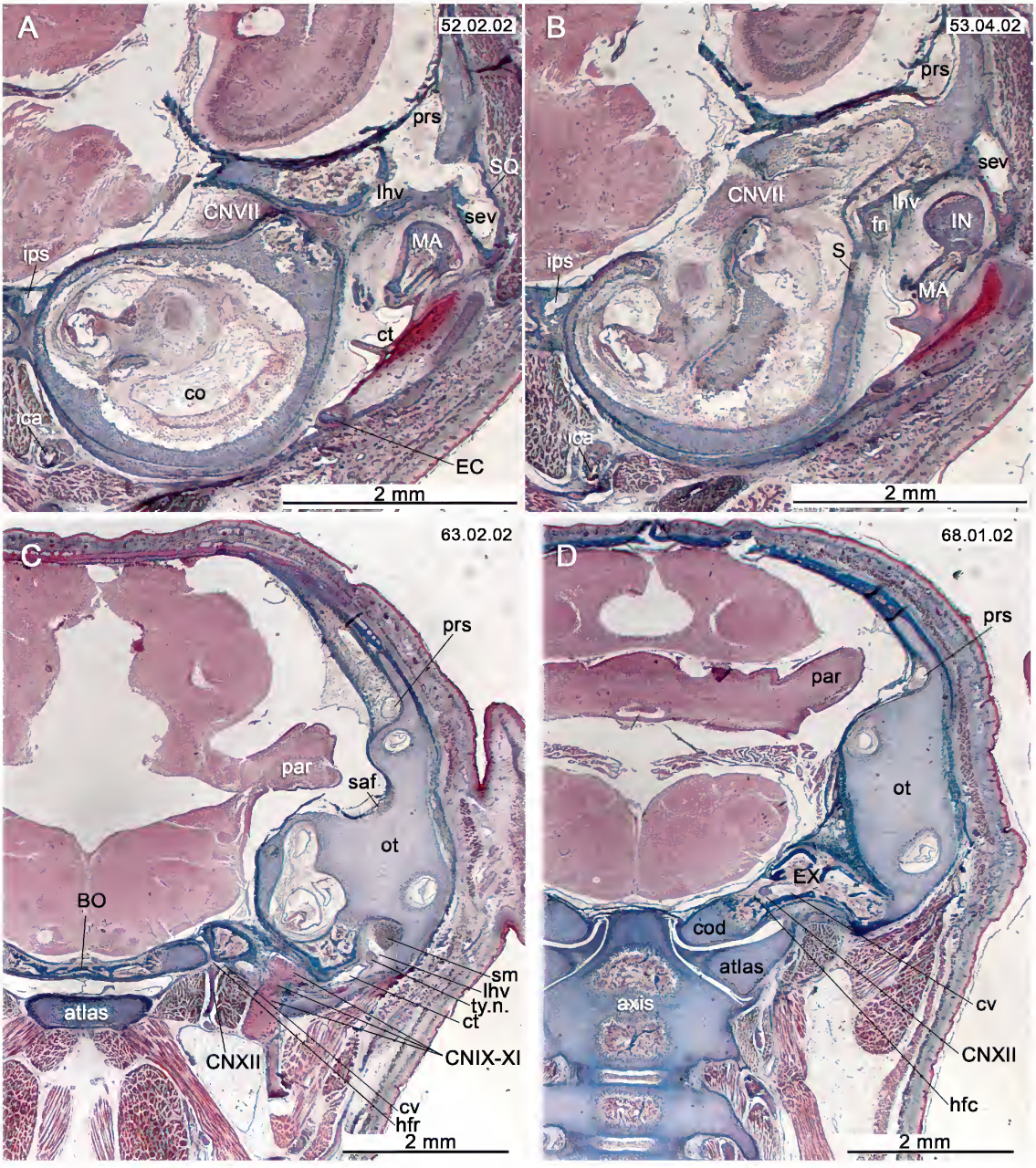
A
52.02.02
prs
SQ
lhv
CNVII
sev
MA
ips
ct
co
ica
EC
2 mm
B
53.04.02
prs
sev
CNVII
lhv
fn
IN
S
ips
MA
ica
2 mm
C
63.02.02
prs
par
saf
ot
BO
sm
lhv
ty.n.
ct
atlas
CNXII
CNIX-XI
cv
hfr
2 mm
D
68.01.02
prs
par
ot
EX
cod
atlas
axis
cv
CNXII
hfc
2 mm

men and the other, smaller one as the hypoglossal foramen. In line with our treatment of these features, we regard both apertures as properly hypoglossal in nature (that is, they each transmitted components of CN XII). Outgroups (e.g., *Asioryctes,* lipotyphlans; Kielan-Jaworowska, 1981; Novacek, 1986) have but one hypoglossal foramen, whereas more distant relatives (e.g., *Vincelestes*; Rougier, 1993) exhibit multiple openings whose contents cannot be resolved through comparative morphology.

Apart from the hypoglossal foramina, what can be interpreted as a true condyloid foramen for a condyloid vein occasionally occurs in extant marsupials (Wible, 2003; fig. 25D). We identified such a foramen in a few cases in which it seemed the most plausible interpretation (e.g., foramen intersecting the basijugular sulcus; fig. 15). When a separate venous aperture is not present, the vein presumably leaves the endocranium jointly with the hypoglossal nerve.

Basijugular sulcus and inferior petrosal sinus: In many and perhaps most sparassodonts (e.g., *Thylacosmilus*, *Sipalocyon*, *Cladosictis*, *Borhyaena*; figs. 6, 9, 14–16, 26A), there is a deep groove on the caudal aspect of the basicranium, here termed the basijugular sulcus. It is easily the largest such excavation on the basicranium, yet it has rarely been mentioned in the literature (but see Forasiepi, 2006). Similar sulci are also seen in some extant marsupials (e.g., *Sarcophilus*; fig. 18). The channel's relations indicate that it conducted a vessel of considerable size from the inferior petrosal sinus to the atlantooccipital articulation via the foramen magnum. Riggs (1934: 15) may have thought that it conducted an artery, since he referred to the caudal aperture of the inferior petrosal sinus as the "posterior carotid foramen," but the sulcus is substantially wider than the true carotid canal in *Thylacosmilus* or carotid sulcus of other sparassodonts. Given its connection with the inferior petrosal sinus, this channel is much more likely to have been venous and is here identified as the craniovertebral vein (see Discussion).

In *Thylacosmilus*, smaller grooves related to the jugular and rostral hypoglossal foramina terminate within the basijugular sulcus, suggesting that all were linked together in a plexiform arrangement. The sulcus itself merges with the caudal hypoglossal foramen, reappearing on the exoccipital's endocranial surface with no diminution in width. The fact that the endocranial section of the sulcus leaves a noticeable trace, and is as large as its ectocranial portion, strongly suggests that this channel conducted a structure additional to the roots of CN XII. The sulcus continues caudally for a short distance, terminating on the lip of foramen magnum. From this and other evidence (see Discussion), we conclude that the sulcus and its various tributaries held branches of a major vascular network that was ancillary to the common routing of cerebral venous flow (i.e., sigmoid sinus–internal jugular–brachiocephalic–vena cava) seen in

FIG. 25. *Perameles* sp. (ZIUT), pouch young, coronal sections through the auditory region. **A–B,** The lateral head vein is seen passing through the petrosal via prootic canal, in close relation to the facial nerve. The lhv is used as a landmark to distinguish the prootic sinus from the sphenoparietal emissary vein (Wible and Hopson, 1995). **C,** Bundles of CNXII fibers are seen passing out of the rostral hypoglossal foramen at transverse level of the jugular foramen (see CNIX–XI). **D,** Additional bundles pass through the caudal hypoglossal foramen at transverse level of dens together with the condyloid vein (aperture depicted is endocranial opening). Abbreviations: **atlas,** first cervical vertebra; **axis,** second cervical vertebra; **BO,** basioccipital; **co,** cochlear duct; **cod,** occipital condyle; **CNVII,** facial (cranial) nerve; **CNIX,** glossopharyngeal (cranial) nerve; **CNX,** vagus (cranial) nerve; **CNXI,** accessory (cranial) nerve; **CNXII,** hypoglossal (cranial) nerve; **ct,** tympanic cavity; **cv,** condyloid vein; **EC,** ectotympanic; **EX,** exoccipital; **fn,** facial nerve (CNVII); **hfc,** caudal hypoglossal foramen; **hfr,** rostral hypoglossal foramen; **ica,** internal carotid artery; **IN,** incus (= anvil); **ips,** inferior petrosal sinus; **lhv,** lateral head vein (= vena capitis lateralis); **MA,** malleus (= hammer); **ot,** otic capsule; **par,** paraflocculus of cerebellum; **prs,** prootic sinus; **S,** stapes (= stirrup); **saf,** subarcuate fossa; **sev,** sphenoparietal emissary vein (= postglenoid vein); **sm,** stapedius muscle (or its tendon); **SQ,** squamosal; **ty.n.,** tympanic nerve (CNIX). Histological serial section number indicated at top left. Numbers ascend in caudal direction.

some but certainly not all placentals. The network in question appears to conform to the cerebrospinal venous system, extensively documented in human and veterinarian anatomies (e.g., Montané and Bourdelle, 1913; Reinhard et al., 1962; Evans and Christensen, 1979; Lang, 1983) but rarely discussed in the paleontological literature (cf. MacPhee, 1994). It is also consistent with the observation that, in monotremes and marsupials, major sigmoid drainage mainly occurs through the foramen magnum (Wible, 1984; see also Rougier and Wible, 2006).

Foramina for rami temporales and post-temporal canal: Rami temporales (MacPhee and Cartmill, 1986) can be thought of as continuations of meningeal branches (both arterial and venous) that penetrate the cranial vault, mostly in the parietal region. In some taxa, major vessels in the upper neck and nuchal region such as the occipital vasculature and the arteria/vena diploetica magna may also communicate with rami temporales. As rami are commonly present in both placentals and marsupials (Wible, 1984; Wible and Hopson, 1995), their existence in sparassodonts is to be expected (figs. 3–5, 8C). As it is usually impossible in fossil material to tell whether both arterial and venous channels passed through these foramina, we have assumed that both are always present (see also Postglenoid Foramen and Suprameatal Foramen).

There appears to be no evidence that the post-temporal canal (for arteria/vena diploetica magna) occurred in sparassodonts (Forasiepi, 2009). Although perforations are evident in the caudal aspect of the cranium of *Thylacosmilus*, the ones we were able to trace in scans were very short and evidently devoted to maintaining local bone tissue (figs. 8E, 10B: nf).

DISCUSSION

Major Osteological Features

The tympanic floor and roof of *Thylacosmilus* are morphologically complex, including no fewer than five elements whose outgrowths participate in their formation (squamosal, alisphenoid, and exoccipital, with petrosal and ectotympanic as constant members). This complexity should not, however, be overemphasized, because the actual shape of roof and floor components is largely the result of intense pneumatization of the middle ear's bony walls. It is the process of pneumatization—involving highly coordinated osteoblastic and osteoclastic activity operating on opposite sides of growing bony elements during ontogeny (MacPhee, 1981)—that determines overall architecture, not the individual bones somehow developing outgrowths in isolation from one another.

The most obvious basicranial difference between *Thylacosmilus* and its relatives within Borhyaenoidea (e.g., *Prothylacynus* and *Borhyaena*; figs. 15, 16) is the apparent lack of a considerable bony floor of the tympanic cavity, other than that provided by the ectotympanic. The tympanic floor was more ossified in hathliacynids, but none approach *Thylacosmilus* in bullar size or completeness. The ectotympanic had to have been present in all sparassodonts, but with the exception of *Thylacosmilus* (this contribution) and *Paraborhyaena* MNHN SAL 5, in which an expanded ectotympanic was described (Petter and Hoffstetter, 1983), no borhyaenoid skull has been recovered with this element in place. This probably indicates it was very lightly attached to the walls of the external acoustic meatus.

Another remarkable character of *Thylacosmilus*, borhyaenids (e.g., *Australohyaena*; Forasiepi et al., 2015), and at least some proborhyaenids (e.g., *Paraborhyaena* and *Callistoe*; Petter and Hoffstetter 1983; Muizon 1999; Babot et al., 2002; Muizon et al., 2018), is reorientation of the auditory capsule (long axis at right angle to the horizontal). The functional correlations of this rearrangement are unknown.

As emphasized throughout this paper, there is no unique pattern of tympanic floor and roof composition in sparassodonts. Coverage varies from complete absence of floor components other than the ectotympanic (e.g., *Borhyaena*, *Prothylacynus*) to ones in which the tympanic cavity was increasingly encased in bone (e.g., *Thylacosmilus*).

Major Vascular Features

The position and relations of most of the large vessels leaving interpretable impressions on the sparassodont basicranium, such as the internal carotid and sphenoparietal emissary vein (Wible, 2003), are not controversial. Also reasonably well documented, and generally applicable to other sparassodonts, are the anatomical correlates of the internal carotid and the absence of a functional arteria diploetica magna. By contrast, the organization of the cerebrospinal venous system, as inferred for *Thylacosmilus* as well as other sparassodonts, has not previously been recognized and is given extended treatment below. We also provide an explanation, founded in comparative craniogenesis, for the notable invariance of the location of the carotid foramen in metatherians (e.g., Sánchez-Villagra and Forasiepi, 2017).

Cerebrospinal Venous System in *Thylacosmilus* and Other Sparassodonts

The morphological correlates of the basijugular sulcus suggest that it bore an important constituent of the cerebrospinal (or vertebral plexus) venous system. The relations of this system are well understood in *Homo* but have been investigated in few other mammals except ones having economic or social importance, such as *Canis*. This and other pathways considered as atypical (from the standpoint of human anatomy) are generally grouped as "collateral channels," but their fundamental components doubtless exist in most mammalian taxa, where they may be of greater significance than in *Homo* (cf. MacPhee, 1994).

In *Canis*, the cerebrospinal venous system consists of a highly plexiform set of valveless channels running from the head to the sacrum, along the vertebrae and within the vertebral canal (Nathoo et al., 2011). The system's rostral end receives venous flow from the cerebral sinuses at the base of the brain (cavernous sinus, petrosal sinuses, basilar plexus), transmitting it to plexuses ringing the foramen magnum and rostral part of the vertebral column. These plexuses anastomose with the azygos vein, various segmental components (e.g., intercostal veins), as well as with each other, ultimately feeding into major collectors like the brachiocephalic veins and rostral vena cava. As noted below, there is some indication that in sparassodonts the cerebrospinal venous system may have actually functioned as the dominant route for returning cerebral blood to the heart, with the internal jugular vein playing a subsidiary role. It is primitive for therians to send the major portion of endocranial venous return through the foramen magnum (Wible, 1984).

In simplified portrayals of cephalic venous return in mammals, the inferior petrosal sinus is depicted as an exclusive tributary of the sigmoid sinus/internal jugular vein. This is misleading, as the inferior petrosal sinus, like the other cerebral sinuses, is significantly plexiform (Mortazavi et al., 2012). For present purposes, the most important of these connections involve the condyloid emissary vein(s) and vertebral plexuses. In *Homo* these are usually small in caliber (Lang, 1983; Mortazavi et al., 2012; Standring, 2016), but in some mammals they are major channels. In *Canis* the inferior petrosal sinus does not terminate anatomically in the internal jugular vein, as in humans, but instead continues caudally to join the condyloid veins. Thus formed, these veins pass through the condyloid canals to the inner surface of the exoccipital, where as "the ultimate cranial extensions of the longitudinal venous sinuses" (Reinhard et al., 1962: 70) they become continuous with the basilar and vertebral plexuses (see also Evans and Christensen, 1979: 122, figs. 4–10; 794, figs. 12–21, 22).

In Evans and Christensen's (1979) nomenclature this continuation of the inferior petrosal sinus is identified as the vertebral vein. From the standpoint of harmonizing human with nonhuman anatomy this usage is somewhat confusing, because the vertebral vein of *Homo* is defined as the trunk that arises from the coalescence of *distal* branches of the vertebral plexus in the cervical region, well away from the foramen magnum. For this

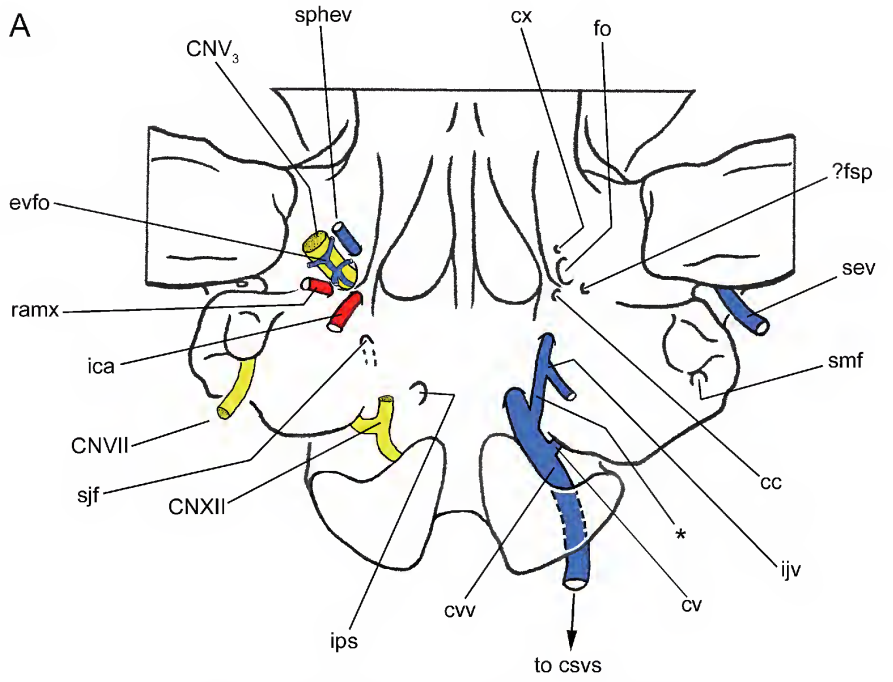

FIG. 26. Features related to blood vessels in representative sparassodonts: **A,** *Thylacosmilus atrox*, external features (based on *Thylacosmilus atrox*, holotype, FMNH P14531); **B–C,** *Lycopsis longirostrus*, external and internal features (based on UCMP 38061 and Marshall, 1977b) Abbreviations: **bsp,** basilar plexus; **cc,** carotid canal; **CNV_3,** mandibular branch of trigeminal (cranial) nerve; **CNVII,** facial (cranial) nerve; **CNXII,** hypoglossal (cranial) nerve; **cars,** cavernous sinus; **csvs,** cerebrospinal venous system; **cv,** condyloid vein; **cvv,** craniovertebral vein; **cx,** canal x (see fig. 6 and text); **evfo,** emissary vein of foramen ovale; **fo,** foramen ovale; **?fsp,** foramen spinosum; **hf,** hypoglossal foramen; **iam,** internal acoustic meatus; **ica,** internal carotid artery; **ijv,** internal jugular vein; **ips,** inferior petrosal sinus; **jf,** jugular foramen; **mmv,** middle meningeal vein; **ophv,** ophthalmic vein; **ramx,** ramus anastomoticus; **sev,** sphenoparietal emissary vein; **sjf,** secondary jugular foramen; **smf,** stylomastoid foramen; **sphev,** sphenoidal emissary vein (= vein of Vesalius); **sphps,** sphenoparietal sinus; **sps,** superior petrosal sinus; **ss,** sigmoid sinus. Only major channels are indicated. The position and relations of most of the large vessels leaving impressions on the basicranium, such as the internal carotid, sphenoparietal emissary vein, and inferior petrosal sinus are not controversial. However, other features, also evidently related to vasculature, have received less attention. As explained in the text, in addition to CNV_3, in *Thylacosmilus* the foramen ovale may have transmitted a large vein to the extracranial pharyngeal plexus. In the absence of a functioning and intact stapedial system, the foramen here identified as the foramen spinosum (?fsp) may have given passage to an anastomotic ramus running from the maxillary artery to the meningeal system, although this task could have been performed by other vessels (e.g., the ophthalmic artery) that have left no mark. The large groove identified as the basijugular sulcus (bjs, see fig. 6), connecting the caudal aperture for the inferior petrosal sinus to the hypoglossal foramen/foramina in many sparassodonts, surely transported the sinus itself. However, instead of leaving for the internal jugular vein, the inferior petrosal sinus seems to have re-entered the endocranium through one or another of the hypoglossal foramina, only to immediately leave again through the foramen magnum, now as the (conjectured) craniovertebral vein (cvv). Asterisk (*) indicates the likely connection between the internal jugular vein and the craniovertebral vein. How drainage through the sinus in this scenario would have related to that through the internal jugular system is unclear. There is some indication that the internal jugular was relatively small in size, although how this affected endocranial drainage cannot be inferred from the material available. In all investigated sparassodonts the posttemporal foramen for the diploic artery and vein are missing. *Thylacosmilus* evidently lacked a transverse venous foramen, but one is present in *Lycopsis* and other taxa (see text).

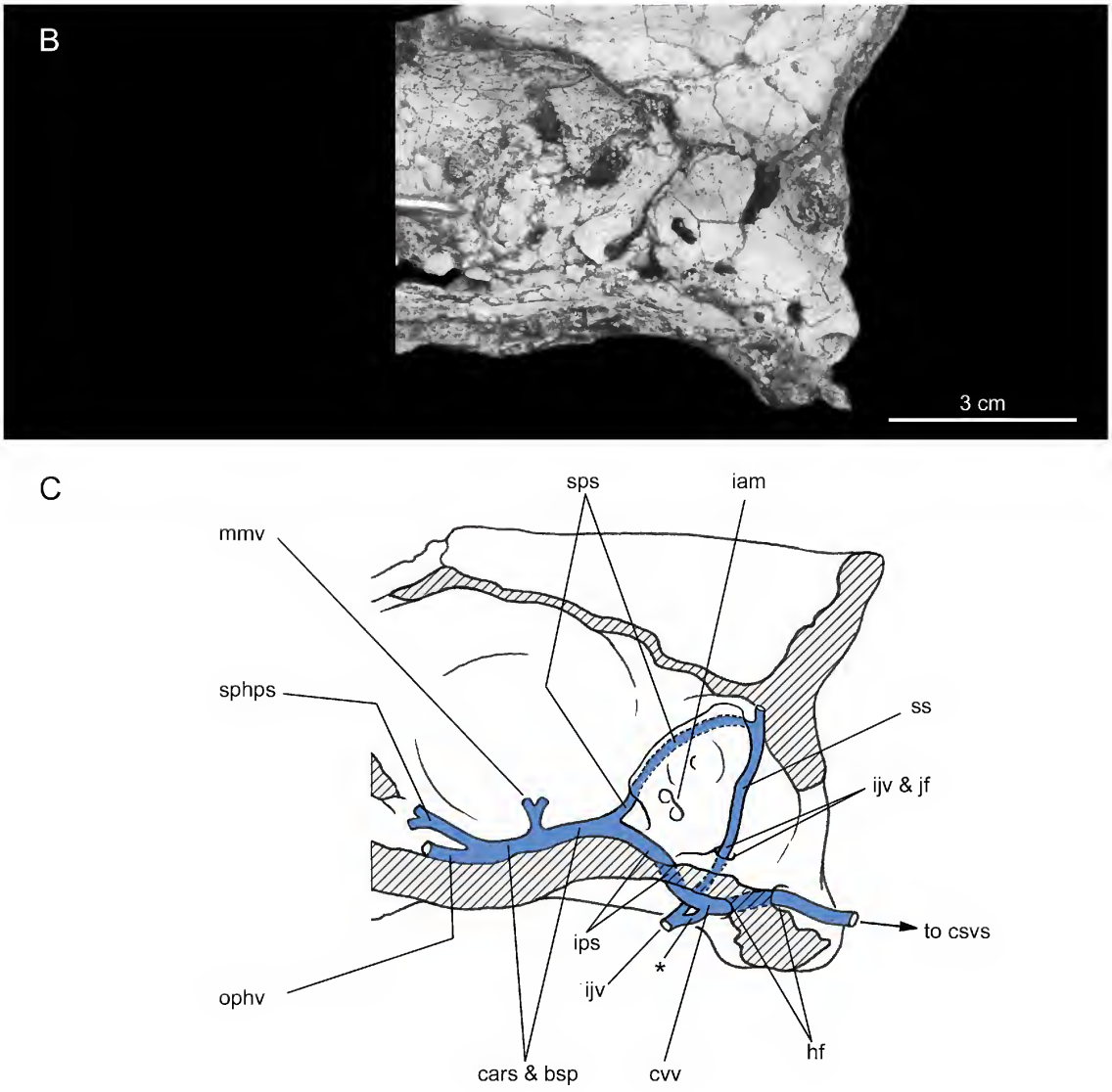

reason we prefer to label the continuation of the inferior petrosal sinus through the basijugular sulcus into the endocranium as the craniovertebral vein (fig. 26A). Since the vertebral vein of *Canis* and the greatly expanded craniovertebral vein inferred for sparassodonts have apparently similar relations, there is a case to be made for considering them as homologs. However, since the incidence of this pathway is so poorly documented for the vast majority of mammals, at present we recommend restricting usage of "craniovertebral vein" to Sparassodonta and, arguably, other metatherians.

As noted, although there is a functional internal jugular in the dog, it is a relatively small vessel ("almost vestigial" according to Reinhard et al., 1962: 72), indicating that a significant part of venous return from the endocranium is actually carried by the inferior petrosal sinus to the vertebral plexus via the condyloid vein. The question arises whether in

sparassodonts the cerebrospinal venous system was likewise dominant over the internal jugular. To test this idea, we measured the jugular canal and basijugular sulcus in the *Thylacosmilus* holotype. The size of the intrabullar canal linking the primary and secondary jugular foramina should provide some indication of the size of the internal jugular vein at its anatomical origin (fig. 8D: jfis). Because in life this canal also gave passage to several nerves, our jugular measurement presumably overestimates the vein's actual caliber. Scaled scan segments through the relevant region of the holotype of *Thylacosmilus* indicate that the minimum width of its jugular canal is approximately 2 mm. In comparison, the width of the basijugular sulcus in the same specimen is 7 mm.

Another indication of the absolute size of the inferior petrosal sinus/craniovertebral vein can be gained from conditions in *Borhyaena* (MACN-A 5922; fig. 16C). In this specimen, postmortem loss of the petrosals has fortuitously exposed a deep, continuous groove on the exposed lateral margins of the central stem, from the area of the carotid canal/cavernous sinus rostrally to the level of the beginning of the basijugular sulcus caudally. Given that the groove passes directly into the sulcus, it is reasonably certain that it contained the inferior petrosal sinus. Because the jugular foramen is ill defined in this taxon (fig. 16), its dimensions cannot be directly compared to those of the basijugular sulcus. However, it is instructive to note the size difference between the sulcus and the more rostrally positioned carotid canal, also visible in figure 16B. Clearly, the inferior petrosal sinus and its continuation, the craniovertebral vein, were major cranial vessels in this taxon.

In summary, this hypothesis concerning the method of cranial venous return in sparassodonts should be considered tentative. Although additional verification is needed, the size of the basijugular sulcus suggests that it was part of a major system of venous return in sparassodonts.

Carotid Foramen Position in Marsupials and Placentals

This study has emphasized the remarkable consistency marsupials display in regard to the presence and location of the carotid canal, in contrast to placentals in which the canal is much more variable. Such consistency requires explanation; here we suggest that it may be correlated with certain features of early cranial development. This treatment is based on ideas originally developed by De Beer (1929, 1937) and Starck (1967) concerning carotid foramen development in tetrapods, but we now extend them explicitly to conditions in marsupials.

In marsupials the endocranial aperture of the carotid foramen—that is, the aperture adjacent to the hypophysis through which the internal carotid artery actually enters the endocranium—varies little in regard to its relative position and relations. In contrast, the foramen's exocranial aperture may be significantly displaced due to postnatal patterns of basicranial growth (Sánchez-Villagra and Forasiepi, 2017). Although many factors are probably involved, ontogenetic events occurring early in cranial development seem to play a possibly fundamental role in carotid foramen positioning.

In late fetal stages of therians, the central stem is usually a solid bar of cartilage, but morphologically it derives from several separate chondrifications (lamina trabecularis, polar cartilages, and hypophyseal and basal plates) that appear early in craniogenesis and later fuse (De Beer, 1937). An important generalization is that in most investigated placentals these chondrifications initially differentiate medial to the internal carotid arteries without enveloping them (De Beer, 1929, 1937; *Lepus*, fig. 27A). Later, a transitory cartilaginous arch develops lateral to the internal carotid at its point of entry into the endocranium. This is the alicochlear commissure that, as its name implies, joins the ala temporalis (an outgrowth of the lamina trabecularis) to the anterior pole of the otic capsule adjacent to the future basi-

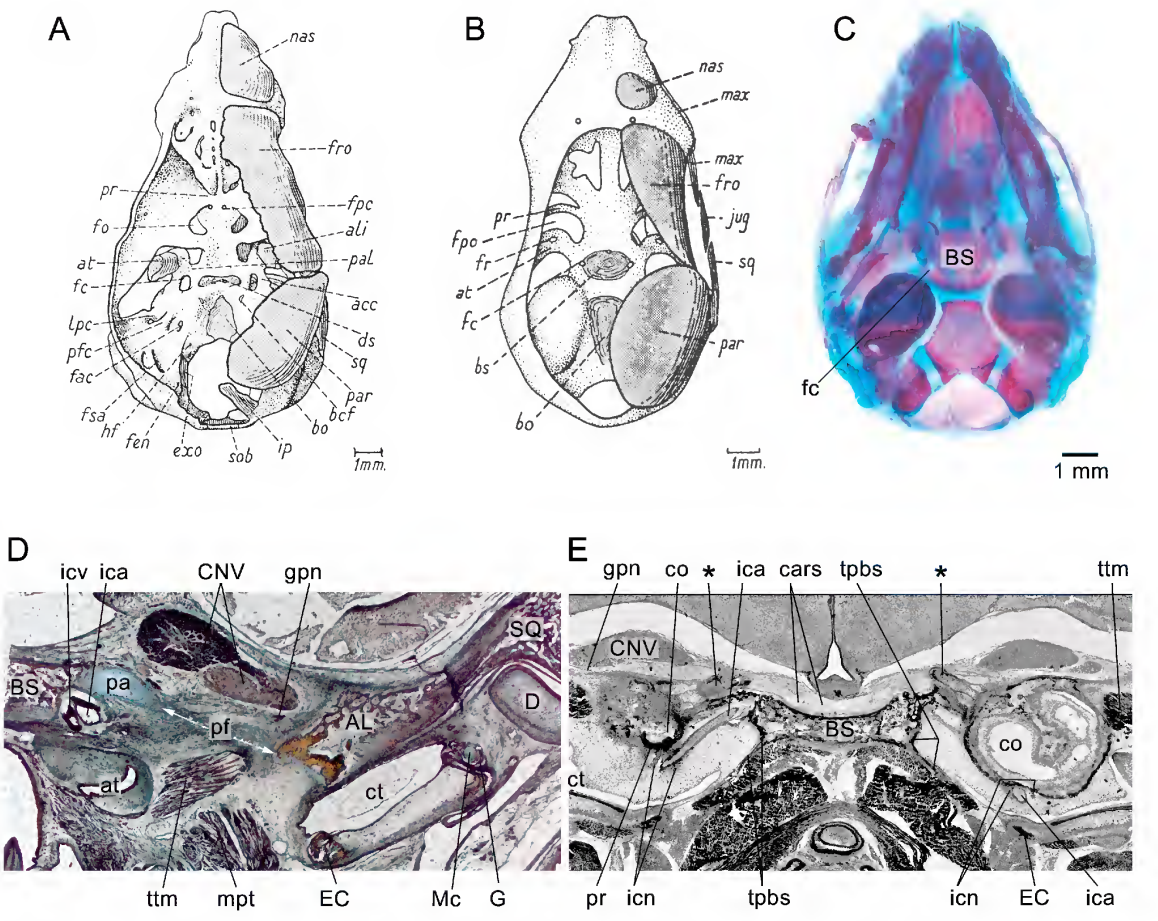

FIG. 27. Developmental contrasts in ontogeny of carotid foramen in representative marsupial and placental taxa: **A,** *Lepus* sp. (reconstruction, 45 mm CRL); **B,** *Perameles* sp. (reconstruction, 23 mm CRL); **C,** *Monodelphis domestica* (ZIUT; 15d postpartum, head, cleared and stained); **D,** *Macropus eugenii* (29 mm CRL); and **E,** *Hemicentetes semispinosus* (MPIH 1964/45, near-term fetus; 40 mm CRL). Abbreviations for A and B (from De Beer, 1937): **acc,** alicochlear commissure; **ali,** alisphenoid bone; **at,** ala temporalis; **bcf,** basicochlear (= basicapsular) fissure; **bo,** basioccipital bone; **bs,** basisphenoid bone; **ds,** dorsum sellae; **exo,** exoccipital bone; **fac,** internal acoustic meatus; **fc,** carotid foramen; **fen,** endolymphatic canal; **fo,** optic foramen; **fpc,** foramen prechiasmaticum; **fpo,** foramen pseudopticum; **fr,** foramen rotundum; **fro,** frontal bone; **fsa,** subarcuate fossa; **hf,** hypoglossal foramen; **ip,** interparietal; **jug,** jugal bone; **lpc,** lateral prefacial commissure; **max,** maxillary bone; **nas,** nasal bone; **pal,** processus alaris; **par,** parietal bone; **pfc,** prefacial commissure; **pr,** preoptic root of orbital cartilage; **sob,** supraoccipital bone; **sq,** squamosal bone. Abbreviations for C –E: **AL,** alisphenoid; **at,** auditory tube; **BS,** basisphenoid; **cars,** cavernous sinus; **CNV,** trigeminal (cranial) nerve; **co,** cochlear duct; **ct,** cavum tympani (= tympanic cavity); **D,** dentary; **EC,** ectotympanic; **fc,** carotid foramen; **G,** gonial; **gpn,** greater petrosal nerve (CNVII); **ica,** internal carotid artery; **icn,** internal carotid nerve; **icv,** internal carotid vein; **Mc,** Meckel's cartilage; **mpt,** medial pterygoid muscle; **pa,** processus alaris; **pf,** piriform fenestra; **pr,** promontorium; **SQ,** squamosal; **tpbs,** tympanic process of basisphenoid; **ttm,** tensor tympani muscle. In E, pair of asterisks (*) indicates the cartilaginous alichochlear commissures being replaced by bone, forming the definitive carotid foramen.

occipital-basisphenoidal synchondrosis. The result is that the artery is now enclosed within a chondrocranial aperture that is immediately adjacent to, but not morphologically within, the central stem. There are exceptions: the alicochlear commissure does not form in lorises, for example, but, interestingly, in these primates the internal carotid is involuted and functionally replaced by an ascending pharyngeal/circulus arteriosus anastomosis (Cartmill, 1975; MacPhee, 1981).

In early fetuses of marsupials, by contrast, the fused lamina trabecularis/hypophyseal plate, which forms the anlage of the basisphenoid, expands laterally to a relatively greater extent than in developing placentals. This may be a reflection of the need to precociously form hard structures in the pharyngeal area in order to facilitate efficient suckling (Maier, 1993). In any case, the result is that the internal carotid, at its point of entry into the endocranium, is surrounded by cartilage from an early stage (*Perameles*; fig. 27B). The alicochlear commissure never develops as a recognizable morphological entity in marsupials (De Beer, 1937; Maier, 1987), although whether its independent existence is suppressed or overtaken by heterochronic expansion of the central stem is uncertain. Alternatively, this form of carotid foramen development may simply be plesiomorphic for mammals, as monotremes follow a similar sequence (De Beer and Fell, 1936).

Although these differences appear minor, they determine later morphology. When the ossification center for the basisphenoid bone appears within the marsupial central stem, it rapidly envelops the internal carotid, thus permanently fixing its position (*Monodelphis*, *Macropus*; fig. 27C, D). Thereafter, the relative position of the osteocranial carotid foramen on the skull will be determined by the local synchondrosal growth center. If relative growth on the basisphenoid side of the synchondrosis outstrips that on the basioccipital side, the foramen's position will appear to move relatively rostrally, as compared with a species in which the converse pattern of growth prevails. (Because the carotid foramen is fixed within basisphenoidal material, in the latter case the foramen's position adjacent to the synchondrosis will not appear to change significantly during later ontogeny; fig. 17).

In placentals, final conditions depend on the nature of skeletal maturation in the area of the piriform fenestra and fetal carotid foramen. In at least some placentals that have been studied for this purpose, such as the tenrec *Hemicentetes semispinosus*, the alicochlear commissure persists well into late fetal life, to be replaced subsequently by ossification proceeding from the basisphenoid (MacPhee, 1981: fig. 56; see also fig. 27E; asterisks). In this way the internal carotid's final position also becomes fixed with respect to surrounding bone territories and the synchondrosis, but in a way appreciably different from and ontogenetically later than the marsupial pattern. In most investigated placentals the alicochlear commissure involutes without ossifying (R.D.E.M., personal obs.), with the result that the presumptive (membrane-bounded) carotid foramen appears to be continuous with the rest of the unossified portion of the basicranium (i.e., piriform fenestra). With further growth and maturation, all or part of the fenestra will become "the" carotid foramen. By contrast, if ossification mostly proceeds from the petrosal, the foramen will appear to perforate that bone. If instead it is the basisphenoid that ossifies the area of the fenestra, the foramen will appear within the latter—but only late in ontogeny, a point De Beer (1937) did not appreciate in the case of *Erinaceus* (MacPhee, 1981: fig. 50), which to him seemed "primitive" (i.e., marsupiallike) in having a basisphenoid-bounded carotid foramen. Note that formation of lengthy carotid canals, something that occurs in many mammals, will not affect the point at which the internal carotid actually enters the endocranium, which as noted is always adjacent to the hypophysis in both marsupials and placentals.

In summary, the real differences between the two groups appear to be three:

(1) In marsupials, there is precocious entrapment of the internal carotid within the trabecular anlage in which the center for the basisphenoid appears, heterochronistically early compared to placental cranial ontogeny.

(2) In placentals, carotid enclosure also occurs, but through the agency of the alicochlear commissure, a laterally positioned structure that does not appear in marsupial development (De Beer, 1937), at least as a morphologically separate entity. In some cases the commissure is later replaced by bone, from the basisphenoid or petrosal (or often both), thus converting the cartilaginous carotid foramen into the bony successor seen in the adult. In other cases the commissure involutes without bony replacement, and the now-unenclosed carotid simply penetrates the membrane covering the piriform fenestra rather than traveling through its own aperture.

(3) In many marsupials the carotid foramen may elongate into a canal, due to later growth, but this does not affect relative relationships determined in the fetus. In placentals there is greater potential variety in the matrix of bones enclosing the internal carotid in the adult, but this too is the result of later growth patterns (such as in the precise way the piriform fenestra closes, if it does).

ACKNOWLEDGMENTS

We are grateful to William Simpson (FMHN), Alejandro Kramarz (MACN), Marcelo Reguero (MLP), Matías Taglioretti and Fernando Scaglia (MMP), Daniel Brinkman (YPM), and Ruth O'Leary and Judy Galkin (AMNH) for permitting access to collections under their care, and to Marcelo Sáchez-Villagra and Wolfang Maier for permitting access to histological serial sections of marsupial embryos. We thank Sergio F. Vizcaíno and Susana Bargo for granting access to sparassodont specimens from recent excavations in the Santa Cruz Formation (fieldwork financially supported by PICT 2013-389 to S.F. Vizcaíno). We also thank Zhe-Xi Luo (University of Chicago) for facilitating arrangements for scanning *Thylacosmilus atrox* (FMNH P14344), Larry Witmer for access to his CT scan of *Thylacosmilus atrox* FMNH P14531, and Camille Grohé for 3-D reconstructions of the inner ear of *Sipalocyon* (AMNH VP 9254) and *Borhyaena* (YPM PU 15120). We are grateful to the reviewers, Robin Beck and Russell Engelman, for their comments on the original manuscript, and to the editor Robert Voss for additional helpful observations. We thank Lorraine Meeker (AMNH) for her excellent photography and line art presented in this paper. We also thank Jorge L. Blanco for cover art and the life reconstruction in figure 2. Copyright for the photos of *Cladosictis patagonica* (YPM PU 15170) and *Borhyaena tuberata* (YPM PU 15120) belongs to the Yale Peabody Museum of Natural History. This is a contribution to projects financially supported by ANPCYT (PICT 2015-966) and the Fulbright-CONICET Scholar Program 2015–2016 (to A.M.F.).

REFERENCES

Alloing-Séguier, L., M.R. Sánchez-Villagra, M.S.Y. Lee, and R. Lebrun. 2013. The bony labyrinth in diprotodontian marsupial mammals: diversity in extant and extinct forms and relationships with size and phylogeny. Journal of Mammalian Evolution 20: 191–198.

Ameghino, F. 1891 Caracteres diagnósticos de cincuenta species nuevas de mamíferos fósiles argentinos. Revista Argentina de Historia Natural 1: 129–167.

Aplin, K. 1990. Basicranial regions of diprotodontian marsupials: anatomy, ontogeny and phylogeny. Ph.D. dissertation, University of New South Wales, Sydney.

Archer, M. 1976. The basicranial region of marsupicarnivores (Marsupialia), relationships of carnivorous marsupials, and affinities of the insectivorous marsupial peramelids. Zoological Journal of the Linnean Society 59: 217–322.

Argot, C. 2003a. Postcranial functional adaptations in the South American Miocene borhyaenoids (Mammalia, Metatheria): *Cladosictis*, *Pseudonotictis*, and *Sipalocyon*. Alcheringa 27: 303–356.

Argot, C. 2003b. Functional adaptations of the postcranial skeleton of two Miocene borhyaenoids (Mammalia, Metatheria), *Borhyaena* and *Prothylacynus*, from South America. Palaeontology 46: 1213–1267.

Argot, C. 2004a. Functional-adaptive features and paleobiologic implications of the postcranial skeleton of the Late Miocene sabretooth borhyaenoid, *Thylacosmilus atrox* (Metatheria). Alcheringa 28: 229–266.

Argot, C. 2004b. Evolution of South American mammalian predators (Borhyaenoidea): anatomical and palaeobiological implications. Zoological Journal of the Linnean Society 140: 487–521.

Babot, M.J. 2005. Los Borhyaenoidea (Mammalia, Metatheria) del Terciario Inferior del Noroeste argentino. Aspectos filogenéticos, paleobiológicos y bioestratigráficos. Ph.D. dissertation, Universidad Nacional de Tucumán, San Miguel de Tucumán, Argentina.

Babot, M.J., and A.M. Forasiepi. 2016. Mamíferos predadores nativos del Cenozoico sudamericano: evidencias filogenéticas y paleoecológicas. *In* F.A. Agnolin, G.L. Lio, F. Brissón Egli, N.R. Chimento, and F.E. Novas (editors), Historia evolutiva y paleobiogeográfica de los vertebrados de América del Sur. Contribuciones del MACN 6: 219–230. Buenos Aires: Museo Argentino de Ciencias Naturales "Bernardino Rivadavia."

Babot, M.J., J.E. Powell, and C. de Muizon. 2002. *Callistoe vincei*, a new Proborhyaenidae (Borhyaenoidea, Metatheria, Mammalia) from the early Eocene of Argentina. Geobios 35: 615–629.

Batson, O.V. 1940. Function of vertebral veins and their role in the spread of metastases. Annals of Surgery 112: 138–149.

Batson, O.V. 1957. The vertebral vein system. American Journal of Roentgenography 78: 195–212.

Beck R.M. 2015. A peculiar faunivorous metatherian from the early Eocene of Australia. Acta Palaeontologica Polonica 60: 123–129.

Billet, G. 2011. Phylogeny of the Notoungulata (Mammalia) based on cranial and dental characters. Journal of Systematic Palaeontology 9: 481–497.

Bugge, J. 1974. The cephalic arterial system in insectivores, primates, rodents and lagomorphs, with special reference to the systematic classification. Acta Anatomica 87 (suppl. 62): 1–159.

Carneiro, L.M. 2018. A new species of *Varalphadon* (Mammalia, Metatheria, Sparassodonta) from the upper Cenomanian of southern Utah, North America: phylogenetic and biogeographic insights. Cretaceous Research 84: 88–96.

Cartmill, M. 1975. Strepsirhine basicranial structures and the affinities of the Cheirogaleidae. *In* W.P. Luckett, F.S. Szalay (editors), Phylogeny of the primates, a multidisciplinary approach: 313–354. New York: Plenum Press.

Cartmill, M., and R.D.E. MacPhee. 1980. Tupaiid affinities: the evidence of the carotid arteries and cranial skeleton. *In* W.P. Luckett (editor), Comparative biology and evolutionary relationships of tree shrews: 95–132. New York: Plenum Press.

Chaffee, R.G. 1952. The Deseadan vertebrate fauna of the Scarritt Pocket, Patagonia. Bulletin of the American Museum of Natural History 98 (6): 507–562.

Chen, Z., H. Feng, G. Zhu, N. Wu, and J. Lin. 2007. Anomalous intracranial venous drainage associated with basal ganglia calcification. American Journal of Neuroradiology 28: 22–24.

Churcher, C.S. 1985. Dental functional morphology in the marsupial sabre-tooth *Thylacosmilus atrox* (Thylacosmilidae) compared to that of felid sabre-tooths. Australian Mammalogy 8: 201–220.

Clemens, W.A. 1966. Fossil mammals of the type Lance Formation. Part II. Marsupialia. University of California Publications in Geological Sciences 62: 1–122.

Coutier, F., L. Hautier, R. Cornette, E. Amson, and G. Billet. 2017. Orientation of the lateral semicircular canal in Xenarthra and its links with head posture and phylogeny. Journal of Morphology 278: 704–717.

Croft, D.A., R.K. Engelman, T. Dolgushina, and G. Wesley. 2018. Diversity and disparity of sparassodonts (Metatheria) reveal non-analogue nature of ancient South American mammalian carnivore guilds. Proceedings of the Royal Society of London B, Biological Sciences 285. [http://dx.doi.org/10.1098/rspb.2017.2012]

De Beer, G.R. 1929. The development of the skull of the shrew. Philosophical Transactions of the Royal Society of London B217: 411–480.

De Beer, G.R. 1937. The development of the vertebrate skull. Oxford: Oxford University Press. [reprinted: University of Chicago Press, 1985]

De Beer, G.R. 1947. How animals hold their head. Proceedings of the Linnean Society of London 159: 125–139.

De Beer, G.R., and W.A. Fell. 1936. The development of the Monotremata. Part III. The development of the skull of *Ornithorhynchus*. Transactions of the Zoological Society of London 23: 1–42.

Echarri S, M.D. Ercoli, M.A. Chemisquy, G. Turazzini, and F.J. Prevosti. 2017. Mandible morphology and diet of the South American extinct metatherian predators (Mammalia, Metatheria, Sparassodonta).

Earth and Environmental Science Transactions of the Royal Society of Edinburgh 106: 277–288.

Ellenberger, W., and H. Baum. 1894. Topographische Anatomie des Pferdes, mit besonderer Berücksichtigung der tierärztlichen Praxis. Vol. 2, Kopf und Hals. Berlin: Verlag Paul Parey.

Engelman, R.K., and D.A. Croft. 2014. A new species of small-bodied sparassodont (Mammalia: Metatheria) from the Middle Miocene locality of Quebrada Honda, Bolivia. Journal of Vertebrate Paleontology 34: 672–688.

Ercoli, M.D., F.J. Prevosti, and A. Álvarez. 2012. Form and function within a phylogenetic framework: locomotory habits of extant predators and some Miocene Sparassodonta (Metatheria). Zoological Journal of the Linnean Society 165: 224–251.

Evans, W.E., and G.C. Christensen. 1979. Miller's Anatomy of the dog. Philadelphia: W.B. Saunders Company.

Falk, D. 1986. Evolution of cranial blood drainage in hominids: enlarged occipital/marginal sinuses and emissary foramina. American Journal of Physical Anthropology 70: 311–324.

Fedorov, A., et al. 2012. 3DSlicer as an image computing platform for the quantitative imaging network. Magnetic Resonance Imaging 30: 1323–1341.

Forasiepi, A.M. 2006. Anatomy of *Arctodictis sinclairi* (Mammalia, Metatheria) and the phylogenetic relationships of Sparassodonta, large carnivores of the Cenozoic of South America. Ph.D. dissertation, University of Louisville, Louisville.

Forasiepi, A.M. 2009. Osteology of *Arctodictis sinclairi* (Mammalia, Metatheria, Sparassodonta) and phylogeny of Cenozoic metatherian carnivores from South America. Monografías del Museo Argentino de Ciencias Naturales 6: 1–174.

Forasiepi, A.M., et al. 2006. A new species of Hathliacynidae (Metatheria, Sparassodonta) from the Middle Miocene of Quebrada Honda, Bolivia. Journal of Vertebrate Paleontology 26: 670–684.

Forasiepi, A.M., M.R. Sánchez-Villagra, T. Schmelzle, and R.F. Kay. 2014. An exceptionally preserved skeleton of *Palaeothentes* from the Miocene of Patagonia, Argentina: new insights on the anatomy of extinct paucituberculatan marsupials. Swiss Journal of Palaeontology 133: 1–21.

Forasiepi, A.M., M.J. Babot, and N. Zimicz. 2015. *Australohyaena antiquua* (Mammalia, Metatheria, Sparassodonta), a large predator from the Late Oligocene of Patagonia, Argentina. Journal of Systematic Palaeontology 13: 503–525.

Gaudin, T.J., J.R. Wible, J.A. Hopson, and W.D. Turnbull. 1996. Reexamination of the morphological evidence for the cohort Epitheria (Mammalia, Eutheria). Journal of Mammalian Evolution 3: 31–79.

Giannini, N.P., F. Abdala, and D.A. Flores. 2004. Comparative postnatal ontogeny of the skull in *Dromiciops gliroides* (Marsupialia: Microbiotheriidae). American Museum Novitates 3460: 1–17.

Goin, F.J. 2003. Early marsupial radiations in South America. *In* M. Jones, C. Dickman, and M. Archer (editors), Predators with pouches. The biology of carnivorous marsupials: 30–42. Victoria: CSIRO Publishing.

Goin, F.J., and A. Candela. 2004. New Paleogene marsupials from the Amazon Basin of Eastern Perú. *In* K.E. Campbell (editor), The Paleogene mammalian fauna of Santa Rosa, Amazonian Perú. Natural History Museum of Los Angeles County, Science Series 40: 15–60.

Goin, F.J., and R. Pascual. 1987. News on the biology and taxonomy of the marsupials Thylacosmilidae (Late Tertiary of Argentina). Anales de la Academia Nacional de Ciencias Exactas Físicas y Naturales de Buenos Aires 39: 219–246.

Goin, F.J., R.M. Palma, R. Pascual, J.E. Powell. 1986. Persistencia de un primitivo Borhyaenidae (Mammalia, Marsupialia) en el Eoceno Temprano de Salta (Fm. Lumbrera, Argentina), aspectos geológicos y paleoambientales relacionados. Ameghiniana 23: 47–56.

Gregory, W.K. 1910. The orders of mammals. Bulletin of the American Museum of Natural History 27: 1–524.

Gregory, W.K. 1920. On the structure and relations of *Notharctus*, an American Eocene primate. Memoirs of the American Museum of Natural History (new series) 3 (pt. 2): 49–243.

Hershkovitz, P. 1992. Ankle bones: the Chilean opossum *Dromiciops gliroides* Thomas, and marsupial phylogeny. Bonner Zoologische Beiträge 43: 181–213.

Hoogland, P.V., W. Vorster, R.J. Groen, and S.H. Kotze. 2012. Possible thermoregulatory functions of the internal vertebral venous plexus in man and various other mammals: evidence from comparative anatomical studies. Clinical Anatomy 25: 45260. [doi: 10.1002/ca.21274]

Horovitz, I., and M.R. Sánchez-Villagra. 2003. A morphological analysis of marsupial mammal higher-level phylogeny relationships. Cladistics 19: 181–212.

Horovitz, I., et al. 2008. The anatomy of *Herpetotherium* cf. *fugax* Cope, 1873, a metatherian from the Oligocene of North America. Palaeontographica Abteilung A 284: 109–141.

Horovitz, I., et al. 2009. Cranial anatomy of the earliest marsupials and the origin of opossums. PloS ONE 4. [doi:10.1371/journal.pone.0008278]

Kielan-Jaworowska, Z. 1981. Evolution of the therian mammals in the Late Cretaceous of Asia. Part IV. Skull structure in *Kennalestes* and *Asioryctes*. Palaeontologia Polonica 42: 25–78.

Ladevèze, S. and C. de Muizon. 2007. The auditory region of early Paleocene Pucadelphydae (Mammalia, Metatheria) from Tiupampa, Bolivia, with phylogenetic implications. Palaeontology 50: 1123–1154.

Lang, J. 1983. Clinical anatomy of the head: neurocranium, orbit, craniocervical regions. New York: Springer-Verlag. [translated from the German by R.R. Wilson and D.P. Winstanley]

Lindenfors, P, J.L. Gittleman, and K.E. Jones. 2007. Sexual size dimorphism in mammals. *In* D.J. Fairbairn, W.U. Blanckenhorn, and T. Székely (editors), Sex, size and gender roles: evolutionary studies of sexual size dimorphism: 16–26. Oxford: Oxford University Press.

López-Aguirre, C., M. Archer, S.J. Hand, and S.W. Laffan. 2016. Extinction of South American sparassodontans (Metatheria): environmental fluctuations or complex ecological processes? Palaeontology 60: 91–115.

MacPhee, R.D.E. 1979. Entotympanics, ontogeny and primates. Folia Primatologica 31: 23–47.

MacPhee, R.D.E. 1981. Auditory regions of primates and eutherian insectivores: morphology, ontogeny, and character analysis. Contributions to Primatology 18: 1–282.

MacPhee, R.D.E. 1994. Morphology, adaptations, and relationships of *Plesiorycteropus*, and a diagnosis of a new order of eutherian mammals. Bulletin of the American Museum of Natural History 220: 1–214.

MacPhee, R.D.E., and M. Cartmill. 1986. Basicranial structures and primate systematics. *In* D.R. Swindler (editor), Comparative primate biology. Vol. 1, systematics, evolution and anatomy: 219–275. New York: Liss.

Maier, W. 1987. The ontogenetic development of the orbitotemporal region in the skull of *Monodelphis domestica* (Didelphidae, Marsupialia), and the problem of the mammalian alisphenoid. *In* H.J. Kuhn and U. Zeller (editors), Morphogenesis of the mammalian skull: 71–90. Hamburg: Verlag Paul Parey.

Maier, W. 1989. Morphologische Untersuchungen am Mittelohr der Marsupialia. Journal of Zoological Systematics and Evolutionary Research 27: 149–168.

Maier, W. 1993. Cranial morphology of the therian common ancestor, as suggested by the adaptations of neonate marsupials. *In* F.S. Szalay, M.J. Novacek, and M.C. McKenna (editors), Mammal phylogeny: 165–181. New York: Springer-Verlag.

Maier, W., J. van den Heever, and F. Durand. 1996. New therapsid specimens and the origin of the secondary hard and soft palate of mammals. Journal of Zoological Systematics and Evolutionary Research 34: 9–19.

Manoussaki, D., et al. 2008. The influence of cochlear shape on low-frequency hearing. Proceedings of the National Academy of Sciences of the United States of America 105: 6162–6166.

Marshall, L.G. 1976a. Evolution of the Thylacosmilidae, extinct saber-tooth marsupials of South America. PaleoBios 23: 1–30.

Marshall, L.G. 1976b. New didelphine marsupials from the La Venta fauna (Miocene) of Colombia, South America. Journal of Paleontology 50: 402–418.

Marshall, L.G. 1977a. Evolution of the carnivorous adaptative zone in South America. *In* M.K. Hecht, P.C. Goody, and B.M. Hecht (editors), Major patters in vertebrate evolution: 709–721. New York: Plenum Press.

Marshall, L.G. 1977b. A new species of *Lycopsis* (Borhyaenidae, Marsupialia) from the La Venta Fauna (Miocene) of Colombia, South America. Journal of Paleontology 51: 633–642.

Marshall, L.G. 1978. Evolution of the Borhyaenidae, extinct South American predaceous marsupials. University of California Publications in Geological Sciences 117: 1–89.

Marshall, L.G. 1981. Review of the Hathlyacyninae, an extinct subfamily of South American "dog-like" marsupials. Fieldiana Geology 7: 1–120.

Marshall, L.G., and Z. Kielan-Jaworowska. 1992. Relationships of the dog-like marsupials, deltatheroidans and early tribosphebic mammals. Lethaia 25: 361–374.

Marshall, L.G., and C. de Muizon. 1995. The skull. *In* C. de Muizon (editor), *Pucadelphys andinus* (Marsupialia, Mammalia) from the Early Paleocene of Bolivia, Part II. Mémoires du Muséum national d'Histoire naturalle 165: 21–90.

Marshall, L.G., J.A. Case, and M.O. Woodburne. 1990. Phylogenetic relationships of the families of marsupials. Current Mammalogy 2: 433–502.

Meng, J., and R.C. Fox. 1995. Osseous inner ear structures and hearing in early marsupials and placentals. Zoological Journal of the Linnean Society 115: 47–71.

Montané, L., and E. Bourdelle. 1913. Anatomie régionale des animaux domestiques, 1. Cheval. Paris: Baillière.

Mortazavi, M.M., et al. 2012. Anatomy and pathology of the cranial emissary veins: a review with surgical implications. Neurosurgery 70: 1312–1319.

Muizon, C. de. 1994. A new carnivorous marsupial from the Paleocene of Bolivia and the problem of marsupial monophyly. Nature 370: 208–211.

Muizon, C. de. 1998. *Mayulestes ferox*, a borhyaenoid (Metatheria, Mammalia) from the early Paleocene of Bolivia. Phylogenetic and palaeobiologic implications. Geodiversitas 20: 19–142.

Muizon, C. de. 1999. Marsupial skulls from the Deseadan (late Oligocene) of Bolivia and phylogenetic analysis of the Borhyaenoidea (Marsupialia, Mammalia). Geobios 32: 483–509.

Muizon, C. de, R.L. Cifelli, and R. Céspedes Paz. 1997. The origin of the dog-like borhyaenoid marsupials of South America. Nature 389: 486–489.

Muizon C. de, S. Ladevèze, C. Selva, R. Vignaud, and F. Goussard. 2018. *Allqokirus australis* (Sparassodonta, Metatheria) from the early Palaeocene of Tiupampa (Bolivia) and the rise of the metatherian carnivorous radiation in South America. Geodiversitas 40: 363–459.

Nathoo, N., E.C. Caris, J.A. Wiener, and E. Mendel. 2011. History of the vertebral venous plexus and the significant contributions of Breschet and Batson. Neurosurgery 69: 1007–1014.

Norris, C.A. 1993. Changes in the composition of the auditory bulla in southern Solomon Islands populations of the grey cuscus, *Phalanger orientalis breviceps* (Marsupialia, Phalangeridae). Zoological Journal of the Linnean Society 107: 93–106.

Novacek, M.J. 1986. The skull of leptictid insectivorans and the higher-level classification of eutherian mammals. Bulletin of the American Museum of Natural History 183 (1): 1–111.

O'Brien, H.D., P.M. Gignac, T.L. Hieronymus, and L.M. Witmer. 2016. A comparison of postnatal arterial patterns in a growth series of giraffe (Artiodactyla: *Giraffa camelopardalis*). PeerJ 4: e1696.

O'Leary, M.A., et al. 2013. The placental mammal ancestor and the post-K-Pg radiation of placentals. Science 339: 662–667.

Osgood, W.H. 1921. A monographic study of the American marsupial, *Caenolestes*. Publications of the Field Museum of Natural History, Zoological series 14: 1–156.

Padget, D. 1957. The development of cranial venous system in man: from the view point of comparative anatomy. Contributions to Embryology 18: 145–191.

Patterson, B. 1965. The auditory region of the borhyaenid marsupial *Cladosictis*. Breviora 217: 1–9.

Pavan, S.E., and R.S. Voss. 2016. A revised subgeneric classification of short-tailed opossums (Didelphidae: *Monodelphis*). American Museum Novitates 3868: 1–44.

Petter, G., and R. Hoffstetter. 1983. Les marsupiaux du Déséadien (Oligocène Inférieur) de Salla (Bolivie). Annales de Paléontologie (Vert.-Invert.) 69: 175–234.

Presley, R. 1979. The primitive course of the internal carotid artery in mammals. Acta Anatomica 103: 238–244.

Prevosti, F.J., and A.M. Forasiepi. 2018. Evolution of South American mammalian predators during the Cenozoic: paleobiogeographic and paleoenvironmental contingencies. Berlin: Springer.

Prevosti, F.J., A.M. Forasiepi, and A.N. Zimicz. 2013. The evolution of the Cenozoic terrestrial mammalian predator guild in South America: competition or replacement? Journal of Mammalian Evolution 20: 3–21.

Reig, O.A., J.A.W. Kirsch, and L.G. Marshall. 1987. Systematic relationships of the living and neocenozoic American "opossum-like" marsupials (suborder Didelphimorphia), with comments on the classification of these and of the Cretaceous and Paleocene New World and European metatherians. *In* M. Archer (editor), Possums and opossums. Studies in evolution, vol. 1: 1–89. Sydney: Surrey Beatty and Sons.

Reinhard, K.R, M.E. Miller, and H.E. Evans. 1962. The craniovertebral veins and sinuses of the dog. American Journal of Anatomy 111: 67–87.

Riggs, E.S. 1933. Preliminary description of a new marsupial saber-tooth from the Pliocene of Argentina. Field Museum of Natural History, Geological series 6: 61–66.

Riggs, E.S. 1934. A new marsupial saber-tooth from the Pliocene of Argentina and its relationships to other South American predaceous marsupials. Transac-

tions of the American Philosophical Society (new series) 24:1–31.

Rosowski, J.J. 1994. Outer and middle ears. *In* R.R. Fay and A.N. Popper (editors), Comparative hearing: mammals: 172–248. New York: Springer.

Rougier, G.W. 1993. *Vincelestes neuquenianus* Bonaparte (Mammalia, Theria) un primitivo mamífero del Cretácico Inferior de la cuenca neuquina. Ph.D. dissertation, Universidad Nacional de Buenos Aires, Buenos Aires.

Rougier, G.W., and J.R. Wible. 2006. Major changes in the ear region and basicranium of early mammals. *In* M. Carrano, T.J. Gaudin, R. Blob, and J.R. Wible (editors), Amniote paleobiology. Phylogenetic and functional perspectives on the evolution of mammals, birds, and reptiles: 269–311. Chicago: University of Chicago Press.

Rougier, G.W., J.R. Wible, and M.J. Novacek. 1998. Implications of *Deltatheridium* specimens for early marsupial history. Nature 396: 459–463.

Ruf, I., Z.-X. Luo, and T. Martin. 2013. Re-investigation of the basicranium of *Haldanodon exspectatus* (Mammaliaformes, Docodonta). Journal of Vertebrate Paleontology 33: 382–400.

Sánchez-Villagra, M.R. 1998. Patterns of morphological change in the ontogeny and phylogeny of the marsupial skull. Ph.D. dissertation, Duke University, Durham, NC.

Sánchez-Villagra, M.R., and A.M. Forasiepi. 2017. On the development of the chondrocranium and the histological anatomy of the head in perinatal stages of marsupial mammals. Zoological Letters 3: 1. [doi: 10.1186/s40851-017-0062-y]

Sánchez-Villagra, M.R., and T. Schmelzle. 2007. Anatomy and development of the bony inner ear in the woolly opossum, *Caluromys philander* (Didelphimorphia, Marsupialia). Mastozoología Neotropical 14: 53–60.

Sánchez-Villagra, M.R., and J.R. Wible. 2002. Patterns of evolutionary transformation in the petrosal bone and some basicranial features in marsupial mammals, with special reference to didelphids. Journal of Zoological Systematics and Evolutionary Research 40: 26–45.

Schindelin, J., et al. 2012. Fiji: an open-source platform for biological-image analysis. Nature Methods 9: 676–682.

Schmelzle, T., M.R. Sánchez-Villagra, and W. Maier. 2007. Vestibular labyrinth evolution in diprotodontian marsupial mammals. Mammal Study 32: 83–97.

Segall, W. 1969a. The middle ear region of *Dromiciops*. Acta Anatomica 72: 489–501.

Segall, W. 1969b. The auditory ossicles (malleus, incus) and their relationships to the tympanic in marsupials. Acta Anatomica 73: 176–191.

Segall, W. 1970. Morphological parallelisms of the bulla and auditory ossicles in some insectivores and marsupials. Fieldiana Zoology 51: 169–205.

Segall, W. 1971. The auditory region (ossicles, sinuses): in gliding mammals and selected representatives of non-gliding genera. Fieldiana Zoology 58: 27–59.

Simpson, G.G. 1948. The beginning of the age of mammals in South America. Part 1. Introduction. Systematics: Marsupialia, Edentata, Condylarthra, Litopterna and Notioprogonia. Bulletin of the American Museum of Natural History 91 (1): 1–232.

Simpson, G.G. 1971. The evolution of marsupials in South America. Anales de la Academia Brasilera de Ciências 43: 103–118.

Sinclair, W.J. 1906. Mammalia of the Santa Cruz beds. Marsupialia. Reports of the Princeton University Expeditions to Patagonia 4: 333–460.

Sisson, S., and J.D. Grossman. 1953. The anatomy of the domestic animals. 4th ed., rev. Philadelphia: Saunders.

Spoor, F., et al. 2007. The primate semicircular canal system and locomotion. Proceedings of the National Academy of Sciences of the United States of America 104: 10808–10812.

Standring, S. 2016. Gray's anatomy: the anatomical basis of clinical practice, 41st ed. London: Elsevier.

Starck, D. 1967. Le crâne de mammifères. *In* P.-P. Grassé (editor), Traité de zoologie, vol. 16.1: 405–549, 1095–1102. Paris, Masson.

Suárez C., A.M. Forasiepi, F.J. Goin, and C. Jaramillo. 2016. Insights into the Neotropics prior to the Great American Biotic Interchange: new evidence of mammalian predators from the Miocene of Northern Colombia. Journal of Vertebrate Paleontology 36 (1): e1029581.

Szalay, F.S. 1982. A new appraisal of marsupial phylogeny and classification. *In* M. Archer (editor), Carnivorous marsupials, vol. 2: 621–640. Sydney: Royal Zoological Society of New South Wales.

Szalay, F.S., and B.A. Trofimov. 1996. The Mongolian Late Cretaceous *Asiatherium* and the early phylogeny and paleobiogeography of Metatheria. Journal of Vertebrate Paleontology 16: 474–509.

Turnbull, W.D. 1978. Another look at dental specialization in the extinct saber-toothed marsupial, *Thylacosmilus*, compared with its placental counterparts. *In* P.M. Butler, and K.A. Joysey (editors), Develop-

ment, function and evolution of teeth: 399–414. London: Academic Press.

Turnbull, W.D., and W. Segall. 1984. The ear region of the marsupial sabertooth, *Thylacosmilus*: influence of the sabertooth lifestyle upon it, and convergence with placental sabertooths. Journal of Morphology 181: 239–270.

van der Klaauw, C.J. 1931. The auditory bulla in some fossil mammals with a general introduction to this region of the skull. Bulletin of the American Museum of Natural History 62 (1): 1–352.

van Kampen, P.N. 1905. Die Tympanalgegend des Säugetierschädels. Morphologisches Jahrbuch 34: 1–722.

Voss, R.S., and S.A. Jansa. 2003. Phylogenetic studies on didelphid marsupials II. Nonmolecular data and new IRBP sequences: separate and combined analyses of didelphine relationships with denser taxon sampling. Bulletin of the American Museum of Natural History 276: 1–82.

Voss, R.S., and S.A. Jansa. 2009. Phylogenetic relationships and classification of didelphid marsupials, an extant radiation of New World metatherian mammals. Bulletin of the American Museum of Natural History 322: 1–177.

Wegner, R.N. 1964. Der Schädel des Beutelbären (*Phascolarctos cinereus* Goldfuss 1819) und seine Umformung durch lufthaltige Nebenhohlen. Abhandlungen der Deutschen Akademie der Wissenschaften zu Berlin, Klasse für Chemie, Geologie und Biologie 4: 1–86.

Wible, J.R. 1983. The internal carotid in early eutherians. Acta Palaeontologica Polonica 28: 174–180.

Wible, J.R. 1984. The ontogeny and phylogeny of the mammalian cranial arterial pattern. Ph.D. dissertation, Duke University, Durham, NC.

Wible, J.R. 1987. The eutherian stapedial artery: character analysis and implications for supraordinal relationships. Zoological Journal of the Linnaean Society 91: 107–135.

Wible, J.R. 1990. Petrosals of Late Cretaceous marsupials from North America, and a cladistic analysis of the petrosal in therian mammals. Journal of Vertebrate Paleontology 10: 183–205.

Wible, J.R. 2003. On the cranial osteology of the short-tailed opossum *Monodelphis brevicaudata* (Didelphidae, Marsupialia). Annals of the Carnegie Museum 72: 137–202.

Wible, J.R. 2009. The ear region of the pen-tailed treeshrew, *Ptilocercus lowii* Gray, 1848 (Placentalia, Scandentia, Ptilocercidae). Journal of Mammalian Evolution 16: 199–233.

Wible, J.R. 2011. On the treeshrew skull (Mammalia, Placentalia, Scandentia). Annals of Carnegie Museum 79: 149–238.

Wible, J.R., and J.A. Hopson. 1995. Homologies of the prootic canal in mammals and non-mammalian cynodonts. Journal of Vertebrate Paleontology 15: 331–356.

Wilson, G.P., E.G. Ekdale, J.W. Hoganson, J.J. Calede, and A. Vander Linden. 2016. A large carnivorous mammal from the Late Cretaceous and the North American origin of marsupials. Nature Communications. [doi: 10.1038/ncomms13734]

Witmer, L.M., S. Chatterjee, J. Franzosa, and T. Rowe. 2003. Neuroanatomy of flying reptiles and implications for flight, posture and behaviour. Nature 425: 950–953.

Wood-Jones, F. 1949. The study of a generalized marsupial (*Dasycercus cristicauda* Krefft). Transactions of the Zoological Society of London 26: 408–501.

Wroe, S., C. Argot, and C. Dickman. 2004. On the rarity of big fierce carnivores and primacy of isolation and area: tracking large mammalian carnivore diversity on two isolated continents. Proceedings of the Royal Society of London B, Biological Sciences 271: 1203–1211.

Wroe, S, et al. 2013. Comparative biomechanical modeling of metatherian and placental saber-tooths: A different kind of bite for an extreme pouched predator. PLoS ONE 8: e66888.

Zimicz, A.N. 2014. Avoiding competition: the ecological history of Late Cenozoic metatherian carnivores in South America. Journal of Mammalian Evolution 21: 383–393.

APPENDIX 1

Glossary

To insure that our terminology is clear and consistent, where appropriate we utilize names and definitions in the glossary developed by MacPhee (1981), with additions from Wible (2003) and other sources. A few additional definitions and clarifications are needed to cover conditions found in *Thylacosmilus* and other fossil metatherians. A source of previous error in identifying apertures associated with the transit of the internal carotid artery through the basicranium may stem from an assumption that marsupials do not differ from placentals. In fact, they do differ.

Emissary veins: Transcranial valveless veins connect intracranial venous sinuses with the extracranial venous system, typically via a number of ports distributed over the neurocranium (Lang, 1983; Standring, 2016). Examples of emissary veins that may attain large caliber in specific taxa include the mastoid emissary vein and the emissary vein or plexus of foramen ovale, which attains large size in *Monodelphis* (R.D.E.M., personal obs.) and perhaps other marsupials.

Emissary veins represent an important class of vascular structures that are rarely considered in morphological studies of fossil mammals. In living taxa, they appear early in ontogeny as the primary channels draining the developing brain, only to later decline in significance as other venous networks take over (e.g., Padget, 1957). Several physiological functions have been attributed to emissary veins, including selective brain cooling due to the fact that blood can flow through them bidirectionally (Hoogland et al., 2012; O'Brien et al., 2016). Although emissary veins probably exist in adults of all mammals, their incidence is well documented only for *Homo*, some domestic animals, and certain species commonly used in physiological studies (e.g., O'Brien et al., 2016). In *Homo* emissary veins are almost always relatively small in caliber except where affected by pathology or developmental error (Falk, 1986; Chen et al., 2007; Mortazavi et al., 2012). In such contexts emissary veins may become important as alternative routes for venous return, if the network can adapt by successfully shunting the flow to these bypasses (Batson, 1940, 1957; Chen et al., 2007). What works in acute disease contexts can presumably also work in evolutionary contexts, given time and appropriate selective forces. This is suggested by instances in which emissaries retain their original importance throughout ontogeny, augmenting or even replacing other channels. A good example is the sphenoparietal emissary vein, which originates in relation to the prootic sinus of early ontogeny (Wible, 1990, 2003). In many mammals, but not normally in humans, this emissary is retained throughout life, acting as the intracranial portion of the retromandibular vein (= postglenoid vein) and draining via the postglenoid foramen to the temporal veins. A speculative effort to reconstruct some elements of cranial vasculature in *Thylacosmilus* is provided in figure 26A.

Entoglenoid region: As used here, the region of the squamosal immediately internal to the mandibular fossa. In many sparassodonts this region is notably elongated mediolaterally, and sometimes bears a depression for reception of the rostral crus of the ectotympanic.

Epitympanic wing: Any outgrowth of a basicranial bone that contributes to the roof of the tympanic cavity (as opposed to a tympanic process, which contributes to the floor of the tympanic cavity). To qualify, the outgrowth must be substantial, not a mere ridge. A useful guide in some but not all cases is the smooth rounding of bony surfaces caused by pneumatization, which tends to increase the volume of the middle ear and thus the number of bone territories that appear within it. In relation to *Thylacosmilus*, we identify epitympanic wings of the alisphenoid, squamosal, and petrosal (i.e., tegmen tympani). Although the tympanic process of the exoccipital is large and well defined, the epitympanic wing in this taxon is confined to the caudal paratympanic sinus and is not visible within the tympanic cavity as such. Although not defined as a (bony) epitympanic wing, from the standpoint of ontogeny, the membrane covering the piriform

fenestra in life certainly qualifies as a roof constituent when incorporated into the middle ear.

Paratympanic space: Any significant pneumatic excavation within the confines of the middle ear but outside the bounds of the tympanic cavity proper. "Paratympanic," as a term applied to secondary spaces (e.g., MacPhee and Cartmill, 1986), are extensions of the ontogenetically primary tympanic cavity, which may be positionally defined as the space that contains the principal organs of hearing (auditory ossicles, muscles, apertures of the cochlear and vestibular windows, and tympanic membrane; MacPhee, 1981). "Paratympanic space" is used here in preference to "hypotympanic sinus" ("the part of the tympanic cavity that contains none of its principal elements, including the auditory ossicles and the fenestrae in the periotic" [van der Klaauw, 1931: 19]). Strictly speaking, the hypotympanic sinus should lie beneath the tympanic cavity proper: "it is formed when the ventral wall loses its flatness and becomes inflated on the medial or caudal side" (van der Klaauw, 1931: 19). However, this term is often used to describe the whole volume circumjacent to the primary tympanic cavity containing the auditory ossicles. Here, paratympanic spaces are named positionally, relative to pars cochlearis. For *Thylacosmilus* we discriminate ventral, lateral, and caudal paratympanic spaces.

Piriform fenestra: Membrane-covered gap in the midbasicranial floor at the level of the basioccipital-basisphenoidal synchondrosis, situated between the alisphenoid/squamosal rostrally, cochlear part of the petrosal caudally, and central stem medially. If persistent, the fenestra appears in the adult as a defect in the basicranium. Its actual borders and appearance, however, vary widely as much depends on how (or whether) the area is ossified by surrounding bones (MacPhee, 1981; Sánchez-Villagra and Forasiepi, 2017). In developing placentals, the fenestra may be morphologically situated entirely within the tympanic cavity as defined by the bony bulla or the fibrous membrane of the tympanic cavity (MacPhee, 1981). In marsupials, the definitive middle ear often fails to incorporate the area of the fenestra, with the result that the gap lies partly or wholly outside the tympanic cavity proper (e.g., *Thylacosmilus*). This feature is sometimes referred to as the foramen lacerum medium in the marsupial literature, a usage we avoid here.

As development continues, basicranial elements may grow together, resulting in the disappearance of the piriform fenestra. However, if ossification is incomplete, the fenestra may act as a single joint aperture for the mandibular nerve (CN V_3), greater petrosal nerve (part of CN VII), and accompanying vasculature (e.g., venous plexuses). It does not transmit the internal carotid artery in marsupials, although it may in placentals due to developmental differences (see Discussion). The degree of bony closure varies within species and it is surely ultimately controlled by developmental programming related to the skull base.

Tympanic cavity: The osseous, topologically unitary chamber that contains the cavum tympani, the membranous sac that fills this chamber during life (MacPhee, 1981). The middle ear includes the tympanic cavity plus the auditory tube and ossicles. Dilatations in the bony walls of the middle ear, variously named mastoid cavity, epitympanic sinus, hypotympanic sinus, paratympanic spaces, and so forth, are the result of highly specific bone remodeling during ontogeny, which explains why there is such uniformity in their relative positioning within, as opposed to between, taxa.

Tympanic process of alisphenoid: Substantial outgrowth of the caudal margin of the alisphenoid that bounds the rostral floor of the tympanic cavity. Found in many but not all metatherians.

Tympanic process of basisphenoid: Substantial outgrowth of lateral margin of the basisphenoid that helps to delimit the medial side of the floor of the tympanic cavity. Absent or not apparent (e.g., *Thylacosmilus*) in metatherians.

Tympanic process of exoccipital: (occasionally, and incorrectly, "mastoid" process)

bounds the caudal part of the floor of the middle ear, caudal to the round window (e.g., *Vombatus*; van Kampen, 1905: 408). In *Thylacosmilus* the exoccipital process is hollowed out by a paratympanic space, which is evidence that it actually contributes to bounding the middle ear and is therefore correctly described as a tympanic process. This feature is not unique to this genus and also occurs in extant marsupials (e.g., wombats; Wegner, 1964). We do not use the terms paroccipital process (e.g., Muizon, 1999) or paracondylar process (e.g., Forasiepi 2009; Forasiepi et al., 2015) for this structure here, even though those terms are in frequent use in the marsupial literature, because these names are more appropriately used in relation to attachment sites for muscles (e.g., digastric muscle).

Tympanic processes of petrosal: These outgrowths are exhaustively treated by MacPhee (1981) and require only minimal definition here:

The rostral tympanic process of the petrosal arises from all or part of the ventral surface of pars cochlearis. May form a major portion of the bony tympanic floor in many marsupials (e.g., *Dromiciops*; Sánchez-Villagra and Wible, 2002).

The caudal tympanic process of the petrosal arises primarily from the rostroventral part of pars canalicularis (MacPhee, 1981) and bounds the rearmost portion of the tympanic cavity. Occasionally very large (e.g., *Dromiciops*; Sánchez-Villagra and Wible, 2002). Although "mastoid process" is often used in a similar sense in metatherian character analyses, we restrict usage of that term to nontympanic outgrowths of pars canalicularis appearing on the nuchal aspect of the skull (e.g., *Didelphis*).

Tympanic processes of squamosal: These processes arise from the squamosal's ventral margin. For metatherians, it is necessary to distinguish two such processes, rostral and caudal, between which the aperture of the external acoustic meatus intervenes. As in the case of the rostral and caudal tympanic processes of the petrosal, both are formed by a single bone and (when both are present) do not form a self-suture. Nevertheless, they can be adequately distinguished as follows (fig. 6A, C):

The rostral tympanic process of the squamosal (= entoglenoid process of squamosal sensu MacPhee, 1981; processus paratympanicus lateralis sensu Wegner, 1964) arises from the entoglenoid region of the squamosal and helps to frame the rostral wall of the tympanic cavity. In some marsupials (e.g., *Vombatus*, *Lasiorhinus*), it forms all of the bony rostral wall (Wegner, 1964), to the exclusion of the alisphenoid tympanic process.

The caudal tympanic process of the squamosal arises from the posttympanic region of the squamosal and frames (together with the caudal crus of the ectotympanic, if expanded, and, in some cases, the exoccipital tympanic process) the caudal wall of the tympanic cavity. We restrictively define the posttympanic process to the projection or ridge on the cranial sidewall that serves as an attachment point for hyoid musculature as seen in living mammals.

Scientific Publications of the American Museum of Natural History

American Museum Novitates
Bulletin of the American Museum of Natural History
Anthropological Papers of the American Museum of Natural History

Submission procedures can be found at http://research.amnh.org/scipubs

All issues of *Novitates* and *Bulletin* are available on the web (http://digitallibrary.amnh.org/dspace). Order printed copies on the web from:
http://shop.amnh.org/a701/shop-by-category/books/scientific-publications.html

or via standard mail from:
American Museum of Natural History—Scientific Publications
Central Park West at 79th Street
New York, NY 10024

♾ This paper meets the requirements of ANSI/NISO Z39.48-1992 (permanence of paper).

On the cover: Artist's reconstruction of *Thylacosmilus atrox* by Jorge L. Blanco, 2019.